University of Nevada, Reno

Developing Tack Coat Specification for Long-Lasting Composite Pavement Performance

A thesis submitted in partial fulfillment of the

requirements for the degree of Master of Science in

Civil and Environmental Engineering

by

Geverson De Jesus Moura

Dr. Adam J. Hand/Thesis Advisor

May, 2023

THE GRADUATE SCHOOL

We recommend that the thesis
prepared under our supervision by

GEVERSON DE JESUS MOURA

entitled

Developing Tack Coat Specification for Long-Lasting Composite Pavement Performance

be accepted in partial fulfillment of the
requirements for the degree of

MASTER OF SCIENCE

Adam J. Hand, Ph.D.
Advisor

Elie Y. Hajj, Ph.D.
Committee Member

Peter E. Sebaaly, Ph.D
Committee Member

Anna K. Panorska, Ph.D.
Graduate School Representative

Erick C. Jones, Ph.D., Dean
Graduate School

May, 2023

Abstract

Pavements are constructed in multiple lifts to efficiently transfer traffic loads from the surface to the underlying layers. It is necessary to apply a tack coat material to ensure complete bonding during the construction of new pavements or rehabilitation processes. Otherwise, the pavement integrity may become compromised. The amount of tack coat and construction quality impact the pavement structure's performance and durability. The required quantity is influenced by factors such as the pavement surface type and condition, preparation of the layer, and appropriate construction practices. The bond strength between layers is also determined by the quality of tack coat and construction/application techniques employed.

This research aimed to determine test methods and best practices to develop a specification for tack coat materials used in composite pavements, which can predict their performance in different environmental conditions, construction techniques, and pavement types. The focus was on tack coat properties related to bonding and durability.

Establishing optimal tack coat specification thresholds required a comprehensive analysis of various rheological properties and an interlayer shear strength test. Rheological tests are fundamental in determining tack coat response to deformation and flow under different conditions. Additionally, interlayer shear strength tests evaluate the adhesive properties of the tack coat by measuring the required force to separate two pavement layers bonded with the tack coat. By correlating the results of rheological properties and interlayer shear strength test results, acceptable thresholds for bonding and durability performance were determined to improve the longevity of composite pavements.

The commonly used parameters of penetration and softening point, for specifying tack coat materials, may not be sensitive enough to reflect the effects of polymer modification. However, the asphalt binder's high-temperature performance grading (PGH) proved to be a good alternative to evaluating tack coat bonding performance. The results suggest that using a tack coat material with a PGH equal to or higher than the binder used in asphalt concrete achieves comparable or better performance than the minimum laboratory-measured ISS of 40 psi required for satisfactory field-level tack coat efficiency based on past research.

An aging index was estimated to assess the impact of aging on rheological properties of tack coat materials and make sure they will perform well throughout the pavement life. The results showed that all materials studied demonstrated good resistance to aging, with aging indexes below 4.0. This parameter was chosen based on a broader range of tack coat materials as part of the NCHRP Project 09-64.

Acknowledgements

First, I would like to thank my academic advisor, Dr. Adam J. Hand, for his invaluable support, guidance, and mentorship throughout my research. His expertise, encouragement, and constructive feedback have been instrumental in shaping my career. I would also like to express my gratitude to Dr. Elie Y. Hajj and Dr. Peter E. Sebaaly for the knowledge I have gained from them during my studies.

I also extend my gratitude to Dr. Anna K. Panaroska for being a valued committee member and Siththarththan Arunthavabalan for his expertise and guidance, which were essential in successfully completing my research.

Lastly, I would like to thank my family and friends for their unwavering support throughout my journey. Their encouragement, love, and guidance have been instrumental in my success.

Table of Contents

Chapter 1: Introduction 1

1.1 Background 1

1.2 Research Objectives 4

1.3 Scope of Work 4

Chapter 2: Literature Review 6

2.1 Composite Pavements 6

2.2 Tack Coat Materials 8

2.3 Tack Coat Application Rate 10

2.4 Tack Coat Setting Time 11

2.5 Tackiness 12

2.6 Effects of Temperature on Tack Coat Performance 13

2.7 Effects of Construction on Tack Coat Performance 14

2.8 Tack Coat Evaluation Test Methods 15

2.8.1 Shear Resistance 15

2.8.2 Tensile Strength 18

2.9 Types of Tack Coat Failure 19

2.10 Pavement Texture 20

Chapter 3: Experimental Plan 23

3.1 Materials & Characterization 24

3.1.1 Tack Coat Materials Selection 24

3.1.2 Emulsion Residue Recovery Tests 25

3.1.3 Tack Coat Performance Characteristics Test Methods 26

3.2 RHEA (Reology Analysis) Software 32

3.3 Bond Strength 33

3.3.1 Portland Cement Concrete Mix Design 34

3.3.2 Portland Cement Concrete Slabs Preparation 35

3.3.3 Tack Coat Materials Application 38

3.3.4 HMA Marshall Mix Design 41

3.3.5 HMA Overlay Compaction 48

3.3.6 AASHTO TP 114 50

Chapter 4: Results and Evaluation 53

4.1 Tack Coat Materials Rheological Evaluation 53

4.1.1 Continuous Performance Grade 53

4.1.2 Rotational Viscometer 55

4.1.3 Complex Modulus (G*) Master Curves 56

4.1.4 Black Space Diagram 58

4.1.5 Non-Recoverable Creep Compliance 60

4.2 Interlayer Shear Strength Test Results 60

4.2.1 ISS Failure Type 63

4.2.2 Statistical Analysis 64

4.3 ISS versus Rheological Properties of Tack Coat Materials 68

4.3.1 Penetration Test 68

4.3.2 Softening Point 69

4.3.3 Viscosity 71

4.3.4 High-Temperature Performance Grade (PGH) 73

4.4 Interface Surface Textures 77

Chapter 5: Findings and Recommendations 83

5.1 Findings 83

5.2 Recommendations 86

References 87

Appendix A 97

List of Tables

Table 1. Classification and Characteristics of Various Tack Coat Materials [15]..... 9

Table 2. Recommended Tack Coat Residual Application Rates [14], [19]..... 11

Table 3. Tack Coat Materials Selected for this Study. 24

Table 4. Test Methods Used for Tack Coat Performance Characteristics..... 27

Table 5. Summary of the Type of Failure for Each Tack Coat Material. 64

Table 6. Mean Profile Depth (MPD) Results for New and Aged PCC Surfaces..... 80

Table 7. Estimated Texture Depth (ETD) Results for New and Aged PCC Surfaces..... 81

Table 8. Mean Profile Depth (MPD) Results for ½-inch and ¾-inch NMAS AC Surfaces. 81

Table 9. Estimated Texture Depth (ETD) Results for ½-inch and ¾-inch NMAS AC Surfaces..... 81

Table A.1. PCC Mix Design. 97

Table A.2. PCC Mix Proportions..... 97

Table A.3. Aggregate Gradation for ¾ inch NMAS PCC Mixture. 98

Table A.4. Aggregate Gradation for ½ inch NMAS HMA Mixture..... 98

Table A.5. ½ inch NMAS HMA Mixture Properties..... 99

Table A.6. Aggregate Gradation for ¾ inch NMAS HMA Mixture..... 99

Table A.7. ¾ inch NMAS HMA Mixture Properties..... 100

Table A.8. Summary of Average Test Results for SS-1 Emulsion Residue [67]. 101

Table A.9. Summary of Average Test Results for SS-1h Emulsion Residue [67]. 102

Table A.10. Summary of Average Test Results for HP NT Emulsion Residue [67]. 103

Table A.11. Summary of Average Test Results for PM NT Emulsion Residue [67]..... 104

Table A.12. Summary of Average Test Results for HPM Emulsion Residue [67]. 105

Table A.13. Summary of Average Test Results for PG 67-22 Binder [67]. 106

Table A.14. Summary of Average Test Results for HP NT Hot-Applied Binder [67]... 107

Table A.15. Summary of Average Test Results for PG 64-22 Binder [67]. 108

Table A.16. ISS Test Results of New AC (½ inch NMAS)/New PCC. 109

Table A.17. ISS Test Results of New AC (¾ inch NMAS)/Aged PCC. 110

Table A.18. ISS Test Results of New AC (½ inch NMAS)/Aged PCC. 111

Table A.19. Analysis of Variance for New AC (½ inch NMAS)/New PCC..... 112

Table A.20. Analysis of Variance for New AC (¾ inch NMAS)/Aged PCC..... 112

Table A.21. Analysis of Variance for New AC (½ inch NMAS)/Aged PCC..... 112

Table A.22. Turkey and Bonferroni Pairwise Tack Coat Comparison for New AC (½ inch NMAS)/New PCC. 112

Table A.23. Turkey and Bonferroni Pairwise Tack Coat Comparison for New AC (¾ inch NMAS)/Aged PCC. 113

Table A.24. Turkey and Bonferroni Pairwise Tack Coat Comparison for New AC (½ inch NMAS)/Aged PCC. 113

List of Figures

Figure 1. (a) Slippage, (b) Delamination, and (c) Top-down Cracking. 2

Figure 2. Project Outline. 5

Figure 3. Typical Cross Sections of Composite Pavements [8]. 8

Figure 4. Effect of curing time on peak shear stress for porous asphalt concrete (PAC) and stone mastic asphalt (SMA) system under normal stress 552 kPa at 25°C [20]. 12

Figure 5. Schematic View of the Leutner Shear Apparatus [32]. 17

Figure 6. Example of Shear Stress-Strain Curve from the Leutner Test [32]. 17

Figure 7. Potential Failure Modes in the BBS test [38]. 20

Figure 8. Diagram illustrating the process of MPD computation [40]. 22

Figure 9. Research Experimental Plan. 23

Figure 10. Three-dimensional (3D) schematic View of the PaveBox [63]. 35

Figure 11. Aggregate Base Course Surface Leveling prior to Pouring PCC Slab. 36

Figure 12. Immediately Tinned-Finished Concrete Slab. 37

Figure 13. PCC Slab After Applying Aging Procedure. 38

Figure 14. (a) Paint Brush used for Emulsified Asphalt Application, (b) Silicone Brush used for Hot-Applied Asphalt Binder Application. 40

Figure 15. Uniform Tack Coat Application on New PCC Pavement Surface. 41

Figure 16. ½-inch NMAS Aggregate Gradation. 43

Figure 17. ½-inch NMAS Mix Optimum Binder Content. 43

Figure 18. ½-inch NMAS Mix Voids in Mineral Aggregate (VMA). 44

Figure 19. ½-inch NMAS Mix Voids Filled with Asphalt (VFA). 44

Figure 20. ½-inch NMAS Mix Unit Weight. 44

Figure 21. ½-inch NMAS Mix Marshall Stability. 45

Figure 22. ½-inch NMAS Mix Plastic Flow. 45

Figure 23. ¾-inch NMAS Aggregate Gradation. 46

Figure 24. ¾-inch NMAS Mix Optimum Binder Content. 46

Figure 25. ¾-inch NMAS Mix Voids in Mineral Aggregate (VMA). 47

Figure 26. ¾-inch NMAS Mix Voids Filled with Asphalt (VFA). 47

Figure 27. ¾-inch NMAS Mix Unit Weight. 47

Figure 28. ¾-inch NMAS Mix Marshall Stability. 48

Figure 29. ¾-inch NMAS Mix Plastic Flow. 48

Figure 30. (a) Heavy-Duty Plate Compactor, (b) Coring Machine, (c) Compacted HMA Overlay and (d) PCC Surface. 50

Figure 31. ISS Testing Samples Tining Direction. 51

Figure 32. Interlayer Shear Strength Test. 52

Figure 33. Continuous PGH of all Tack Coat Materials. 54

Figure 34. Continuous PGL of all Tack Coat Materials. 55

Figure 35. Viscosity vs. Emulsion Type. 56

Figure 36. 4-mm DSR Data (SS-1). 57

Figure 37. Master Curves at 25°C (Original). 58

Figure 38. Black Space Diagram of a Laboratory vs. Plant Mixtures [58]. 59

Figure 39. Black Space Diagram (Original). 59

Figure 40. Non-Recoverable Creep Compliance for all Tack Coat Materials at PGH. 60

Figure 41. ISS Test Results of New AC (½ inch NMAS)/New PCC Samples using Different Tack Coat Types at Medium and High Application Rate. 61

Figure 42. ISS Test Results of New AC (¾ inch NMAS)/Aged PCC Samples using Different Tack Coat Types at Medium and High Application Rate. 61

Figure 43. ISS Test Results of New AC (½ inch NMAS)/Aged PCC Samples using Different Tack Coat Types at Medium and High Application Rate. 62

Figure 44. (a) New AC (½ inch NMAS)/Aged PCC Adhesive Failure (SS-1); (b) New AC (½ inch NMAS)/Aged PCC Cohesive Failure (HP NT). 64

Figure 45. ISS Prediction at 7% Air Voids for New AC (½ inch NMAS)/New PCC..... 66

Figure 46. ISS Prediction at 7% Air Voids for New AC (¾ inch NMAS)/Aged PCC..... 66

Figure 47. ISS Prediction at 7% Air Voids for New AC (½ inch NMAS)/Aged PCC..... 67

Figure 48. Predicted ISS vs. Penetration for New AC (½ inch NMAS)/New PCC. 68

Figure 49. Predicted ISS vs. Penetration for New AC (¾ inch NMAS)/Aged PCC. 69

Figure 50. Predicted ISS vs. Penetration for New AC (½ inch NMAS)/Aged PCC. 69

Figure 51. Predicted ISS vs. Softening Point for New AC (½ inch NMAS)/New PCC... 70

Figure 52. Predicted ISS vs. Softening Point for New AC (¾ inch NMAS)/Aged PCC. 70

Figure 53. Predicted ISS vs. Softening Point for New AC (½ inch NMAS)/Aged PCC. 70

Figure 54. Predicted ISS vs. Viscosity for New AC (½ inch NMAS)/New PCC. 71

Figure 55. Predicted ISS vs. Viscosity for New AC (¾ inch NMAS)/Aged PCC. 72

Figure 56. Predicted ISS vs. Viscosity for New AC (½ inch NMAS)/Aged PCC. 72

Figure 57. ISS vs. Tack Coat PGH for New AC (½ inch NMAS)/New PCC. 74

Figure 58. ISS vs. Tack Coat PGH for New AC (¾ inch NMAS)/Aged PCC. 74

Figure 59. ISS vs. Tack Coat PGH for New AC (½ inch NMAS)/Aged PCC. 74

Figure 60. ISS Normalization for New AC (½ inch NMAS)/New PCC. 76

Figure 61. ISS Normalization for New AC (¾ inch NMAS)/Aged PCC. 77

Figure 62. ISS Normalization for New AC (½ inch NMAS)/Aged PCC. 77

Figure 63. Laser Texture Scanner. 78

Figure 64. (a) 3D Coordinates of Scanned New PCC Surface ;(b) 3D Coordinates of Scanned Aged PCC Surface. 79

Figure 65. Intensity Image of (a) New PCC Surface; and (b) Aged PCC Surface. 79

Figure 66. ISS vs. MPD (PCC) Results. 82

Figure 67. ISS vs. MPD (AC) Results. 82

Chapter 1: Introduction

This chapter provides essential background information about the proposed research topic, the study objective, and the scope of work followed to achieve the outcomes. Its purpose is to establish the context for the entire research project by presenting justification, goals, and relevance in the field for the study.

1.1 Background

A pavement is constructed of multiple layers, each containing distinct road materials. To ensure optimal transfer of traffic and environmental stresses and strains throughout a composite pavement, the hot-mix asphalt (HMA) and Portland cement concrete (PCC) layers must be fully bonded, allowing the pavement to function as a single, integrated structure. When pavement layers adhere well to each other, they experience minimal shear and permanent deformations and exhibit superior elastic recovery. These factors contribute to the creation of long-lasting pavements [1].

Typically, a thin layer of unmodified or polymer-modified bituminous material is applied as a tack coat on existing or new pavements before placement and compaction of a top layer. This tack coat is the primary means for fully bonding between the two pavement layers during construction. Therefore, selecting and correctly applying the most suitable tack coat material for a specific project is crucial.

Traditionally, the selection of tack coat materials has been based on experience, convenience, and empirical judgment due to the need for more sufficient guidelines for the proper use of them [2]. The quantity of tack coat material needed during construction is influenced by factors such as the type and surface condition of the pavement layer it is

applied to, surface preparation, and proper construction techniques. The amount and quality of tack coat applied have a significant impact on the overall performance of the pavement structure.

In composite pavements, the quality of the bond between HMA overlays and PCC pavements is widely recognized as a critical factor in determining the performance of the overlay. When the bond between these layers deteriorates, it can lead to pavement deformation various premature distresses, such as slippage, delamination, and top-down surface cracking, as demonstrated in Figure 1. This can ultimately lead to increased pavement rehabilitation and maintenance costs [1], [3].

(a) (b) (c)

Figure 1. (a) Slippage, (b) Delamination, and (c) Top-down Cracking.

Al-Qadi et al. examined how surface texture influences the bond strength of the tack coat between PCC pavement surfaces and HMA overlays [4]. The authors discovered that the orientation of tining does not affect interface shear strength (ISS), while the impact of tack coat application rate on ISS is more significant on smooth surfaces than on tined or milled surfaces. This is attributed to the interlocking of HMA aggregates with the rougher milled surface. When the tack coat application rate is low compared to a smooth surface, surface tining can improve interface shear strength. Furthermore, the milled surface provides

significantly higher interface shear strength than tined and smooth surfaces at various tack coat application rates.

Numerous research studies have investigated the factors that impact bond strength. King and May found that a 10% decrease in ISS can lead to a 50% reduction in pavement fatigue life, demonstrating the negative impact of dust on tack coat bond quality [5]. Other authors have suggested that the separation of pavement layers can occur when subjected to shear stress higher than the ISS. In cases where the bond between two pavement layers is weak, the pavement's lifespan may be reduced from 20 to 7 years [6], [7].

Regarding tack coat material, asphalt emulsions have been the primary selection; among them, slow-setting and rapid-setting emulsions are the most frequently employed types. However, using asphalt emulsions as tack coat material can present some challenges, including the time required for the emulsion to break and set and the potential for tracking, which involves the transfer of tack coat material from the pavement surface to the tires of vehicles and equipment driven on the emulsion, with tracking often caused by construction vehicles or equipment [2].

Some asphalt emulsion and hot-applied asphalt binder materials made with high-stiffness binders, referred to as "non-tracking," have gained popularity in recent times as a means of preventing material pick-up on tires. The reason for this is that when tracking occurs, it can lead to bond failure in certain areas, which compromises pavement overall integrity and durability.

1.2 Research Objectives

The research was conducted to create a specification for tack coat materials, along with relevant laboratory testing techniques, to promote the appropriate use of tack coats for composite pavements. This specification was conducted to assess tack coat performance in various settings, such as different construction methods, pavement types, and environmental needs, regardless of the condition of the underlying pavement surface. The research specifically concentrated on test methods that pertain to tack coat properties related to bonding and durability in diverse environmental conditions for composite pavements.

1.3 Scope of Work

Figure 2 presents an outline of the experimental plan developed to establish laboratory test methods and thresholds for evaluating the bonding and durability performance of tack coat materials for composite pavements. The plan considers several factors, including equipment acquisition and material testing costs, current practices, repeatability, and the probability of the proposed methods being adopted by state Departments of Transportation (DOTs) and industry.

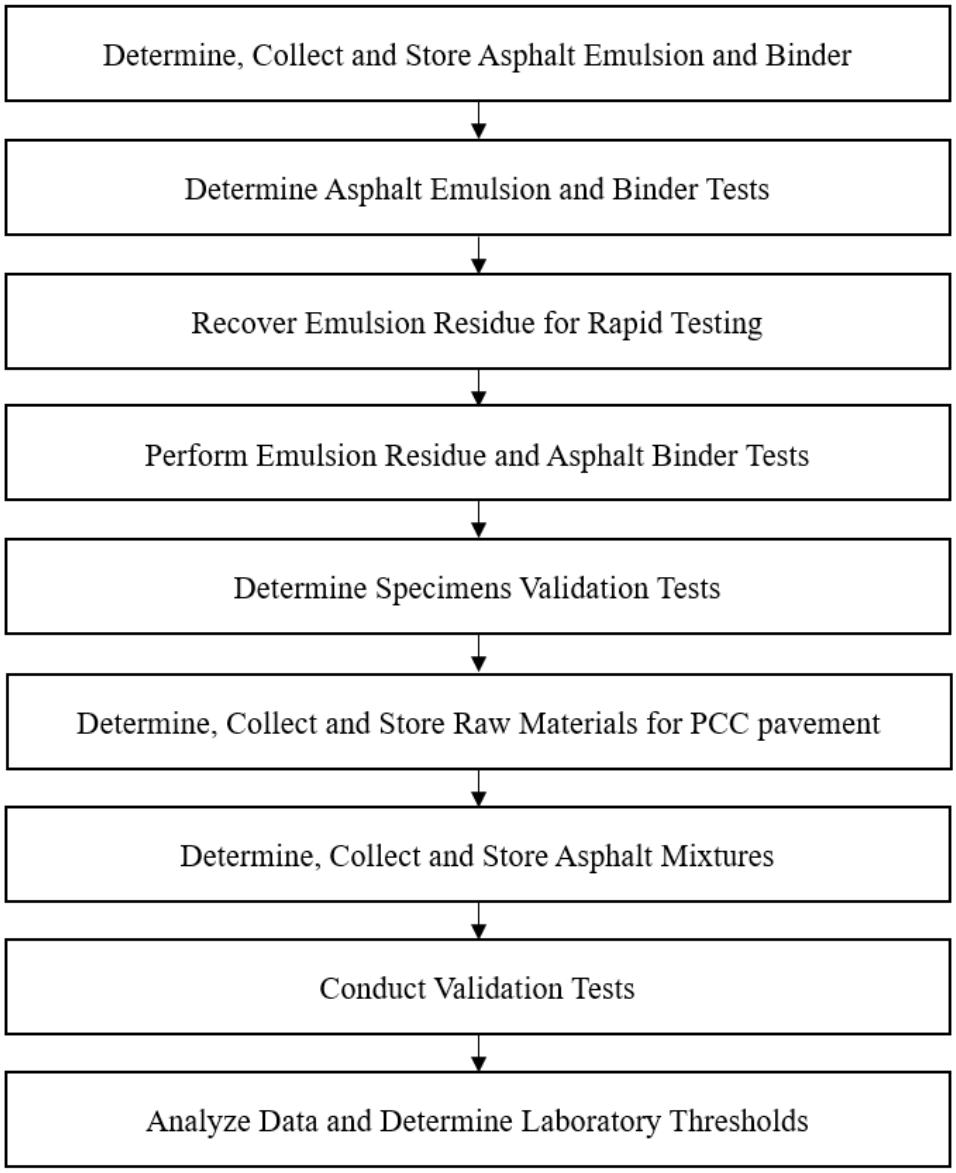

Figure 2. Project Outline.

Chapter 2: Literature Review

This section presents a thorough literature review on tack coat materials used in construction of composite pavements. The review contains recent studies on tack coat material characteristics and their efficacy in enhancing the adhesion between composite pavement layers. The significance of the insights provided in this section lies in facilitating the comprehension of the present knowledge on tack coat materials and guiding future research endeavors in this field.

2.1 Composite Pavements

In the past, transportation agencies and the road construction industry have been responsible for designing and building flexible and rigid pavement types. With the assistance of technology, pavement engineers can now determine the most cost-effective pavement type that can accommodate expected traffic demands while providing drivers with safety and comfort on the existing road. Before selecting a particular pavement type, the pavement type selection (PTS) method is generally utilized to determine the best pavement option for a given project [8].

As pavements age and are subjected to increased usage, they tend to deteriorate more rapidly. While preventive and corrective maintenance can help prolong their lifespan, eventually, pavements will require rehabilitation. Various rehabilitation methods are available to restore a pavement's structural capacity, depending on the extent of the damage or distress [9].

One popular approach for repairing deteriorated and cracked PCC pavements is to use Asphalt Concrete (AC) overlays [10]. AC overlays will significantly reduce deflections

and extend the pavement life for several years when the existing pavement is appropriately repaired prior to overlaying it [11]. In instances where concrete slabs are severely damaged, full-depth slab repair techniques involving the removal and replacement of damaged concrete slabs with either PCC or asphalt mixture should be utilized. If necessary, corrective work should also be undertaken on the underlying subbase or subgrade layers [12].

Composite pavement systems have demonstrated potential as an economical alternative for high-traffic roadways. They can offer higher structural and functional performance levels when compared to conventional flexible or rigid pavements. Although there are many other composite pavement systems, for this study, a composite structure is defined as a multi-layer structure where dense-graded HMA (flexible layer) is placed above PCC (rigid layer). The flexible layer offers a smooth, safe, and quiet driving surface supported by a solid, strong base. The classic pavement concept, which states that layer moduli decrease as layer depth increases, is generally changed. In composite structures, the rigid layer at the bottom is stiffer than the surface layer [8]. Figure 3 shows typical cross sections of composite pavements.

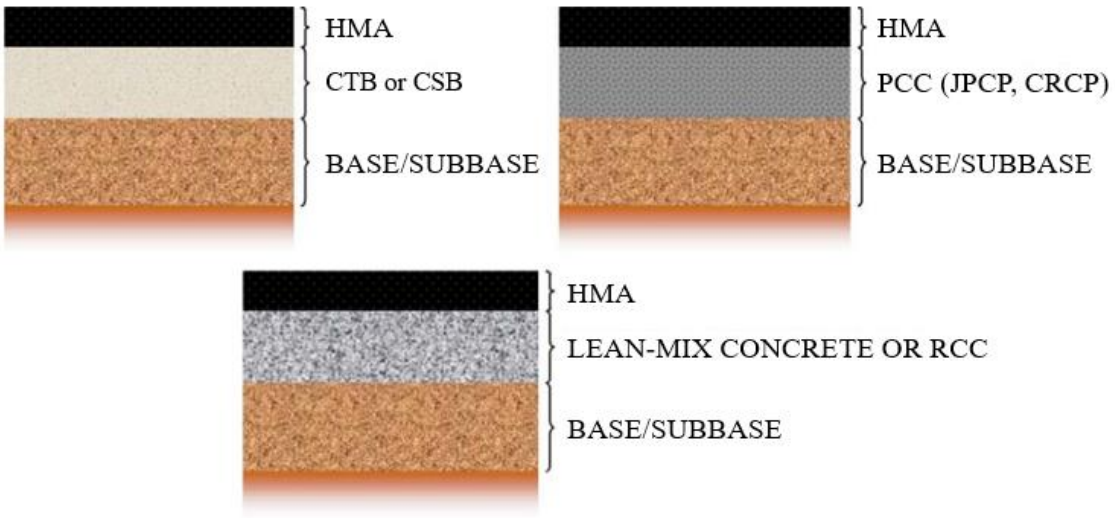

Figure 3. Typical Cross Sections of Composite Pavements [8].

The tack coat between two pavement layers must be evenly distributed and break before the new asphalt concrete layer is laid down for optimal performance. When an emulsion breaks, the liquid asphalt and water separate into two distinct phases. After the water evaporates, the remaining asphalt adheres to the underlying surface, enhancing the interlayer shear strength [13].

2.2 Tack Coat Materials

Traditionally, three materials have been utilized as tack coats: 1) asphalt emulsions, 2) performance-graded (PG) asphalt binders, and 3) cutback asphalt. However, the use of cutback asphalts has become less prevalent due to environmental concerns associated with diluent material evaporation [14]. Table 1 outlines various tack coat types and their respective characteristics [15].

Table 1. Classification and Characteristics of Various Tack Coat Materials [15].

Tack Coat Type	Classification	Characteristics
Hot-Applied Asphalt Binder	PG 58-28 PG 64-22 PG 76-22 Epoxy Asphalt	High bond strength, and difficult to spray.
Asphalt Emulsion	Slow Setting (SS-1, SS-1h, SS-1hp, CSS-1, CSS-1h, SS-1vh (non-tracking) Rapid Setting (RS-1, RS-2, CRS-1, CRS-2, CRS-2P (polymer-modified), CRS-2L (latex-modified) Trackless Tack Coat (a polymer modified emulsion with a hard-base asphalt binder)	Easy handling, energy saving, environmentally and safety friendly.
Cutback Asphalt	MC-70 (Medium Curing) RC-70 (Rapid Curing)	Consumes high energy and has environmental problems.

Note: SS-1 (Slow-Setting, Low Viscosity); SS-1h (Slow-Setting, Low Viscosity with Hard Base Asphalt); SS-1hp (Slow-Setting, Low Viscosity, Polymer Modified with Hard Base Asphalt); SS-1vh (Slow-Setting, Low Viscosity with Very Hard Base Asphalt); CSS-1 (Cationic Slow-Setting, Low Viscosity); CRS-2 (Cationic Rapid-Setting, High Viscosity); CRS-2P (Cationic Rapid-Setting, High Viscosity, Polymer Modified Asphalt); CRS-2L (Cationic Rapid-Setting, High Viscosity, Latex Modified); MC- 70 (Medium Curing Cutback Asphalt), RC-70 (Rapid Curing Cutback Asphalt).

Although some research has shown that hot-applied asphalt binders provide stronger interface bonding than emulsified asphalt, these materials must be heated to elevated temperatures to enable spray applications. If the asphalt binder does not reach adequate temperatures during construction, applying it uniformly to the surface layer would be difficult, especially at lower application rates [15]. Furthermore, test results show that hot-melt coatings, which are high-content copolymer-modified asphalt, have higher interface shear strength than solvent-born coatings (polymer-based cement) at high temperatures. After the solvent has evaporated, the residue provides an adhesive bonding, achieved by the hot-melt coating after spraying over the surface [16].

Emulsified asphalt or asphalt emulsion is a suspension of asphalt cement droplets in water, which a cationic or anionic emulsifying agent assists. The most common emulsified asphalt

types are slow-setting (SS) emulsion grades such as SS-1, SS-1h, CSS-1, and CSS-1h, and the rapid-setting (RS) emulsion grades such as RS-1, RS-2, CRS-1, CRS-2, CRS-2P, and CRS-2L [14]. Because they can be applied at intermediate temperatures, asphalt emulsions are the most popular tack coat materials, replacing hot asphalt binders and cutback asphalt. They are also safer to manipulate as they are not flammable or pose a risk to workers' health [17].

Most state DOTs constantly update a list of qualified or approved tack coat products on their websites. Factors like material availability, environmental conditions, and field experience can influence the choice of tack coat materials for a particular project.

2.3 Tack Coat Application Rate

Uniformity of application and a proper application rate are key to achieving a successful bonding [12]. The tack coat application rate must be optimized to achieve good interface bonding at the lowest possible cost. Varied application rates may be required to ensure good adhesion between the existing and overlay layers on pavement surfaces of multiple ages [18]. Most importantly, it is the residual amount of asphalt cement, not the application rate of diluted asphalt emulsion, that should be specified [14].

It is crucial to consider the many variables affecting tack coat application rate, including surface type, temperature, curing time, mixture type, and tack coat material. The pavement surface must also be cleaned and dried before applying the tack coat material to provide maximum bonding. For example, a power sweep should be used to clean milled pavements to prevent the tack coat from adhering to dust particles rather than the pavement surface.

Table 2 presents recommended tack coat residual application rates in gallons per square yard (gsy) for different pavement conditions [14], [19].

Table 2. Recommended Tack Coat Residual Application Rates [14], [19].

Surface Type	Residual Application Rate (gsy)	
	NCHRP Project 09-40 [14]	Asphalt Institute (AI) [19]
New Asphalt Mixture	0.035	0.020 – 0.045
Oxidized Asphalt Mixture	0.055	0.040 – 0.070
Milled Asphalt Mixture	0.055	0.040 – 0.080
Portland Cement Concrete	0.045	0.030 – 0.050

2.4 Tack Coat Setting Time

Diluted emulsions containing asphalt binder and water are brown when applied to a pavement surface and turn black after evaporation of the water in the emulsion. Once water molecules in tack coat materials evaporate, leaving the asphalt residue on the surface, the breaking process occurs. Due to different formulations in emulsifying agents, curing times vary with different tack coat material types. Rapid-setting emulsions often take significantly less time than slow-setting emulsions. As soon as the emulsion breaks, a bonding between the interlayer surfaces begins to form. Most tack coat materials take one to two hours to cure completely. So, it is recommended to wait until the tack coat has fully dried before placing a new pavement layer on top [18]. Figure 4 shows the effect of curing time on the shear strength of a Cationic Rapid-Setting emulsion (CRS) and modified asphalt emulsion (MAE). Shear strength can be increased by extending the curing time to a certain point, after which it will remain stable [20].

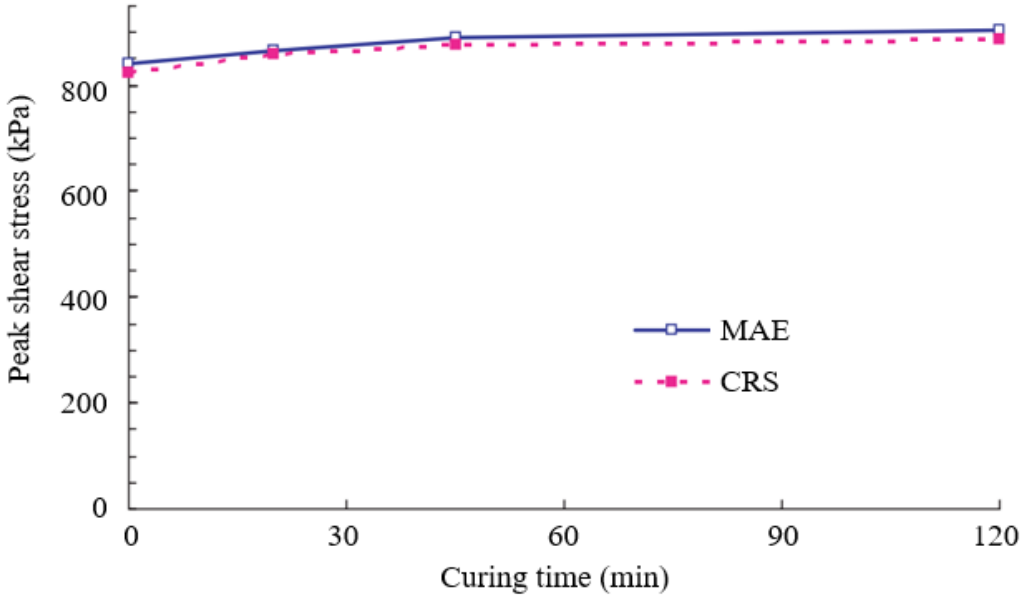

Figure 4. Effect of curing time on peak shear stress for porous asphalt concrete (PAC) and stone mastic asphalt (SMA) system under normal stress 552 kPa at 25°C [20].

2.5 Tackiness

For an asphalt emulsion to be considered "non-tracking," its strength (cohesion) must be higher than its adhesion to vehicle tires. In addition, the adhesion between the existing pavement surface and the emulsion must also be stronger than the adhesion of the tack coat to the tires. Tracking can happen on the wet (unbroken and unset) emulsion or the asphalt residue after curing. To mitigate the first problem, the emulsion must have enough time to break and cure before traffic is allowed on the tacked surface. Pavement temperature was found to be the most critical factor affecting tracking after the emulsion had fully cured. The tracking behavior will mostly depend on properties of the tack coat when subjected to different pavement temperatures (stiffer residual asphalt will track less). Surface cleanliness, paving over an unbroken/uncured asphalt emulsion, and selecting the wrong

stiffness of the residual asphalt binder are the three most critical issues that might cause tracking [21].

2.6 Effects of Temperature on Tack Coat Performance

Many researchers have emphasized the importance of considering the emulsion temperature during tack coat application to evaluate bond strength and tack coat performance. The emulsion residue stiffens at low temperatures and demonstrates a high shear strength. In contrast, as the temperature approaches the softening point of the emulsified asphalt binder, the material becomes more flowable, resulting in a gradual reduction of the shear strength [22].

Tack coat pull-off tests have shown a strong correlation between the maximum tensile strength and the softening point of the tack coat material. It was found that an increase in the softening point of the asphalt binder led to a corresponding increase in the optimal tack coat application temperature [23].

Changes in the properties of the asphalt binder are observed when application temperatures vary. The behavior of the pavement interface can be described using three parameters - the interface reaction modulus (slope of the shear stress-displacement curve), maximum shear strength, and friction coefficient after failure. These parameters characterize the interaction between the two pavement layers and have been found to be significantly influenced by temperature variation [24].

Conversely, other research contradicts previous findings and proposes that higher temperatures will result in a stronger bond between pavement layers. It can be attributed to the boiling of the emulsion when the new HMA layer is placed. This boiling process

evaporates water from the emulsion, enabling complete coating and adhesion of the asphalt binder to the existing pavement surface. Moreover, boiling helps to eliminate excess moisture from the pavement surface, which enhances bond strength and minimizes the potential for moisture-related pavement damage [25].

2.7 Effects of Construction on Tack Coat Performance

The condition of an existing pavement notably influences the interlayer bonding strength. However, research endeavors have determined that multiple factors related to construction could lead to the failure of a tack coat material, including the existence of moisture, inadequate curing, and contamination originating from paving equipment [26].

In the past, asphalt distributor trucks were the go-to equipment for applying tack coats. Still, many equipment companies have developed specialized pavers with integrated emulsion tanks and spray bars. Studies have found that using spray pavers for tack coat application results in higher interlayer bonding strength than conventional methods, such as distributors and HMA pavers, which can be attributed to higher application rates. Although spray pavers offer advantages such as time and cost-effectiveness, functional issues may arise during paving, such as uneven application of the sprayed material [26].

Applying tack coat using distributor trucks is challenging because haul trucks often drive on the applied material, which causes it to be tracked and removed from the surface layer. To overcome this issue, several methods have been developed. One option is to use trackless tack coat material. Alternatively, using a material transfer vehicle (MTV) along with a second tank is also an effective solution to this problem [14].

To improve interlayer bond strength, it is crucial to achieving precise and uniformly distributed application of tack coat. Uneven distribution of asphalt emulsion can occur horizontally on the pavement surface due to differences in emulsion output and fan patterns among the distributor nozzles. Additionally, longitudinal variations can occur along the length of the pavement due to changes in distributor speed and flow rates. Moreover, the existing pavement surface can absorb a portion of the emulsion applied, reducing its efficacy as a bonding agent for subsequent layers of aggregate or asphalt concrete [27].

Distributor trucks typically come equipped with computerized systems that feature tachometers to precisely monitor and control the vehicle's speed and volume measuring devices to monitor the amount of emulsion in the tank. Additionally, these systems include pressure gauges, thermometers, and controls that enable the operator to adjust the pressure and application rate, as well as the height and width of the spray bar. This allows for quick adjustments and shutting off individual spray bar sections directly from the cab. These systems are designed to compensate for vehicle speed variations and ensure precise and efficient emulsion application [28].

2.8 Tack Coat Evaluation Test Methods

2.8.1 Shear Resistance

Shear testing has become the most commonly used method to assess pavement interlayer bonding properties. Uzan et al. developed the first shearing mode test to evaluate the interface bond strength of cube specimens at varying temperatures, analyzing the effects of tack coat rate and normal stress on shear strength [29].

Modifications using cylindrical specimens were made to Uzan's test method, and a simple shear test device was developed by the Ancona Shear Testing Research and Analysis (ASTRA) program. Several studies have shown that interlayer bonding characterization is more accurate when a normal stress of about 0.2 MPa is used, as it better represents critical traffic loading conditions. This device can conduct direct shear tests while applying different levels of normal load, making it more suitable for simulating real-world in situ conditions [30].

The Leutner test, originated in Germany in 1979, is the simplest test method used to measure the interlayer bond strength between two pavement layers without the application of normal stresses at the interface. The dimensions of the equipment are illustrated in Figure 5, and expressed in millimeters. This test applies a constant rate of shear displacement across the bonded cross-section while recording the resulting shear force and the applied displacement throughout the test. Figure 6 presents an example of the shear stress-displacement curve resultant from the test. The maximum shear stress at the point of failure can be easily calculated by considering the cross-sectional area at the interface of double-layered specimens using Equation 1 [31].

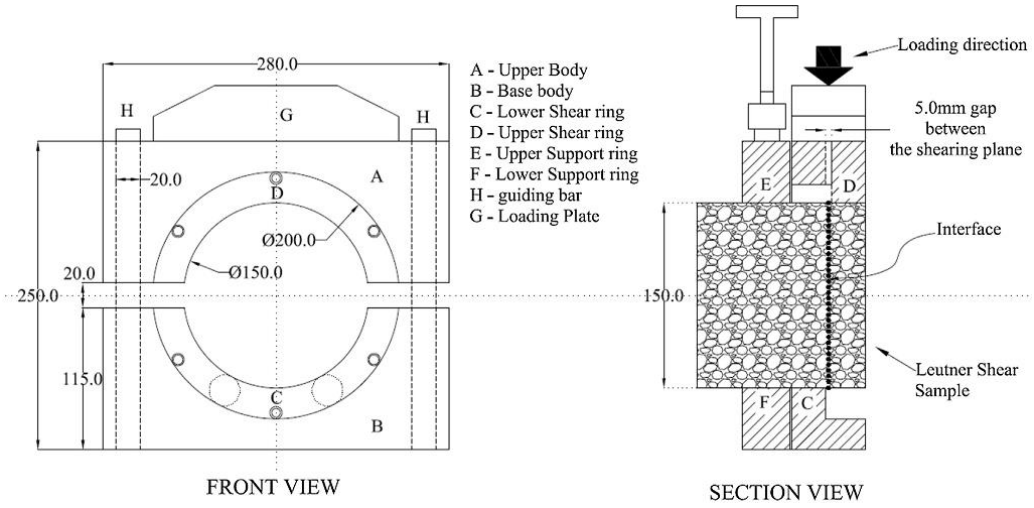

Figure 5. Schematic View of the Leutner Shear Apparatus [32].

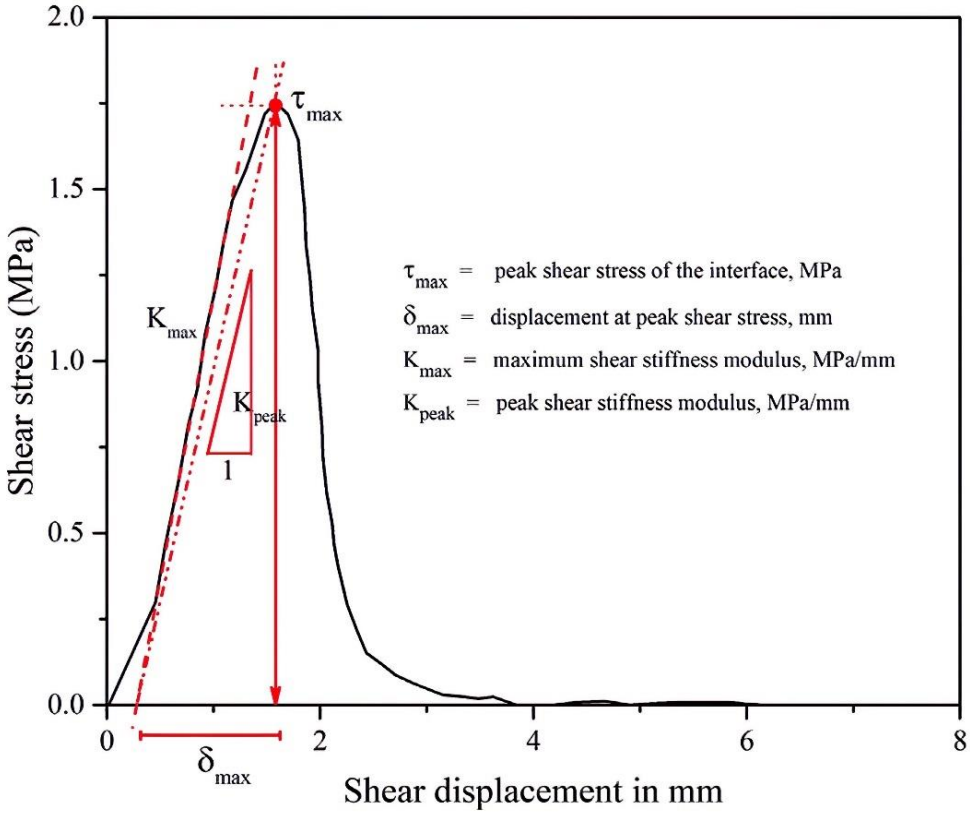

Figure 6. Example of Shear Stress-Strain Curve from the Leutner Test [32].

$$\tau_{max} = \frac{F_{max}}{A} = \frac{F_{max}}{\frac{\pi * D^2}{4}} \quad (1)$$

Where:

τ_{max} = maximum shear stress, MPa.

F_{max} = maximum shear force, N.

A = cross section area of Leutner shear sample, mm^2.

D = diameter of Leutner shear sample, mm.

Several researchers have utilized modified versions of the Leutner shear test, which resulted in the development of AASHTO TP 114 *Determining the Interlayer Shear Strength (ISS) of Asphalt Pavement Layers* [33]. The determination of interlayer shear strength for asphalt pavement layers is accomplished through this method, using both laboratory-prepared and field-compacted samples.

NCHRP Project 09-40 [14] showed that achieving satisfactory field-level tack coat efficiency and optimal residual tack coat application rates on various pavement surfaces requires a minimum laboratory-measured ISS of 40 psi.

2.8.2 Tensile Strength

Tensile strength testing is the second most commonly used approach for evaluating interlayer bond strength. This test involves pulling the top layer perpendicular to the interface plane until the maximum load is achieved to examine the adhesive failure mechanism of the tack coat. This test method is covered by AASHTO TP 115 *Standard Method of Test for Determining the Quality of Tack Coat Adhesion to the Surface of an*

Asphalt Pavement in the Field or Laboratory [34] and is applicable for both field and laboratory tests.

2.9 Types of Tack Coat Failure

In pavement design and construction, preventing debonding between asphalt and concrete pavement layers is crucial. This phenomenon occurs when non-negligible shear stress is generated as vehicles accelerate and brake. Additionally, the shear forces in longitudinal and transverse directions become more significant with increased slope, particularly for heavy traffic. This increased shear force can cause layers to debond, posing a risk to the pavement [35].

Establishing a proper interface bond between adjacent pavement layers depends significantly on the characteristics of the existing pavement surface before overlay construction. The micro- and macro-textures of the underlying layer's surface play a crucial role in achieving good bonding. Therefore, higher surface roughness is often associated with higher interlayer shear resistance [36].

The Binder Bond Strength (BBS) Test is a laboratory method described in AASHTO T 361 *Determining Asphalt Binder Bond Strength by Means of the Binder Bond Strength (BBS) Test* [37]. It measures the force necessary to detach a pull-off stub bonded to a solid substrate with asphalt binder. When pull-off strength values are measured under various environmental conditions and curing times, they provide information about the bond strength at the interface between the substrate and hot-applied or emulsified asphalt binders. Two primary failure modes are observed in this test: adhesive and cohesive failures. Adhesive failure occurs when the failure appears at the interface of the asphalt

binder-substrate or asphalt binder-stub, while cohesive failure happens when the failure occurs within the asphalt itself. Figure 7 illustrates a schematic of potential failure modes in the modified BBS test [38].

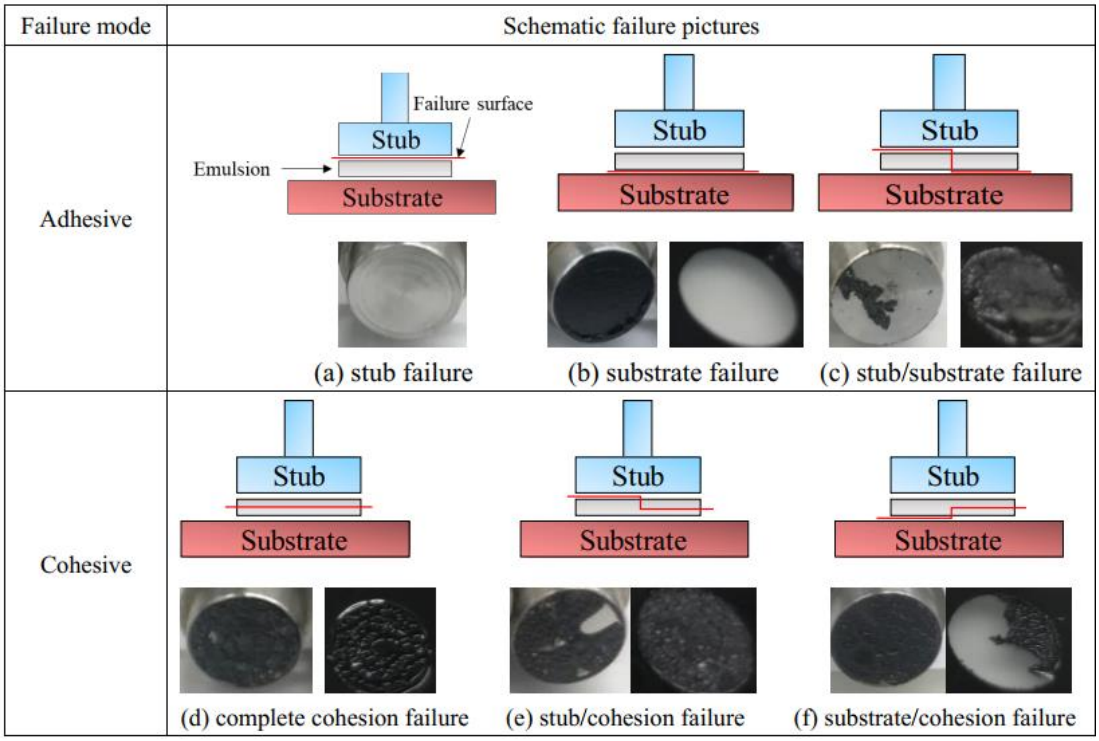

Figure 7. Potential Failure Modes in the BBS test [38].

2.10 Pavement Texture

The decrease in friction of pavement as it ages can be attributed to two primary factors. The first factor is the polishing of the aggregate due to constant traffic, which causes a reduction in microtexture. The second factor is the wearing out of the aggregate, leading to a decrease in macrotexture. To restore Portland cement concrete surfaces, techniques such as grooving and diamond grinding are employed, while micro-surfacing and seal coats are utilized for asphalt concrete pavements. Microtexture comprises wavelengths ranging

from 1 micrometer to 0.5 mm (0.0004 in. to 0.02 in.), while macrotexture encompasses wavelengths in the range of 0.5 mm to 50 mm (0.02 in. to 2 in.) [39].

The size of the particles in the mixture influences the texture of the pavement. The macrotexture of the pavement contributes to the hysteresis component of friction and facilitates rapid water drainage. On the other hand, microtexture enables direct contact between the tire and pavement and contributes to the adhesion component of friction [40].

To prevent disruptions in traffic flow, vehicle-mounted laser devices are often used to measure macrotexture. ASTM E-1845 *Standard Practice for Calculating Pavement Macrotexture Mean Profile Depth* [40] determines the mean profile depth (MPD) of pavement macrotexture from a pavement profile. The measured profile is divided into segments with a base length of 100 mm (3.9 in.) for analysis. The segment is then divided in half, and the highest peak in each half segment is measured. The difference between the peak's height and the segment's average level is calculated, and the average of these differences for all segments in the profile is reported as the MPD, as depicted in Figure 8. Some equipment manufacturers may use the profile's root mean square (RMS) to remove wavelengths longer than 100 mm after filtering. However, MPD, an area-based measurement, is more closely related to the volumetric patch method and friction. Estimating the mean texture depth (MTD) using a transformation equation (Equation 2) based on the mean profile depth (MPD) results in the computed value known as the estimated texture depth (ETD) [40], [41].

$$ETD = 0.2+0.8\ MPD \quad (2)$$

Where:

ETD = estimated texture depth, mm.

MPD = mean profile depth, mm.

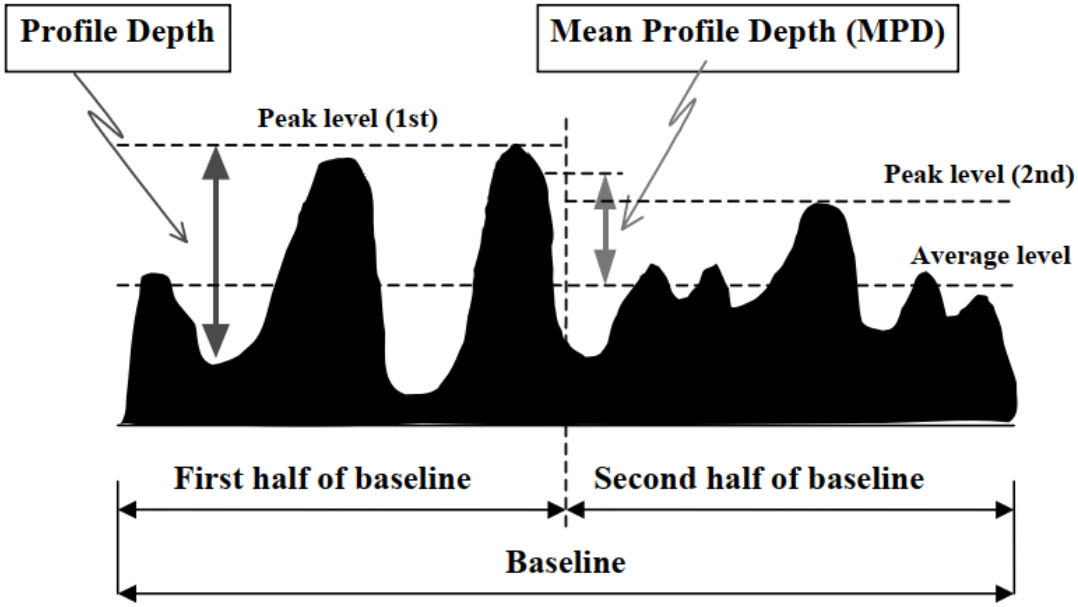

Figure 8. Diagram illustrating the process of MPD computation [40].

Chapter 3: Experimental Plan

This section outlines an experimental plan to characterize tack coat materials for improved bonding and durability performance in composite pavements. The primary objective of the plan was to ensure the reliability of results through a comprehensive testing approach. A detailed overview of the experimental plan is presented in Figure 9, highlighting the critical stages and procedures to be followed throughout the study.

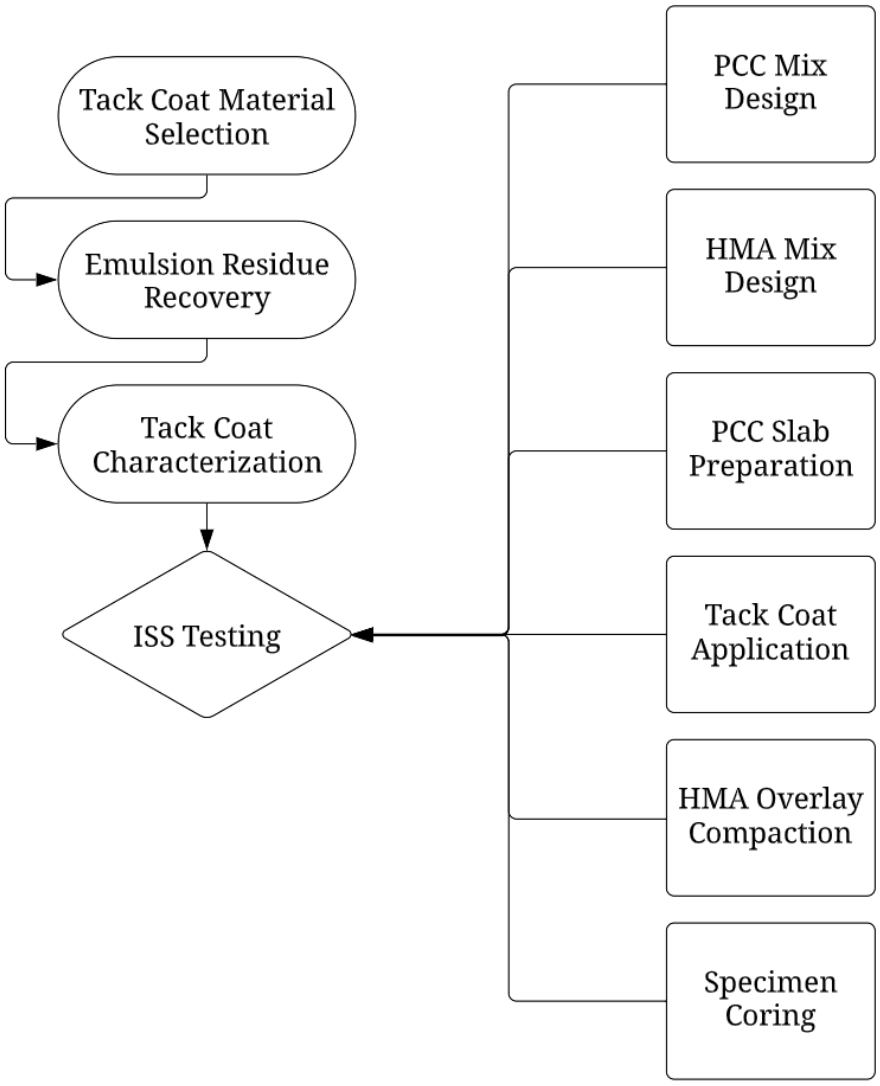

Figure 9. Research Experimental Plan.

3.1 Materials & Characterization

3.1.1 Tack Coat Materials Selection

Table 3 presents the various tack coat materials selected for this study to cover a broad spectrum of residue stiffness values and polymer modification. This selection aimed to ensure that a wide range of residual binder properties was covered, which could be applied in cold and hot climates, regardless of the specific construction techniques employed. The importance of this approach lies in the fact that residual asphalt can vary significantly in its rheological characteristics, depending on factors such as temperature. Using diverse tack coat materials enables the construction industry to select the most suitable material for their specific needs based on their particular environmental conditions and construction methods.

Table 3. Tack Coat Materials Selected for this Study.

Material ID	Tack Coat Characteristics
SS-1	Slow-setting emulsion (120-150 mm penetration residue, non-polymer modified)
SS-1h	Slow-setting emulsion (60-100 mm penetration residue, non-polymer modified)
HP NT	Hard penetration-based tack coat (non-tracking)
PM NT	Polymer modified tack coat (non-tracking)
HPM	Highly polymer modified tack coat (typically used with spray pavers for bonded thin lifts)
PG 67-22	Hot-applied asphalt binder
HP NT_HA	Hard penetration-based hot applied non-tracking tack coat/membrane (can be polymer modified for crack relief applications)

3.1.2 Emulsion Residue Recovery Tests

Different approved procedures for recovering asphalt emulsion residue are available, each with pros and cons. AASHTO (American Association of State Highway and Transportation Officials) T 59 *Standard Method of Test for Emulsified Asphalts* [42] is a distillation-based process for residue recovery that has been found to be lacking in that it does not accurately reflect real-world conditions, given the high temperatures used. Additionally, the process allows for a broad time tolerance of up to 60 ± 15 minutes, leading to inconsistent residue properties. Another disadvantage is that the high temperatures can cause degradation and irreversible reactions of polymer modifiers, thus producing a far-removed residue from what is found in the field. The manufacturer may suggest alternative distillation temperature ranges for assessing polymer-modified samples, but the customer must approve it.

The low-temperature evaporation (LTE) technique as per AASHTO R 78 *Standard Practice for Recovering Residue from Emulsified Asphalt Using Low-temperature Evaporative* [43] has been adopted as the preferred method among the available options, as it effectively simulates field conditions. However, the downside to this method is the long duration of 6 hours for method B and 48 hours for method A, excluding the time spent on sample preparation. Another area for improvement is the difficulty of creating Bending Beam Rheometer (BBR) test specimens due to the limited residue it generates. Moreover, the Emulsion Task Force (ETF)'s efforts to develop the AASHTO specification for surface treatments have highlighted the variability of residue characteristics. The research concluded that an inconsistent film thickness during sample preparation and varying

residual moisture content in the recovered residue were the most important sources of the considerable variation [44].

Using vacuum ovens at 60 ± 5°C for 3 hours following ASTM D7944 *Standard Practice for Recovery of Emulsified Asphalt Residue Using a Vacuum Oven* [45] is the most effective technique to produce consistent results regarding recovered residue properties. The short test time and a high vacuum applied guarantee complete moisture removal from the residue. Although the method is more expensive because of the equipment it requires, the amount of residue it produces is similar to the LTE method. Additionally, one needs to determine the atmospheric pressure in the laboratory or use an expensive absolute pressure gauge to guarantee consistent results in residue recovery.

3.1.3 Tack Coat Performance Characteristics Test Methods

A comprehensive summary of the chosen test methods for predicting the performance of tack coat materials under various environmental conditions, pavement types, and construction techniques can be found in Table 4. These test methods have been selected based on extensive research and analysis to ensure that they are reliable and appropriate for the task at hand.

A third-party entity was responsible for conducting all the tests to assess the characteristics of the tack coat. These tests were carried out with the utmost precision, and in strict compliance with the standards the AASHTO set forth. By adhering to these rigorous standards, the results of the tests can be trusted to provide accurate data regarding the performance of the tack coat.

Table 4. Test Methods Used for Tack Coat Performance Characteristics.

Test Method	AASHTO Standard	Material Tested		Performance Characteristics	
		Asphalt Binder	Emulsion Residue	Bonding	Durability
Dynamic Shear Rheometer (DSR)	AASHTO T 315	✓	✓	✓	✓
Bending Beam Rheometer (BBR)	AASHTO T 313	✓	✓	✗	✓
Multiple Stress Creep and Recovery (MSCR)	AASHTO T 350	✓	✓	✓	✓
Viscosity	AASHTO T 316	✓	✓	✓	✓
Penetration	AASHTO T 49	✓	✓	✗	✓
Softening Point	AASHTO T 53	✓	✓	✗	✓
4-mm DSR	TBD[1]	✓	✓	✗	✓

[1]To be determined.

Recent and historical research shows a strong correlation between interlayer bond strength and the stiffness of emulsion residue [14], [46]. The viscosity measurement is critical in determining the performance of asphalt emulsion residue as a tack coat material. The rotational viscometer is commonly used to measure the viscosity of the binder at higher temperatures than those experienced by the tack coat during use.

In contrast, the MSCR and complex shear modulus (G*) tests are conducted at expected pavement temperatures. These tests do not directly measure viscosity, but they are closely related to it through the non-recoverable creep compliance (J_{nr}) obtained from the MSCR test and stiffness evaluation via G*, which is related to the elastic modulus. This

information is essential because it helps to determine the potential for the asphalt emulsion residue to perform well as a tack coat material under expected pavement temperatures.

Evaluating the durability of asphalt emulsion residue as a tack coat material involves considering the results of all these tests in addition to traditional methods like penetration and softening point tests that have been widely used for many years.

3.1.3.1 Dynamic Shear Rheometer (DSR)

When the asphalt sample is subjected to shearing forces, its ability to resist repeated deformation can be described by G*. The phase angle (δ) represents the time gap between applying shear stress and the corresponding shear strain response. These rheological properties are determined according to AASHTO T 315 *Standard Method of Test for Determining the Rheological Properties of Asphalt Binder Using a Dynamic Shear Rheometer (DSR)* [47] with parallel plate test geometry. The test temperature is controlled using a forced air chamber, while the range of loading frequencies is assessed between 1 and 100 rad/sec. Since test temperatures exceeded 46°C, a parallel plate configuration with 25 mm plates and a 1.0 mm gap was employed.

3.1.3.2 Bending Beam Rheometer (BBR)

The BBR test, described as per AASHTO T 313 *Standard Method of Test for Determining the Flexural Creep Stiffness of Asphalt Binder Using the Bending Beam Rheometer (BBR)* [48] is used to assess the low-temperature stiffness (S) of an asphalt binder subjected to a static load and understand its ability to withstand thermal cracking, a significant issue in cold weather. The test also calculates the m-value, a parameter that reflects the ability of the asphalt binder to relieve the stresses induced by the load applied during the test.

The BBR test produces another important parameter, the ΔTc, representing the difference between the m-value critical temperature at 60 seconds of loading (the temperature at which the m-value equals the specification value of 0.300) and the stiffness-critical temperature at 60 seconds (the temperature at which the S-value equals the specification value of 300 MPa). The ΔTc parameter demonstrates how asphalt binder responds to aging and how incorporating additives might impact its response [49].

Studies on the aging of asphalt binders have introduced longer PAV aging cycles of 40 hours compared to the standard 20-hour cycle in order to assess the effects of aging on long-term durability. AI IS (Asphalt Institute Information Series) 240 [50] reveals a clear trend where increasing levels of aging result in more negative ΔTc values. The findings demonstrated that three different binders studied exhibit a positive value of ΔTc in an unaged condition. At 20 hours of PAV aging, the standard duration for PG binder analyses according to AASHTO M 320 *Standard Specification for Performance-Graded Asphalt Binder* [51], one binder remains positive and is S-controlled. However, for the extended 40-hour PAV aging, all binders become m-controlled, displaying more negative values. Thus, the laboratory aging required to assess ΔTc properly depends on the type of ΔTc analysis conducted.

3.1.3.3 Multiple Stress Creep Recovery (MSCR)

The Multiple Stress Creep Recovery test is the latest improvement to the Superpave Performance Grade (PG) specification, which eliminates the need for individual tests previously used to indicate polymer modification of asphalt binders, such as elastic recovery, toughness and tenacity, and force ductility [52]. This test provides the

performance and formulation of the asphalt binder, including the binder's recovery properties under different stress and temperature conditions.

The MSCR test, following the AASHTO T 350 *Standard Method of Test for Multiple Stress Creep Recovery (MSCR) Test of Asphalt Binder Using a Dynamic Shear Rheometer (DSR)* [53], is performed on Rolling-Thin Film Oven (RTFO)-aged asphalt samples subjected to 10 loading cycles with a 1-second load and a 9-second rest period at two stress levels (0.1 kPa and 3.2 kPa). The change in shear strain is measured and recorded after each cycle, enabling the non-recoverable creep compliance (J_{nr}) parameter calculation. This property describes the material's time-dependent, irreversible deformation under constant stress and can be expressed by Equation 3.

$$J_{nr} = \frac{\gamma_{10}}{\tau_{applied}} \text{ , kPa}^{-1} \quad (3)$$

Where:

γ = non-recoverable strain at the 10^{th} cycle, mm/mm.

τ = applied shear stress, kPa.

3.1.3.4 Viscosity

The AASHTO T 316 *Standard Method of Test for Viscosity Determination of Asphalt Binder Using Rotational Viscometer* [54] specifies a test method for determining the viscosity of asphalt binder at high application temperatures to ensure it can be pumped during construction without clogging or damaging the pumps. The test uses the Brookfield Rotational Viscometer, equipped with cylindrical spindles and a thermal chamber. The viscosity of the binder is determined by measuring the torque required to maintain a

constant rotational speed (20 rpm) of a cylindrical spindle immersed in the asphalt binder sample at a constant temperature, enabling measurement of the relative resistance to rotation. The viscosity is expressed in pascal seconds (Pa.s) and is calculated based on the torque and speed measurements.

3.1.3.5 Penetration Test

AASHTO T 49 *Standard Method of Test for Penetration of Bituminous Materials* [55] describes a test method used to determine the depth to which a standard needle will penetrate vertically into an asphalt binder sample. The test procedure requires that the specimen be conditioned to 25°C. The material is then leveled into a container, and the standard needle (weighing 100g) allowed to penetrate the sample for 5 seconds. The distance the needle penetrates the material is recorded as the penetration value in tenths of a millimeter. The test provides a measure of the bituminous material's consistency, with higher penetration values indicating softer binders while lower values suggesting stiffer materials.

3.1.3.6 Softening Point Test

The AASHTO T 53 *Standard Method of Test for Softening Point of Bitumen (Ring-and-Ball Apparatus)* [56] determines the temperature at which an asphalt binder loses its ability to support a standardized steel ball. The test procedure involves heating a disk-shaped asphalt sample within a ring-and-ball apparatus consisting of a steel ring, two supports, and a steel ball resting on top of the sample. The entire apparatus is then submerged in a water bath and heated at a fixed rate. As the temperature rises, the asphalt sample softens, causing

the ball to sink into the sample until it touches the supports. The temperature at which this occurs is recorded as the softening point.

3.2 RHEA (Reology Analysis) Software

RHEA software, developed by Abatech Inc., is designed to analyze rheological data obtained from various tests and comprehensively analyze the properties of viscoelastic materials. Dynamic or creep data can be used to generate master curves of stiffness or compliance information in either the time or frequency domain [57].

RHEA has several features, including determining complex viscosity, phase angle, and black space diagram, as well as relaxation and retardation spectra. It can also calculate the MEPDG master curve and corresponding shift factors, Glover-Rowe parameter, and ΔTc from stiffness and m-value (for BBR and 4mm DSR tests). Other features of RHEA include those not listed here.

The Black Space diagram is a valuable tool for monitoring the effects of aging on the rheological properties of an asphalt binder. It is a plot of the complex modulus versus the phase angle and is often used to investigate the cracking resistance of materials. Utilizing the 4-mm DSR test results, the Black Space diagram and complex modulus master curves can be generated for each tack coat material. The diagram shows that oxidation can increase the binder complex modulus and thereby increase rutting resistance. However, it also causes a significant drop in the phase angle and m-value obtained from the BBR. This leads to a more elastic behavior and faster damage accumulation, highlighting the importance of understanding the viscoelastic properties of asphalt binders under different conditions [58].

Formulating a master curve is a regular procedure that minimizes the significant test data necessary for viscoelastic materials. Developing a master curve for an asphalt binder involves the measurement of its stiffness at various temperature-frequency combinations. The original data is horizontally shifted based on a reference temperature by employing the time-temperature superposition principle, obtaining the same rheological behavior at varying experimental conditions [59]–[61].

3.3 Bond Strength

The Interlayer Shear Strength (ISS) test is a well-established method used to measure the maximum force required to shear the interface between two pavement layers and determine the maximum shear strength of these layers. The testing protocol is described in detail in AASHTO TP 114.

The ISS test was implemented on two distinct pavement configurations to gain a more comprehensive understanding of the various factors that may affect the shear strength of composite pavements. The first configuration involved laying a new HMA layer on top of the new PCC. The second configuration involved placing a new HMA layer on an aged PCC surface.

The seven types of emulsion residue and asphalt binder used to conduct the tack coat performance tests (Table 3) were applied between the two pavement layers to perform the mixture validation test. The test aimed to assess the effectiveness of the different emulsion types by evaluating their ability to achieve the desired levels of adhesion between the pavement layers. Two different application rates were selected for the PCC surface type to determine the optimal application rate that would result in maximum bond strength. This

test made it possible to identify the best-performing emulsion types and the optimal application rate for each emulsion type, thereby providing valuable insights into the effectiveness of different tack coat materials and application methods used for composite pavements.

3.3.1 Portland Cement Concrete Mix Design

The mix designs for PCC and HMA mixtures were performed by a third-party organization, enabling a more extensive production process capable of meeting the project's required scale.

The PCC mix design adhered to the guidelines and specifications outlined in American Concrete Institute (ACI) 301 [62], resulting in a ¾-inch NMAS (Nominal Maximum Aggregate Size) mix for this study. The NMAS is defined as the maximum size of aggregate particles present in the mixture and is determined by the sieve size immediately above the first sieve that retains at least 10% of the total aggregate mass.

The mix design followed the recommended procedures for selecting materials, determining the water-cement ratio, and adjusting the mix proportions to achieve the desired strength, durability, and workability. The specification was used as a reference document to ensure that the PCC mix design met the necessary performance requirements and complied with industry standards. Following the guidelines outlined in AC 301, the PCC mix was optimized for the specific application and met expectations to exhibit the desired properties and performance in the field. Materials used and test results are presented in Table A.1 through Table A.3 in Appendix A.

3.3.2 Portland Cement Concrete Slabs Preparation

In order to conduct accurate and reliable interlayer shear strength testing of the composite specimens (HMA over PCC), several test samples were fabricated using a specially designed large-scale test form known as the PaveBox, which allowed for precise control and measurement of factors that can affect bond strength, such as curing, and environmental conditions.

The PaveBox is a testing device constructed inside the Scrugham Engineering and Mines Building at the University of Nevada, Reno (UNR) to replicate real-world pavement construction and testing conditions. The box is supported on a base plate grouted to the floor, filled with several feet of subgrade and aggregate base material, and typically surfaced with asphalt or PCC mixture. The internal measurements of the box are 124 inches in length, 124 inches in width, and 72 inches in height [63]. Figure 10 shows a three-dimensional schematic view of the PaveBox, with dimensions in inches.

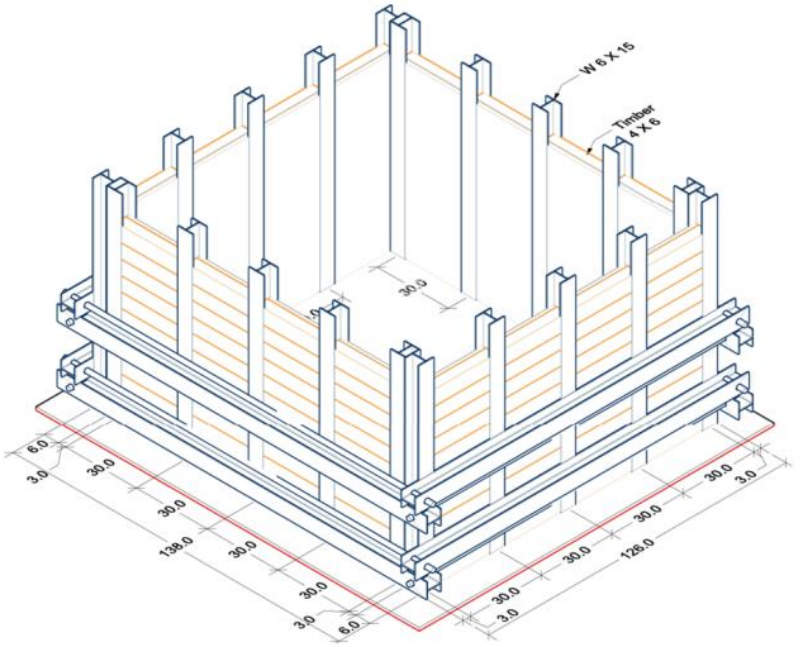

Figure 10. Three-dimensional (3D) schematic View of the PaveBox [63].

To prepare the concrete slabs, wooden forms were utilized to mark out the entire area to pour concrete over the compacted base layer. Initially, a thin layer of concrete was poured to create a level surface (Figure 11), ensuring that the subsequent PCC pavement layer would be precisely 3 inches thick as per the design. The wood chosen for the forms was durable, warp-resistant, and capable of supporting the weight of the concrete mix without bending or breaking, perfectly delineating the internal dimensions and exact shape of the slab and acting as a barrier to retain the concrete mix while it cured.

Figure 11. Aggregate Base Course Surface Leveling prior to Pouring PCC Slab.

After the concrete was poured into the wood forms, a vibration was applied to eliminate air pockets. This is an essential step because it increases the density and strength of the concrete. Once the pouring and vibrating were completed, the pavement surface was finished to simulate a real-life scenario. Initially, the surface was screed and floated to create a smooth pavement and remove minor imperfections. Then, a tining rake, which

measured 36 inches wide and had 1/8-inch-thick blades spaced 3/4 inch apart, was used to create the desired texture on the pavement surface. Tining is a texturing technique commonly used on PCC pavements to produce macrotexture, which enhances safety at high speeds. The tining rake was passed over each concrete slab in a single motion to ensure the texture was uniform and consistent.

Before applying the HMA mixture on top, the slab was allowed to cure for 7 days. It was crucial to maintain the moisture of the concrete during this period to prevent quick drying and cracking, which could negatively affect ISS results. To accomplish this, the surface of the slab was watered every day with a gentle stream of water, which helped keep it damp and allowed for a gradual and consistent curing of the concrete. Figure 12 exhibits the finished concrete slab surface.

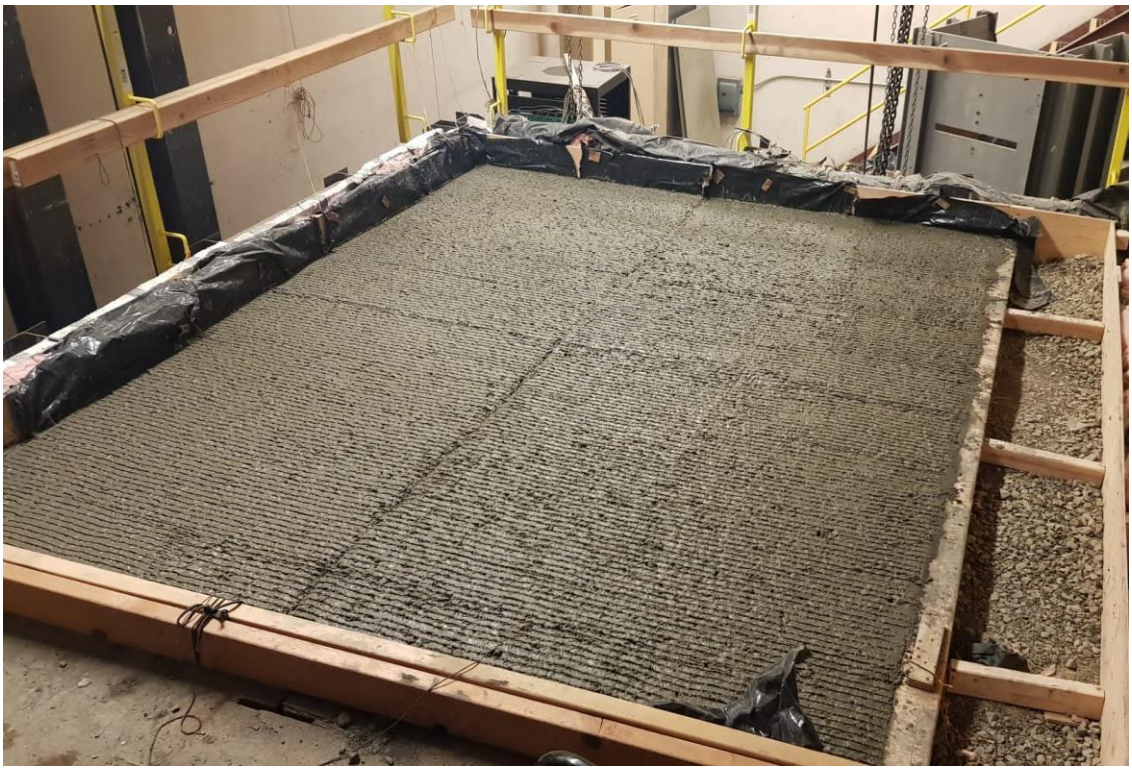

Figure 12. Immediately Tinned-Finished Concrete Slab.

In order to prepare the aged PCC slab, the same initial procedure of pouring the concrete into the forms and tining the surface with the tining rake was followed. The surface was then polished using a belt sander with 50-grit paper. This process was undertaken to accurately replicate the natural wear and tear that occurs over ten or more years on PCC pavements and ensure that the ISS test conducted on it would yield results reflective of its real-life usage. Figure 13 illustrates the aged PCC slab, after sanding reduced the tining depth and polished the surface.

Figure 13. PCC Slab After Applying Aging Procedure.

3.3.3 Tack Coat Materials Application

Several key factors must be considered to ensure an optimal tack coat application rate on a pavement surface. The amount of tack coat to be applied to the pavement surface was determined based on the desired residual application rate (in gallons per square yard) specified in NCHRP Project 09-40 [14] and presented in Table 2. This desired rate was

then used in Equation 4 to calculate the weight, in grams, of the tack coat applied on the bottom pavement layer. The calculation considers the cross-sectional area where the tack coat material was applied, the specific gravity of the tack coat material, and the percent asphalt residue for the emulsion (i.e., the amount of residual asphalt to water in the tack coat material). The constant used in the formula was used to convert the units of gallons to liters and yards squared to square inches, ensuring consistency across all measurements. By carefully calculating and applying the appropriate amount of tack coat based on these factors, the bond between asphalt layers can be strengthened, improving the overall performance and longevity of the pavement.

$$\text{Tack Coat Weight} = \frac{2.9205 \text{ x Targeted Residual Application Rate x Area x Specific Gravity}}{\text{\% Asphalt Residue}} \quad (4)$$

The quantity of tack coat required for optimal application onto a pavement surface is contingent upon the type and condition of the underlying layer, while the bond strength is predicated upon the quality of the tack coat material as well as the construction or application methods used. In light of Table 2, this study utilized a medium application rate of 0.045 gsy and a high application rate of 0.074 gsy to determine the amount of tack coat to be applied to both new and aged PCC. These rates were selected based on recommendations from NCHRP Project 09-40 for New PCC and were used as a guide for applying the tack coat in the study.

To ensure the accurate and precise application of the seven types of tack coat materials utilized in the study, a calibrated and leveled laboratory scale was employed to measure

the exact weight of the tack coat that needed to be applied. The pavement surface was prepared by brooming it before tack coat application to ensure optimal bonding of the tack coat material. This critical step ensured that debris or loose particles were removed from the surface, creating a clean and suitable substrate for the emulsion residue or asphalt binder to adhere to.

Seven identical areas were then designated and marked out using a chalk line to ensure consistency on the PCC pavement surface. These areas were delineated meticulously, taking great care to avoid the longitudinal construction joint, which has been identified as one of the principal causes of reflective cracking, negatively impacting the ISS results.

The asphalt emulsions were applied at an ambient temperature of 77ºF (25ºC) using a paintbrush, while the hot-applied binders were heated to 300ºF (148ºC) and applied using a silicone brush, as illustrated in Figure 14. Upon completion of the application process, the tack coat was allowed to cure for at least an hour, which has been established as a generally sufficient duration for curing all types of tack coat. All seven materials were carefully applied to the pavement surface to achieve a uniform rate, as shown in Figure 15.

(a) (b)

Figure 14. (a) Paint Brush used for Emulsified Asphalt Application, (b) Silicone Brush used for Hot-Applied Asphalt Binder Application.

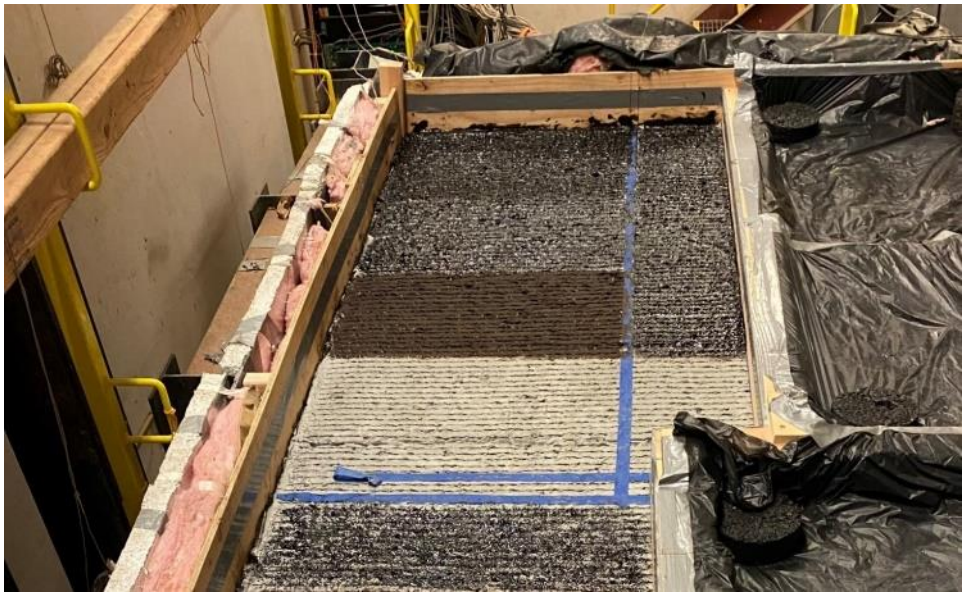

Figure 15. Uniform Tack Coat Application on New PCC Pavement Surface.

3.3.4 HMA Marshall Mix Design

In order to conduct a comprehensive study on the impact of the type of asphalt mixes on bond strength, this research project selected and evaluated two distinct HMA mix designs. The first design was a ½-inch NMAS mix, while the second was a ¾-inch NMAS mix.

These specific asphalt mixes were chosen because most Department of Transportation (DOT) agencies recommend ½-inch surface course materials for overlays or mill-and-fill projects. Furthermore, the research aimed to investigate and comprehend the impact of changing the overlay mixes' nominal maximum aggregate size from ½" (12.5 mm) to ¾" (19.0 mm) on the bond strength.

The mixtures used in this research were composed of a PG 64-22 binder. This binder is designed to withstand a maximum pavement temperature of 64 degrees Celsius and a minimum temperature of -22 degrees Celsius. This means the binder can endure these temperature extremes without risk of failure.

The Marshall mix design method is a popular and widely used approach for designing and producing asphalt concrete due to its simplicity and cost-effectiveness. It was used to obtain the HMA mixtures employed in this study. The mix design was meticulously prepared in strict compliance with the most current version of the 2012 Standard Specification for Public Works Construction (SSPWC) sponsored by the Regional Transportation Commission (RTC) of Washoe County, Nevada, and the Asphalt Institute Manual Series No. 2 (MS-2) [64], [65].

Both mixes contained 15% Reclaimed Asphalt Pavement (RAP) and 1.26% hydrated lime in terms of the dry weight of aggregates, which contributes to the finished product's durability, strength, and overall performance. The Marshall mix design involves varying compaction levels, with the number of blows applied depending on the anticipated traffic. For this study, the samples were compacted with 50 blows per face to simulate medium traffic. The properties of the ½-inch mixture are depicted in Figure 16 to Figure 22, while the properties of the ¾-inch mixture are illustrated in Figure 23 to Figure 29. Table A.4 to Table A.7 in Appendix A provide complete data on the percentage of bins, aggregate properties, and mixture properties for both mixture types.

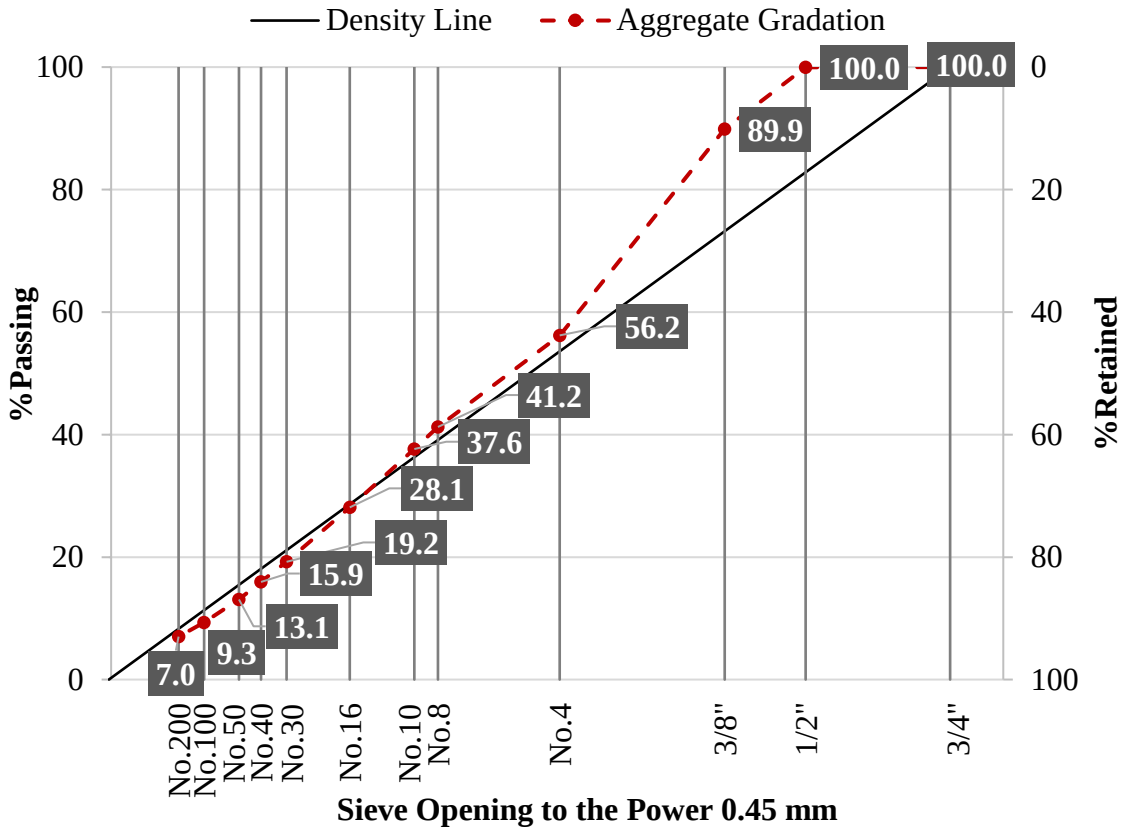

Figure 16. ½-inch NMAS Aggregate Gradation.

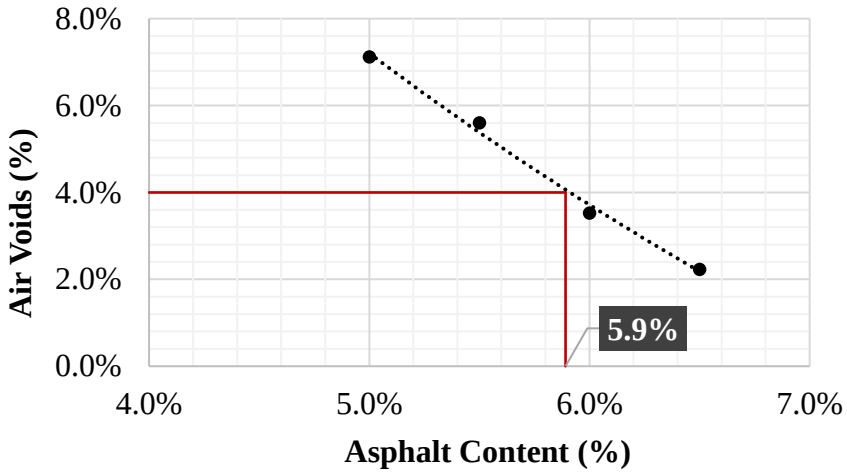

Figure 17. ½-inch NMAS Mix Optimum Binder Content.

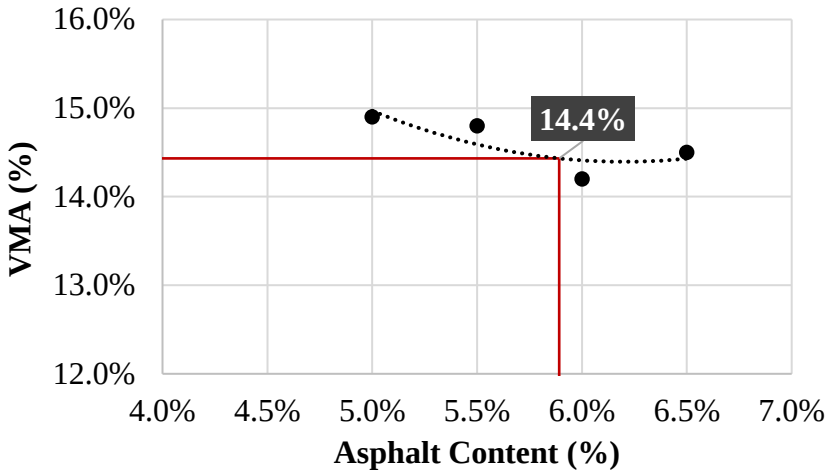

Figure 18. ½-inch NMAS Mix Voids in Mineral Aggregate (VMA).

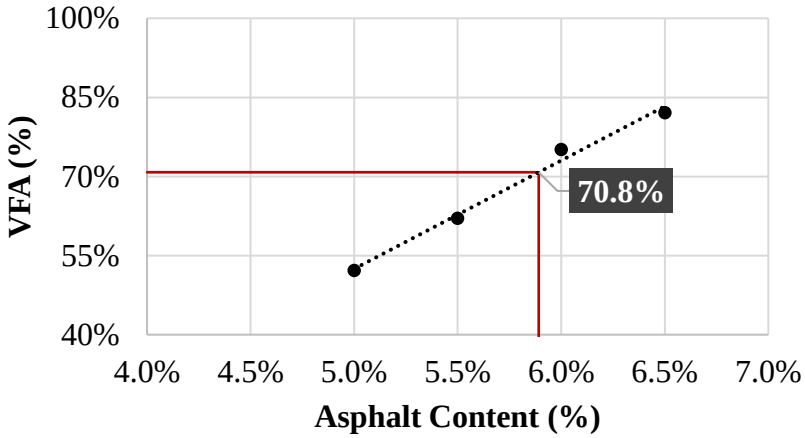

Figure 19. ½-inch NMAS Mix Voids Filled with Asphalt (VFA).

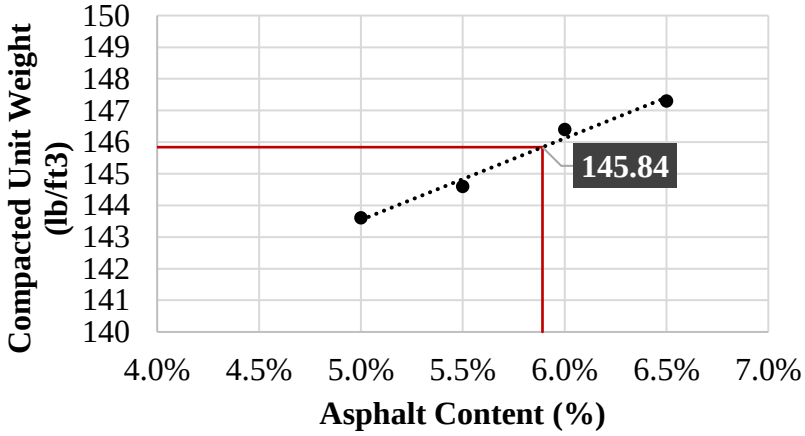

Figure 20. ½-inch NMAS Mix Unit Weight.

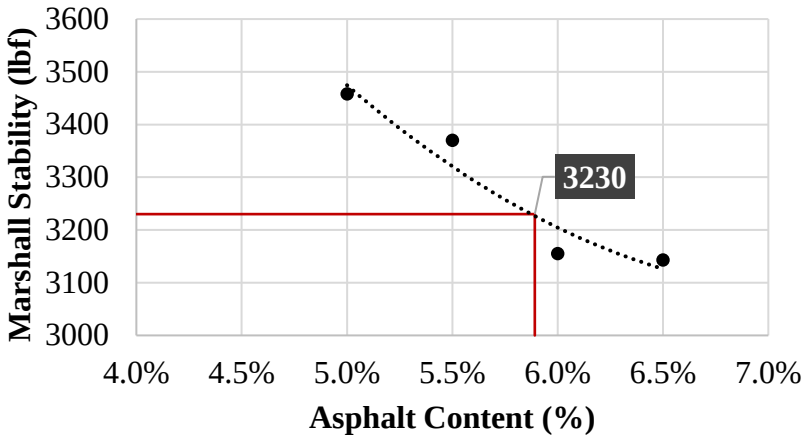

Figure 21. ½-inch NMAS Mix Marshall Stability.

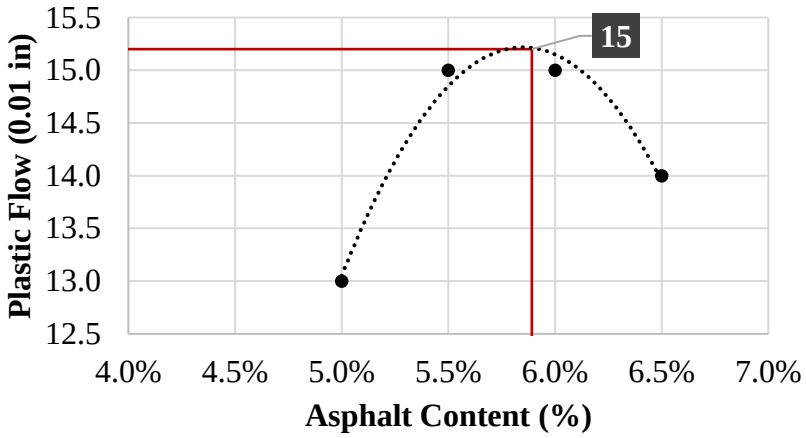

Figure 22. ½-inch NMAS Mix Plastic Flow.

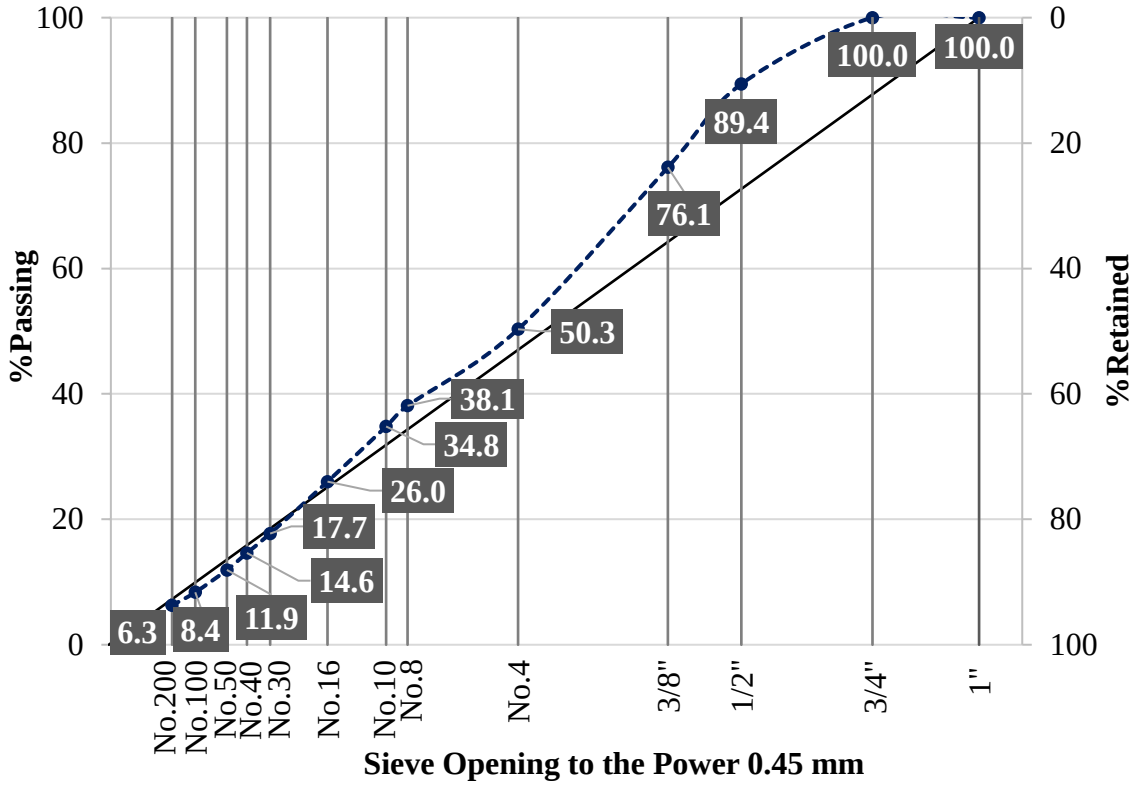

Figure 23. ¾-inch NMAS Aggregate Gradation.

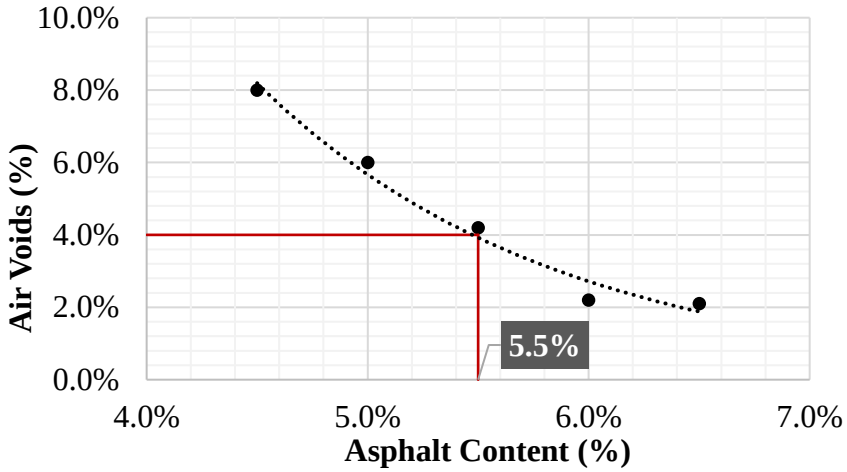

Figure 24. ¾-inch NMAS Mix Optimum Binder Content.

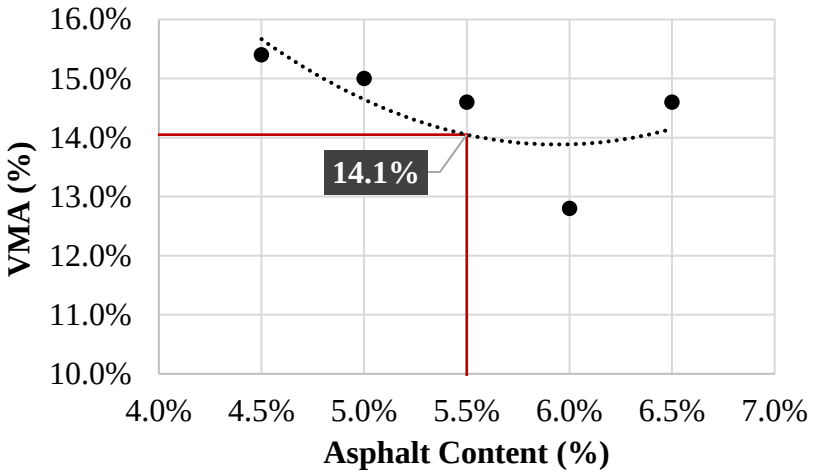

Figure 25. ¾-inch NMAS Mix Voids in Mineral Aggregate (VMA).

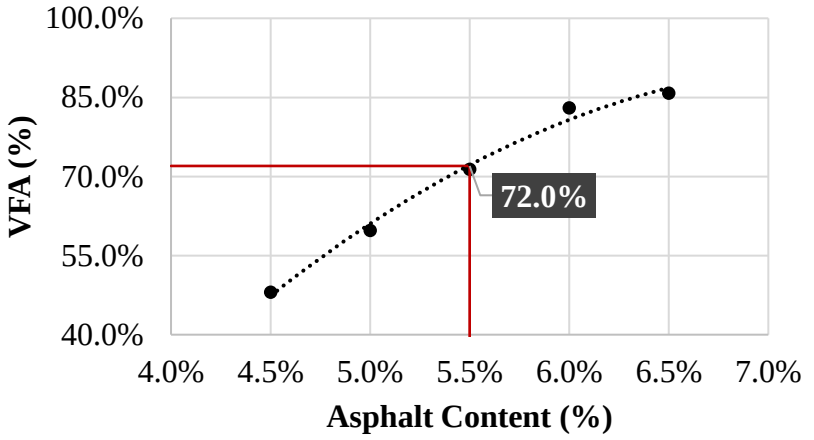

Figure 26. ¾-inch NMAS Mix Voids Filled with Asphalt (VFA).

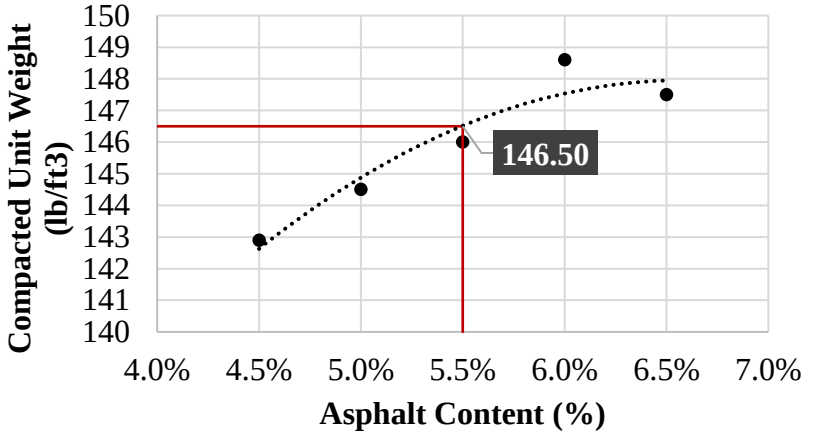

Figure 27. ¾-inch NMAS Mix Unit Weight.

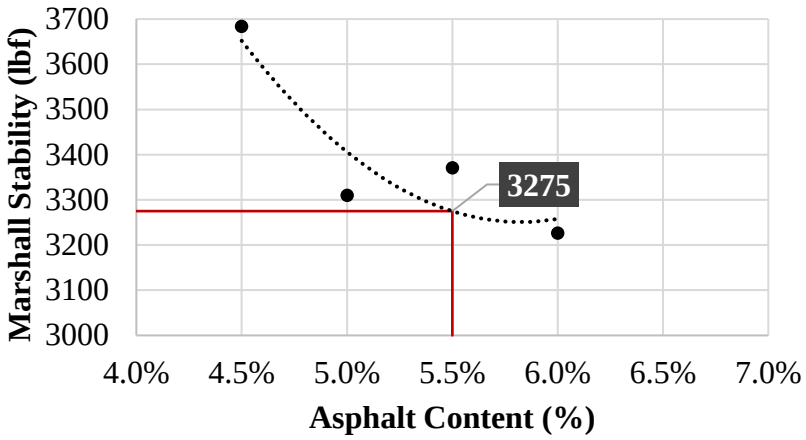

Figure 28. ¾-inch NMAS Mix Marshall Stability.

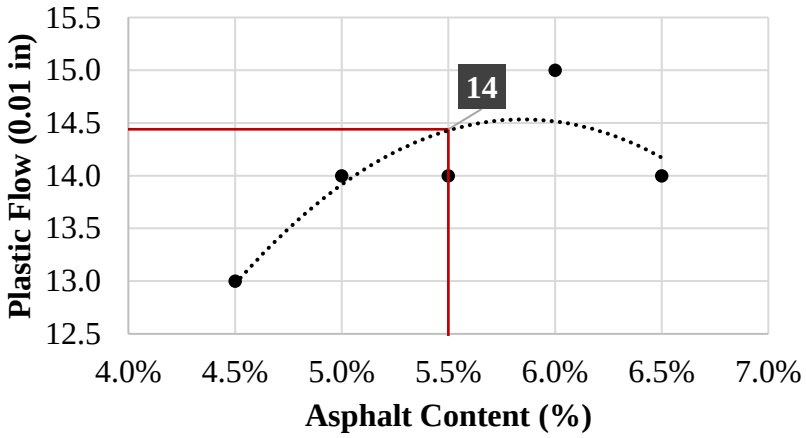

Figure 29. ¾-inch NMAS Mix Plastic Flow.

3.3.5 HMA Overlay Compaction

The asphalt mixtures used in the experiment were transported to UNR in 5-gallon steel pails as per AASHTO R 97 *Standard Practice for Sampling Asphalt Mixtures* [66]. To ensure accurate sampling of the mixture from the truck bed, the top portion was shoveled away to a depth of at least 12 inches, eliminating the possibility of segregated material, which could affect sample accuracy. Next, the material was obtained from at least three distinct locations. It is essential to take a portion of each area and place it in each bucket to ensure a representative sample is acquired.

To guarantee that the asphalt concrete (AC) layer is adequately compacted and adheres to the existing pavement surface, it was crucial to maintain the bottom surface layer at an appropriate temperature. This is why infrared lights were installed around the perimeter of the PaveBox. The lights helped to heat the prepared bottom slab (with tack coat materials applied) and maintain a consistent temperature throughout the paving process.

Controlling the pavement temperature is especially important for asphalt overlay projects. If the temperature is too low, the mix may not adhere properly to the existing pavement surface, resulting in a weak bond. This could lead to cracks and other damage to the pavement in real-world conditions. On the other hand, if the temperature is too high, the mixture becomes tender, which makes it challenging to reach proper density levels.

The asphalt mixture was heated to 293°F (145°C) using a force-draft oven and transported to its final destination, the PaveBox, where it was applied to the PCC surface. Careful planning was necessary to ensure the mixture remained at a high temperature throughout the course. This was essential for its successful application, as a drop in temperature could negatively impact its properties.

Once the mixture had been evenly distributed, the subsequent task involved compacting it using a heavy-duty plate compactor until it reached a height of 2 inches. The desired level of air voids was 7%, as this is the most suitable level for guaranteeing the longevity of the pavement surface. Figure 30 is an overview of the PCC surface ready to receive the tack coat material, a compacted HMA overlay slab, the equipment used for compaction, and the coring machine utilized to extract the ISS samples.

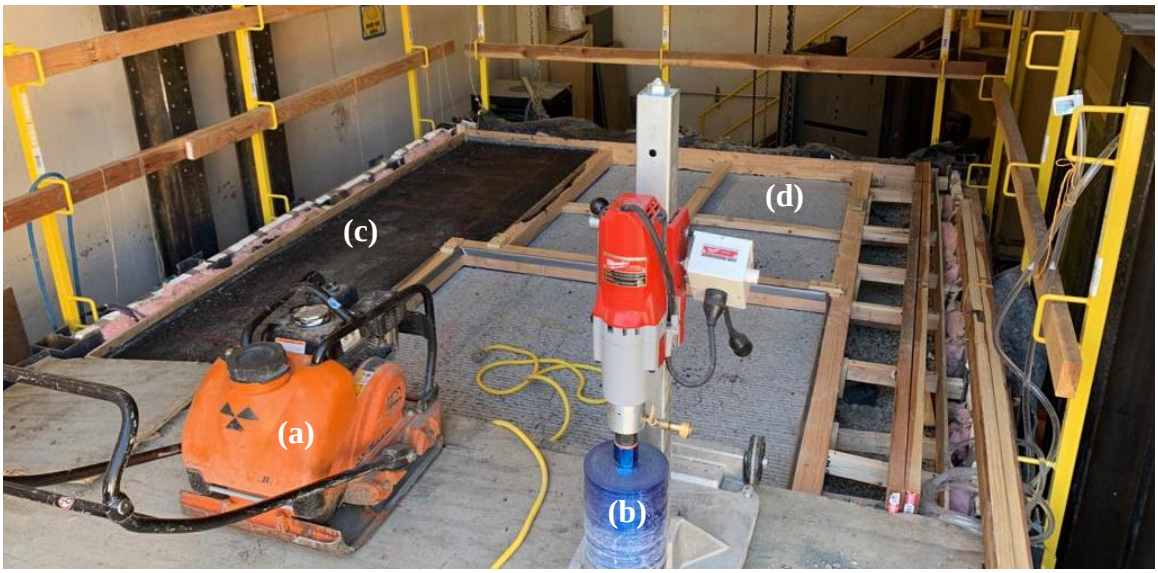

Figure 30. (a) Heavy-Duty Plate Compactor, (b) Coring Machine, (c) Compacted HMA Overlay and (d) PCC Surface.

3.3.6 AASHTO TP 114

A thorough and detailed method was employed to obtain accurate data on the interlayer shear strength of pavement layers bonded with various tack coat materials and application rates. The first step involved using a diamond coring machine, ensuring the specimens collected were uniform and consistent in size.

Before proceeding with the extraction process, the direction of tining on the PCC surface was carefully marked on top of the asphalt concrete layer at each core location. This step was crucial to ensure the correct orientation of the specimen was maintained throughout the ISS testing procedure (Figure 31). The specimens were extracted 3 inches from the edges and 1 inch apart. This decision was made because obtaining the desired density closer to the wood frame edges is more challenging. As such, selecting a location further away from the edges is more likely to produce a representative sample. Additionally, waiting for 24 hours before coring the samples ensured that the asphalt concrete had cooled sufficiently to avoid damaging the core samples during extraction.

Figure 31. ISS Testing Samples Tining Direction.

In order to conduct the ISS testing, a total of 135 specimens were extracted for analysis. These specimens included 90 samples with a ½ inch NMAS mixture and 45 samples with a ¾-inch NMAS mixture. The test to determine interlayer shear or bond strength was conducted following AASHTO TP 114 guidelines. The testing was performed on 6-inch diameter cores at 77ºF (25°C). To ensure that the specimens were at the correct temperature, they were conditioned for at least two hours in a force-draft oven at the test temperature.

To simulate the effect of traffic on the pavement surface, the specimens were loaded in the direction of the tining orientation marked on top of the AC layer (Figure 32). The frame consisted of a loading frame, which could move up and down and apply pressure to the specimens, and a reaction frame, which remained stationary. During testing, a continuous

displacement rate of 0.1 in/min was employed to load the specimens until they failed. The purpose of this procedure was to determine the ultimate load applied to each specimen, which was then used to calculate their ISS using Equation 1.

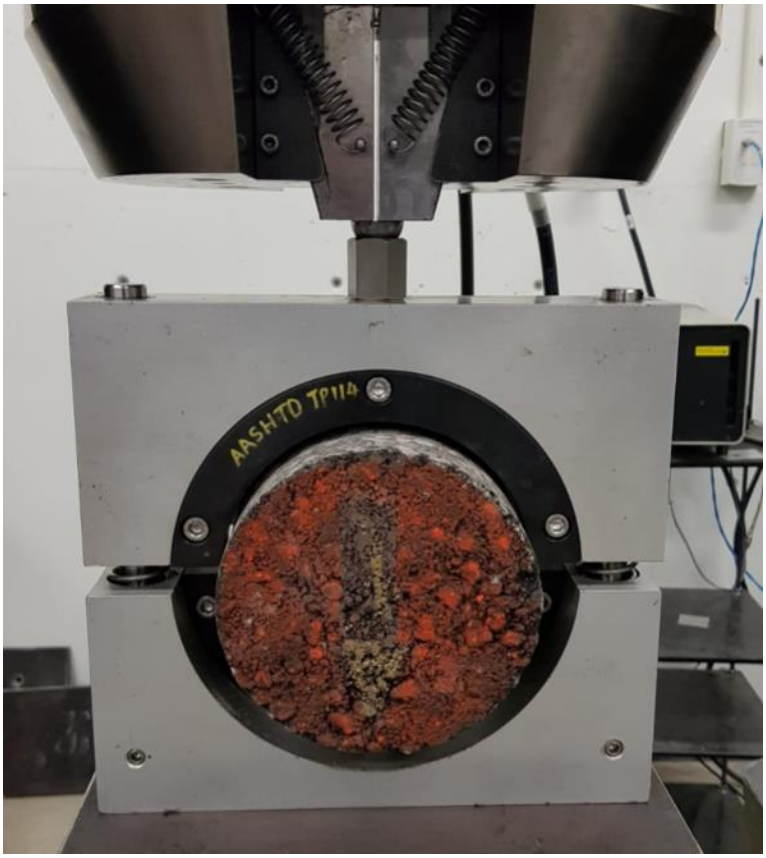

Figure 32. Interlayer Shear Strength Test.

Chapter 4: Results and Evaluation

This chapter presents analysis of critical properties and performance of various tack coat materials and their impact on composite pavement strength and durability.

4.1 Tack Coat Materials Rheological Evaluation

As part of NCHRP Project 09-64 [67], a detailed methodology was employed to select the best method for recovering emulsion residue. The experiment considered three methods: distillation, low-temperature evaporation, and vacuum. As the research showed that the recovery methods used had no significant effect on the rheological properties of the tack coat materials, the distillation method was selected to obtain the residue required for all subsequent rheological tests after considering the advantages and disadvantages discussed in Section 3.1.2.

In NCHRP Project 9-64 [67], several tests were conducted on the tack coats to develop selection criteria for tack coat specification. These tests included obtaining performance grade (PG), penetration, softening point, and aging index (G* measured at 15°C on RTFO−aged residue/G* measured at 15°C on original binder), which were then correlated with ISS to determine the appropriate tack coat specification criteria. The results of these tests are presented in Table A.8 to Table A.15 in Appendix A and were used to perform additional analysis on the stiffness of the materials and better understand the influence of polymer modification on the behavior of the tack coat materials, as follows.

4.1.1 Continuous Performance Grade

Figure 33 illustrates the continuous PGH of all tack coat materials and the binder used in the HMA mixtures. This parameter was obtained from the DSR and indicates the stiffness

of the binder. The higher the grade, the stiffer the binder is. The figure shows that only the slow-setting emulsions, namely SS-1 and SS-1h, are softer than the binder used in the mixture. This is a crucial parameter that will be later associated with ISS results to determine the relationship between the PGH of the binder used in the mixture and the PGH of each tack coat material. This evaluation will be used to assess the bonding performance of the materials.

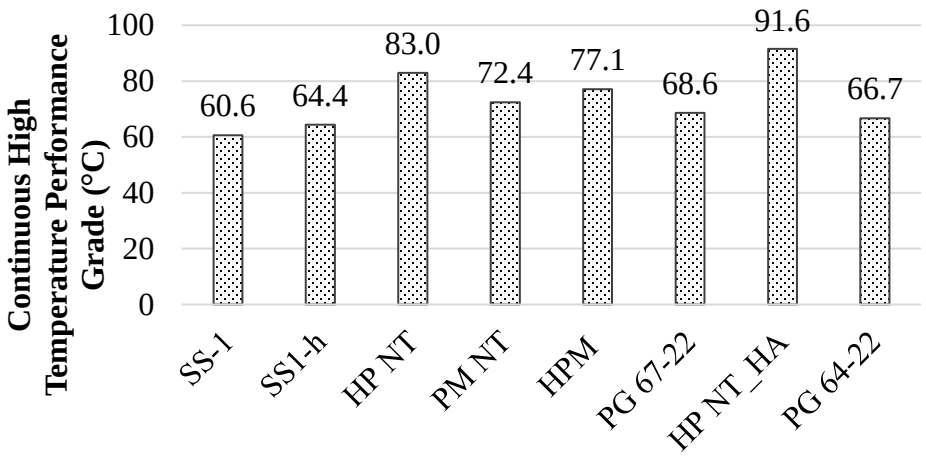

Figure 33. Continuous PGH of all Tack Coat Materials.

Polymer-modified asphalt binders have recently been used as an alternative to increasing resistance to rutting under heavy traffic loads, a crucial performance parameter for asphalt pavements. As shown in Figure 33, the PM NT and HPM emulsions had significant improvement on the PGH, achieving comparable levels to stiffer base binders such as HP NT. The observed improvement can be attributed to the increased viscosity of polymer-modified binders relative to unmodified binders. This enhancement in viscosity leads to greater shear resistance, which ultimately translates into improved high-temperature performance.

Figure 34 demonstrates that polymer addition also enhances the relaxation properties of the binder, thereby improving its ability to cope with the stress and strain caused by low temperatures. The improved relaxation properties of the polymer-modified binders ensure they can withstand the cyclic loading associated with temperature changes, thus reducing the likelihood of cracking. This is an important consideration, as low-temperature cracking is prevalent in many regions and can significantly impact the durability and service life of asphalt pavements.

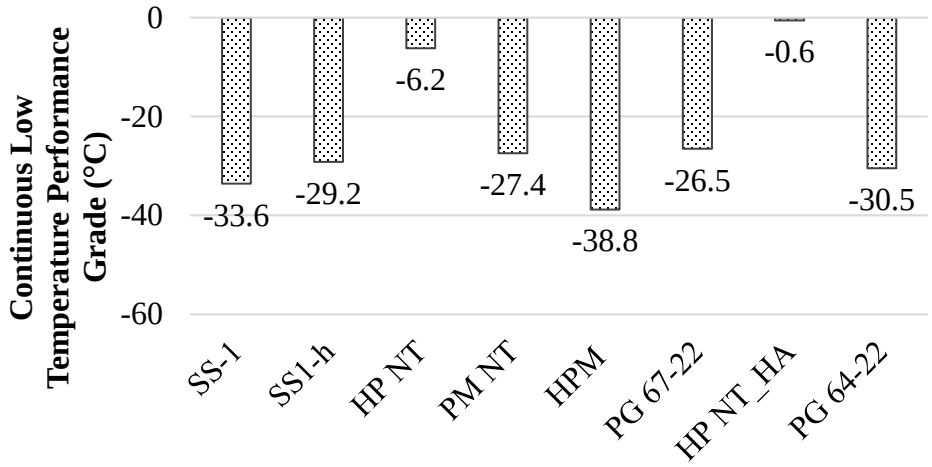

Figure 34. Continuous PGL of all Tack Coat Materials.

4.1.2 Rotational Viscometer

The resistance of a fluid to flow is measured by its viscosity. In the case of asphalt binders, a higher viscosity implies a thicker material with better shear resistance. As shown in Figure 35, the polymer's addition significantly affects the material's viscosity. Specifically, adding a large amount of polymer to the base binder results in a notably high viscosity of 5663 Centipoise (cP). This increase in viscosity may make the material suitable for use in high-temperature or high-traffic areas where durability and stability are essential.

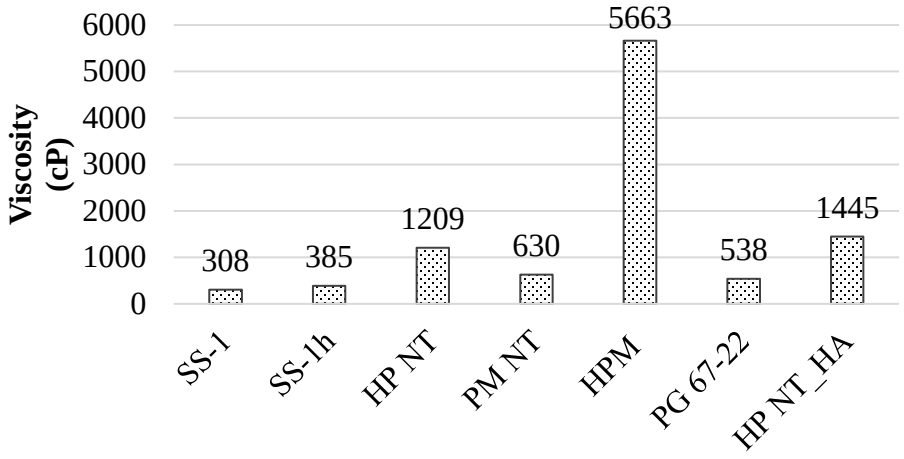

Figure 35. Viscosity vs. Emulsion Type.

4.1.3 Complex Modulus (G) Master Curves*

One of the rheological models recently studied is the Christensen-Anderson (CA). This model was specifically developed to study the behavior of asphalt binders under dynamic shear loading. The complex modulus and phase angle expressions in this model are described by Equations 5 and 6, respectively [59].

$$G^* = G^*_e + \frac{G^*_g - G^*_e}{\left(1+\left(\frac{f}{f_c}\right)^k\right)^{\frac{me}{k}}} \quad (5)$$

$$\delta = \frac{90\ m_e}{1+\left(\frac{f}{f_c}\right)^k} \quad (6)$$

Where:

G^*_g = glassy modulus.

G^*_e = elastic modulus.

f_c = crossover frequency ($\delta = 45°$).

f = reduced angular frequency.

m_e and k = fitting parameters.

The Williams-Landel-Ferry (WLF) shift function (Equation 7) is a widely used mathematical model to describe the temperature dependence of viscoelastic materials. In the context of the present study, the WLF shift function was employed to shift the test data and construct a smooth master curve [59].

$$\log \alpha_t = \frac{-C_1 (T - T_g)}{C_2 (T - T_g)} \quad (7)$$

Where:

C_1, C_2 = fitting coefficients.

T = test temperature, °C.

T_g = glassy transition temperature often taken as the reference temperature, °C.

Figure 36 and Figure 37 display the complex modulus versus the angular frequency obtained from the 4-mm DSR for the SS-1 material and the master curves developed for all tack coat materials at a reference temperature of 25°C, respectively.

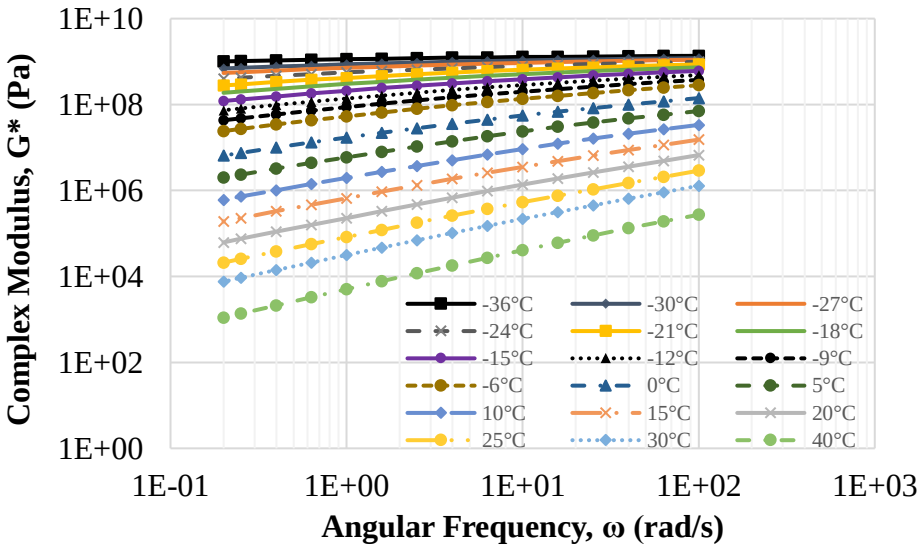

Figure 36. 4-mm DSR Data (SS-1).

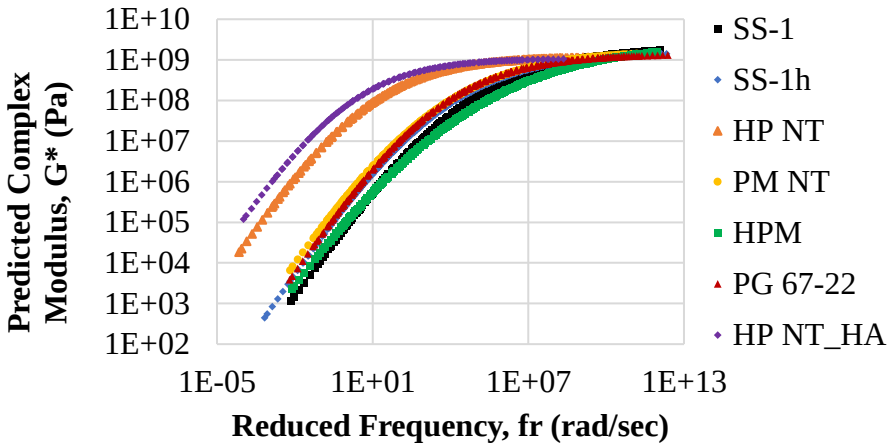

Figure 37. Master Curves at 25°C (Original).

Based on the data presented in Figure 37, it can be observed that stiffer materials exhibit an upward shift in the master curve in comparison to softer materials. It is worth noting that although adding a high percentage of polymer can increase the high-temperature performance grade of the HPM material, some polymers used in asphalt binders may have a higher temperature susceptibility than the base asphalt. This means that at higher temperatures, the polymer becomes softer, which can cause a decrease in the complex modulus of the material—in this case, creating a product comparable with the slow-setting emulsion. Another possible explanation is that the base binder used in the emulsion formulation is excessively soft.

4.1.4 Black Space Diagram

A comparison between laboratory and plant mixtures is shown in Figure 38 through a black space diagram, which provides insights into how the diagram can be interpreted. A low phase angle value on the diagram indicates a more elastic mixture, whereas a high phase angle value indicates a more viscous mixture. Higher values of G* will result in an upwards shift of the curve, indicating a stiffer material [58].

Figure 39 illustrates this phenomenon by displaying a black space diagram for each tack coat material. The diagram clearly shows that the HP NT and HP NT_HA materials have stiffer and more viscous behavior, which is indicative of their ability to resist deformation under load.

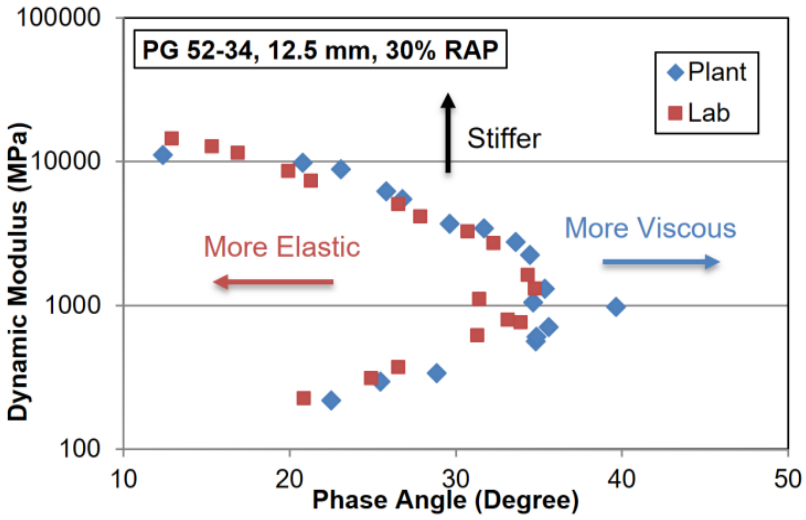

Figure 38. Black Space Diagram of a Laboratory vs. Plant Mixtures [58]**.**

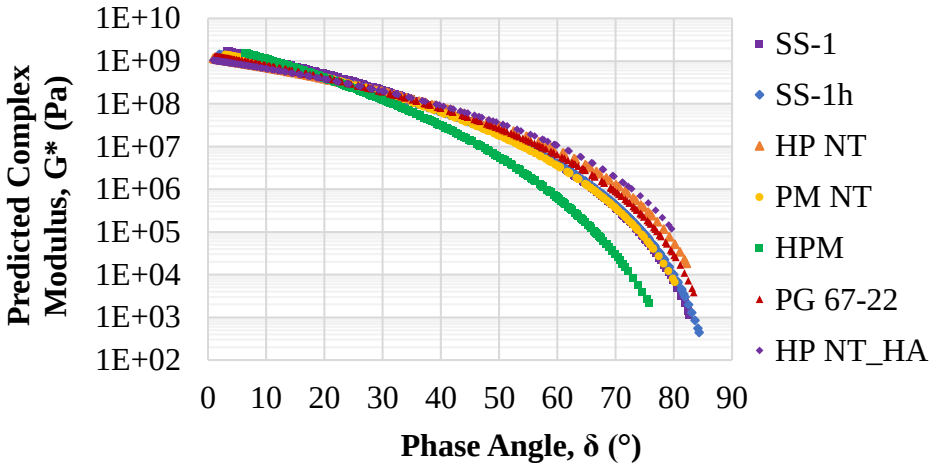

Figure 39. Black Space Diagram (Original).

4.1.5 Non-Recoverable Creep Compliance

A higher Jnr value of an asphalt binder indicates the material is more prone to deformation and less able to recover its shape over time. This could result in a weaker interlayer bond between pavement layers, as it may contribute to ineffective load transferring—leading to potential pavement failure. This behavior can be easily identified for the softer emulsions (SS-1 and SS-1h) in Figure 40. On the other hand, stiffer materials or the emulsions modified with polymer present lower Jnr values, indicating better recovery properties.

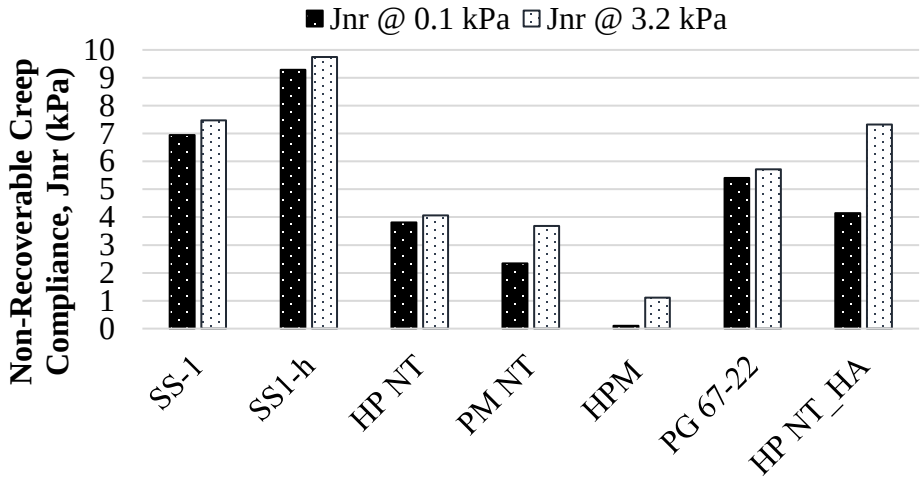

Figure 40. Non-Recoverable Creep Compliance for all Tack Coat Materials at PGH.

4.2 Interlayer Shear Strength Test Results

The findings of the ISS results are presented in Figure 41 to Figure 43, where the ISS values for each tested specimen are plotted on the primary vertical axis, and the corresponding percent air voids (%AV) of the AC layer measurements are illustrated on the secondary vertical axis. A clear correlation between the ISS and %AV can be observed, with the ISS displaying a consistent increase as the %AV decreases, regardless of the PCC surface type

or the tack coat material utilized. Appendix A summarizes the raw ISS data through Table A.16 to Table A.18.

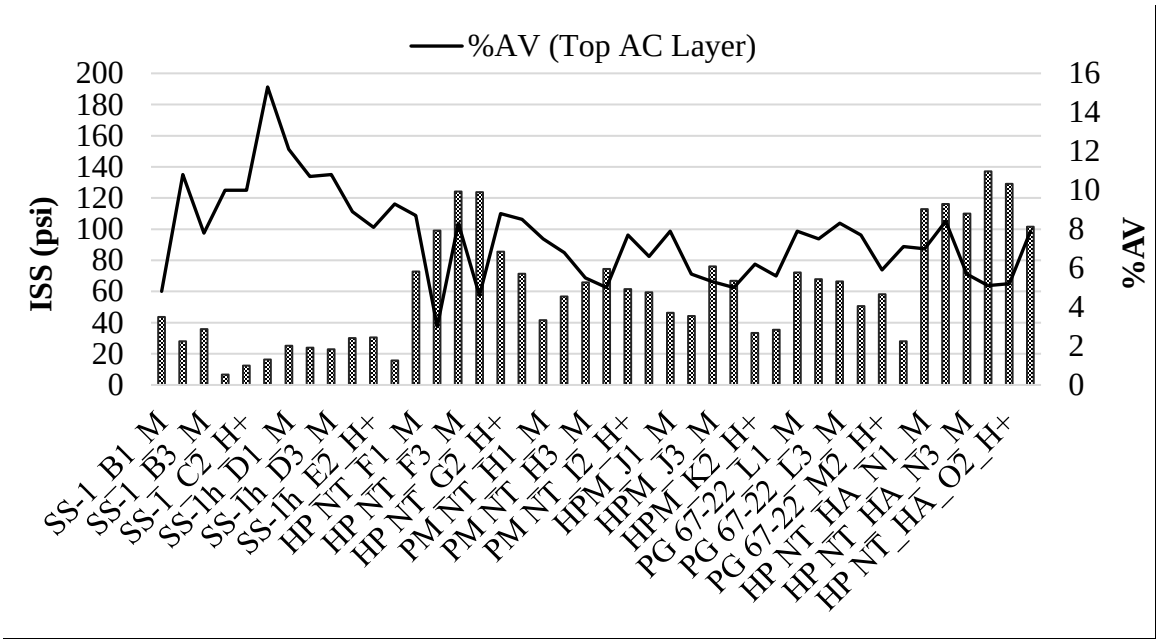

Figure 41. ISS Test Results of New AC (½ inch NMAS)/New PCC Samples using Different Tack Coat Types at Medium and High Application Rate.

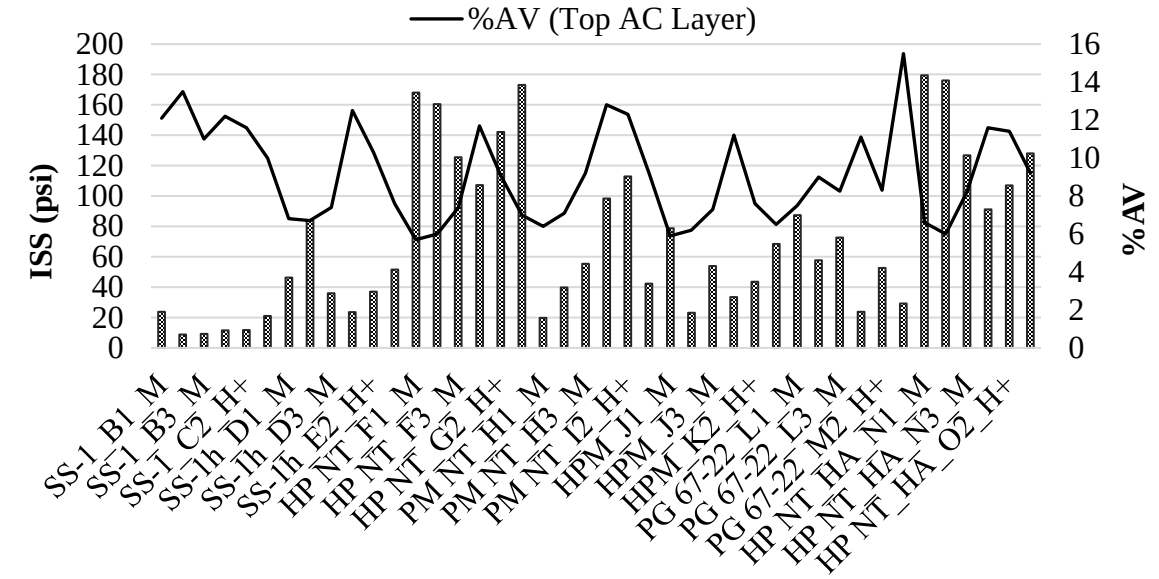

Figure 42. ISS Test Results of New AC (¾ inch NMAS)/Aged PCC Samples using Different Tack Coat Types at Medium and High Application Rate.

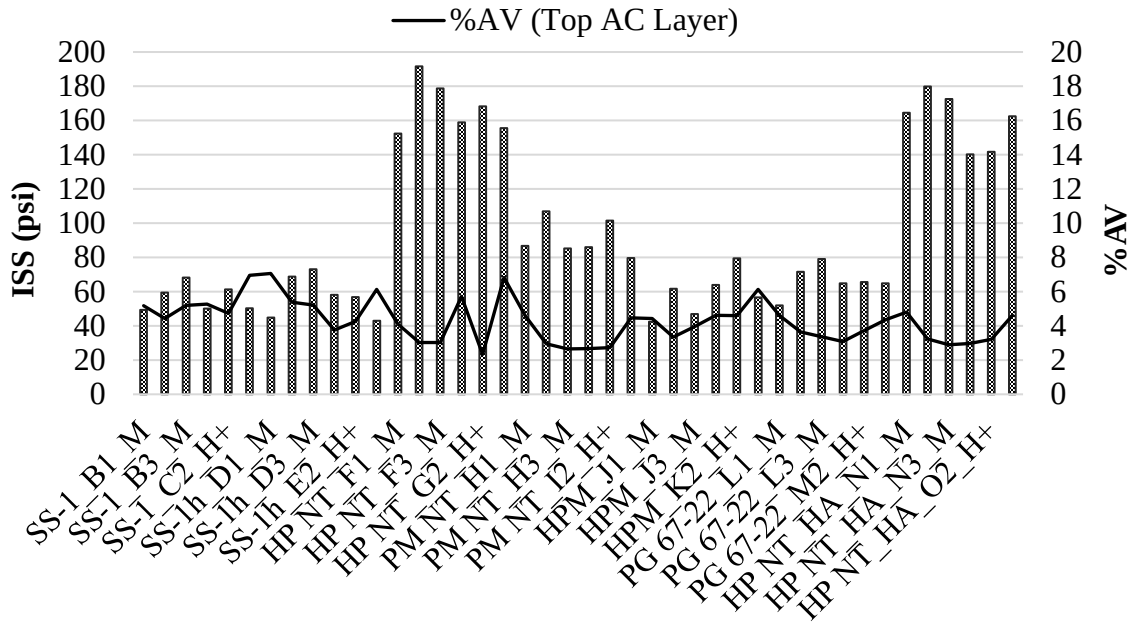

Figure 43. ISS Test Results of New AC (½ inch NMAS)/Aged PCC Samples using Different Tack Coat Types at Medium and High Application Rate.

Because during the coring process, the samples with no tack coat applied experienced instant debonding for all pavement configurations, it can be inferred that tack coat materials play a critical role in enhancing the interface shear strength. Regardless of the surface condition of the PCC slabs, it was observed that all specimens exhibited the same trend, with the samples treated with Hard-Pen Non-Tracking Hot-Applied (HP NT_HA) and Hard-Pen Non-Tracking (HP NT) materials exhibiting higher ISS values. The primary reason behind this phenomenon is that these materials comprise a harder base binder than the one used in the asphalt concrete mixture, contributing to their superior performance. In contrast, the emulsions containing a softer base binder (such as SS-1 and SS-1h) were expected to present lower ISS values.

Additionally, since the majority of the ¾ inch NMAS/Aged PCC slab specimens had higher air voids than the desired 7% target, a more efficient compactor was used to continue the

experiment, which led to a maximum %AV of 7.1% for the New AC (½ inch NMAS)/Aged PCC slab, thereby affecting the magnitude of the ISS values.

4.2.1 ISS Failure Type

When evaluating the performance of tack coat materials, it is crucial to consider the shape and location of the shear failure surface. Two types of failure were observed after the ISS testing in the NCHRP Project 09-64 [67]. As shown in Figure 44a, adhesive failure occurs at the interface between the HMA and the PCC layers, right at the surface at which the tack coat is applied. This can happen due to insufficient tack coat coverage or poor adhesion properties of the tack coat. In contrast, Figure 44b shows an example of cohesive failure within the asphalt mix itself. This type of failure can happen when a strong bond is created between the asphalt mix and the underlying layer, causing tensile stress within the asphalt mix during loading. If the internal strength of the asphalt mix is insufficient to withstand the tensile stresses, it can lead to cohesive failure, resulting in cracking or complete breakage.

The failure pattern observed for each tack coat material is summarized in Table 5. It is worth noting that the type of failure can also be affected by the surface condition, whether a new or aged PCC. A smoother and less damaged new PCC surface may result in a stronger bond between both layers. Therefore, it is crucial to consider the surface condition when selecting and evaluating tack coat materials to ensure optimal performance and longevity of the pavement.

Table 5. Summary of the Type of Failure for Each Tack Coat Material.

Tack Coat Material	PGH	ΔPGH[1]	Failure Type (New PCC)	Failure Type (Aged PCC)
SS-1	60.6	-6.1	Adhesive	Adhesive
SS-1h	64.4	-2.3	Adhesive	Adhesive
HP NT	83.0	16.3	Cohesive	Cohesive
PM NT	72.4	5.7	Cohesive	Adhesive
HPM	77.1	10.4	Cohesive	Adhesive
PG 67-22	68.6	1.85	Cohesive	Cohesive
HP NT_HA	91.6	24.9	Cohesive	Cohesive

[1] ΔPGH = Tack Coat PGH – Binder used in the AC Mixture PGH.

(a) (b)

Figure 44. (a) New AC (½ inch NMAS)/Aged PCC Adhesive Failure (SS-1); (b) New AC (½ inch NMAS)/Aged PCC Cohesive Failure (HP NT).

4.2.2 Statistical Analysis

Statistical analysis was performed using a general linear model (GLM) to investigate the correlation between the ISS and different types of tack coats. The GLM is a widely used statistical modeling method that establishes a connection between a dependent variable (ISS) and one or more independent variables, including tack coat types.

The results of the statistical analysis are presented in Table A.19 to Table A.21, which can be found in Appendix A. The analysis indicates that the type of tack coat utilized substantially influences the values of ISS, as indicated by a p-value of less than 0.05. On the other hand, the tack coat's application rate does not significantly impact ISS values, as indicated by a p-value greater than 0.05. These findings suggest that selecting an appropriate tack coat type is crucial for achieving the desired level of interlayer shear strength in the pavement structure. At the same time, the application rate may be less critical in this regard.

Based on the findings above, a new analysis was conducted by removing the application rate factor from the model. This modified GLM was then used to predict the ISS values at 7% air voids for all tack coat materials. This air void percentage was chosen as asphalt pavements are typically constructed at this void level. The predicted ISS values for each pavement configuration are presented in Figure 45 to Figure 47, with the error bars representing the 95% confidence interval (CI) around the predicted values. These figures provide a visual representation of the predicted ISS values for each tack coat material, aiding in identifying the most effective material for achieving the desired level of interlayer shear strength.

Once the ISS values for all pavement configurations at the same air void levels have been determined, they can be compared directly. It was expected that the new PCC surface, which had been ground to enhance its texture, would have higher ISS values than an aged surface. However, the results showed the opposite. This could be attributed to the fact that the AC layer was compacted with higher effort on top of the aged PCC layer, resulting in

lower air void levels. Thus, it highlights the importance of the construction technique in determining ISS values.

According to Figure 46 and Figure 47, selecting a different NMAS for the AC mixture did not have a notable impact on the ISS values. This implies that the NMAS of the AC mixture has minimal influence on ISS, and other factors, such as the type and properties of the binder and the compaction process, are likely to have a more significant impact on determining the pavement's bond strength.

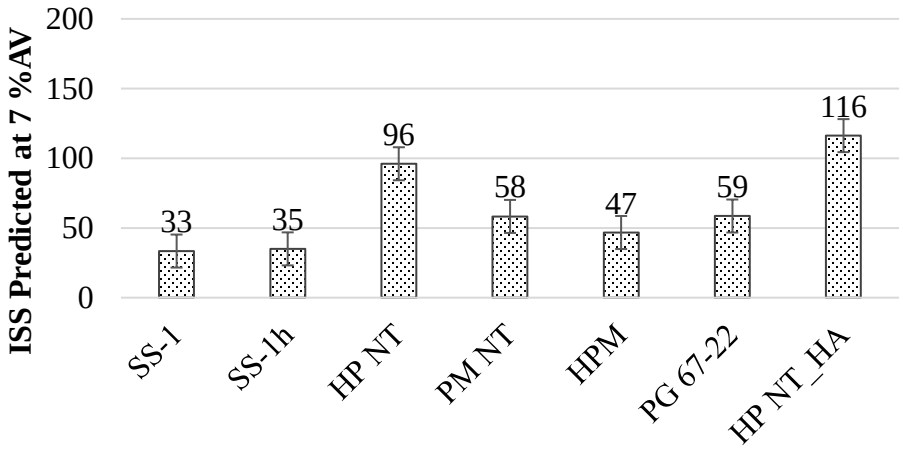

Figure 45. ISS Prediction at 7% Air Voids for New AC (½ inch NMAS)/New PCC.

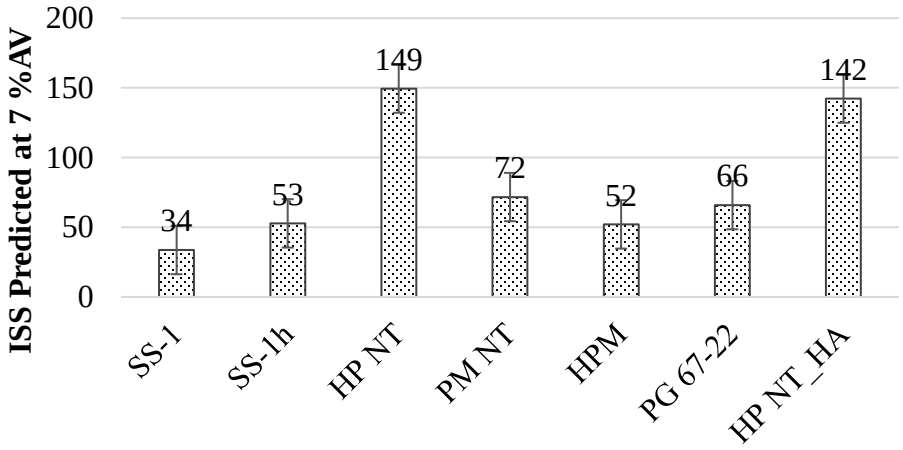

Figure 46. ISS Prediction at 7% Air Voids for New AC (¾ inch NMAS)/Aged PCC.

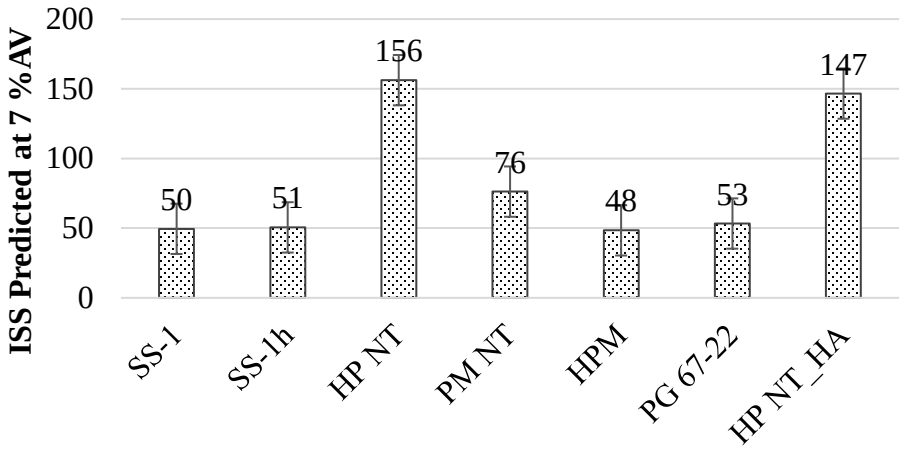

Figure 47. ISS Prediction at 7% Air Voids for New AC (½ inch NMAS)/Aged PCC.

The Turkey and Bonferroni comparison methods, commonly used in statistical analysis to compare multiple groups and identify significant differences between group means, were utilized to distinguish any discrepancies among the various tack coat groups. The outcomes of this analysis are available in Appendix A. Table A.22 and Table A.23 indicate that the average ISS can be categorized into two groups: A and B. Group A comprises HP NT_HA and HP NT, whereas the remaining coat types are in Group B. The ISS means for coat types in the same group are not significantly different. However, the ISS means for coat types in different groups are statistically different. In Table A.24, a new group C has been introduced for specific tack coats, indicating that an increased compaction effort has had an impact on the performance of the tack coat materials.

Furthermore, aside from contrasting the tack coat groups, the predicted Interlayer Shear Strength values will also be evaluated against the rheological properties mentioned in Section 4.1 to gain a deeper understanding of the factors influencing the ISS of pavement layers and how the choice of tack coat can impact these factors.

4.3 ISS versus Rheological Properties of Tack Coat Materials

The ISS results predicted at 7% air voids were used to examine the influence of the rheological properties of tack coats on the interlayer bonding performance within pavement layers.

4.3.1 Penetration Test

Figure 48 to Figure 50 show data that suggests that when a stiffer tack coat material is used (with lower penetration values), the resulting interlayer shear strength is higher. The trend exhibited by the graphs provides evidence that the choice of tack coat material can significantly impact the structural integrity of a pavement system, regardless of the surface type.

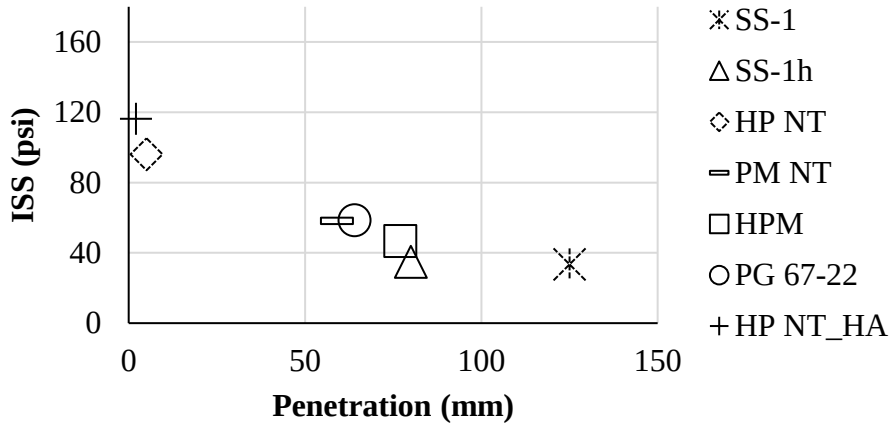

Figure 48. Predicted ISS vs. Penetration for New AC (½ inch NMAS)/New PCC.

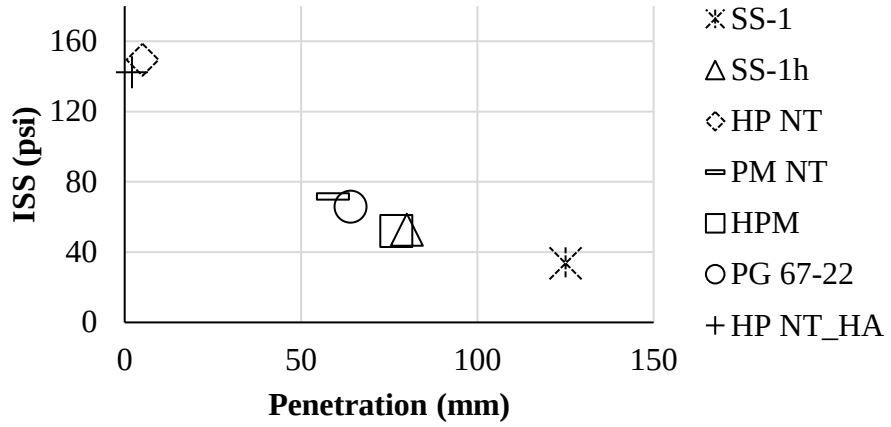

Figure 49. Predicted ISS vs. Penetration for New AC (¾ inch NMAS)/Aged PCC.

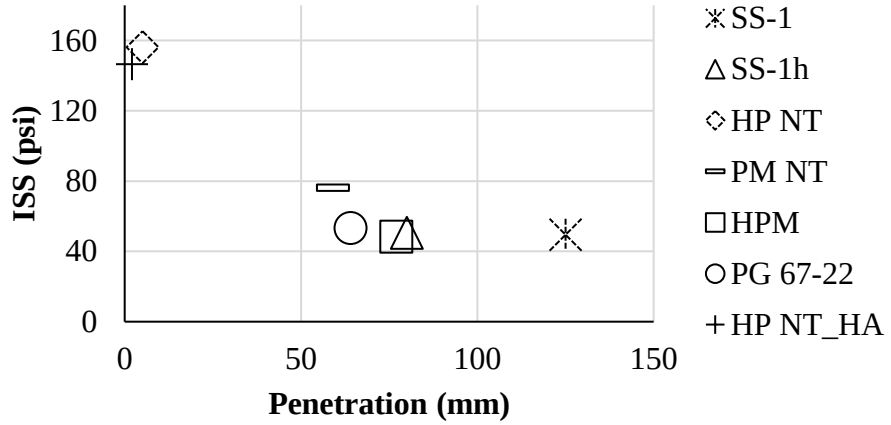

Figure 50. Predicted ISS vs. Penetration for New AC (½ inch NMAS)/Aged PCC.

4.3.2 Softening Point

A tack coat material with a high softening point can better withstand high temperatures, preventing softening or deformation and promoting a stronger bond between pavement layers. Figure 51 to Figure 53 illustrate that ISS values increase when the softening point of the tack coat also increases. This correlation suggests that a tack coat material with a high softening point can produce a more durable pavement system.

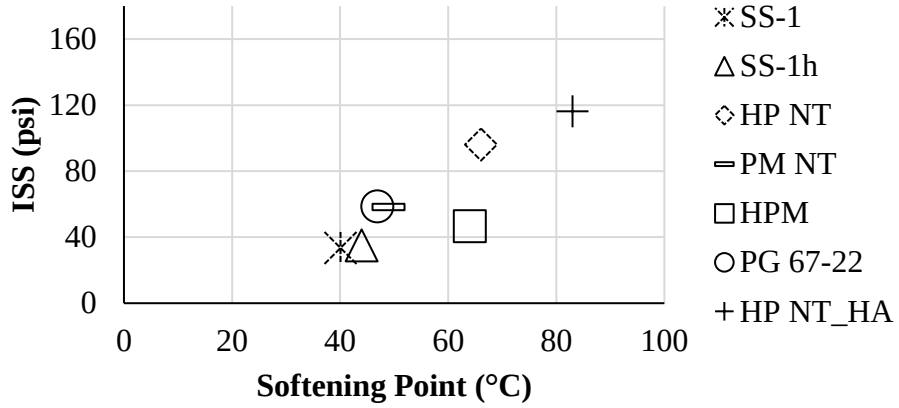

Figure 51. Predicted ISS vs. Softening Point for New AC (½ inch NMAS)/New PCC.

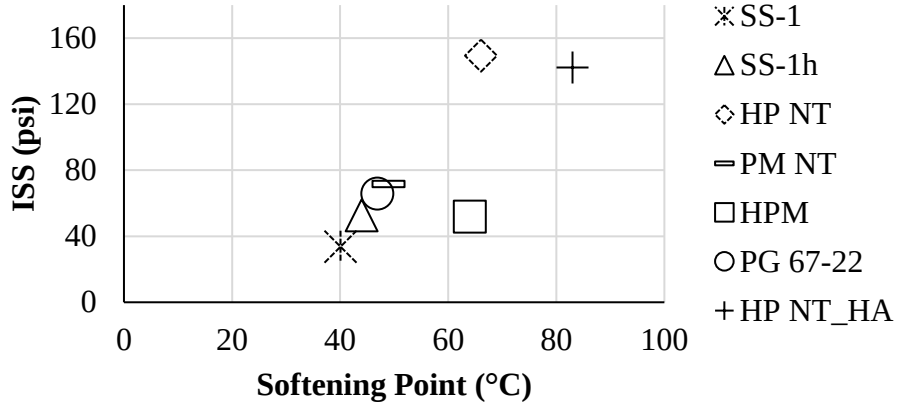

Figure 52. Predicted ISS vs. Softening Point for New AC (¾ inch NMAS)/Aged PCC.

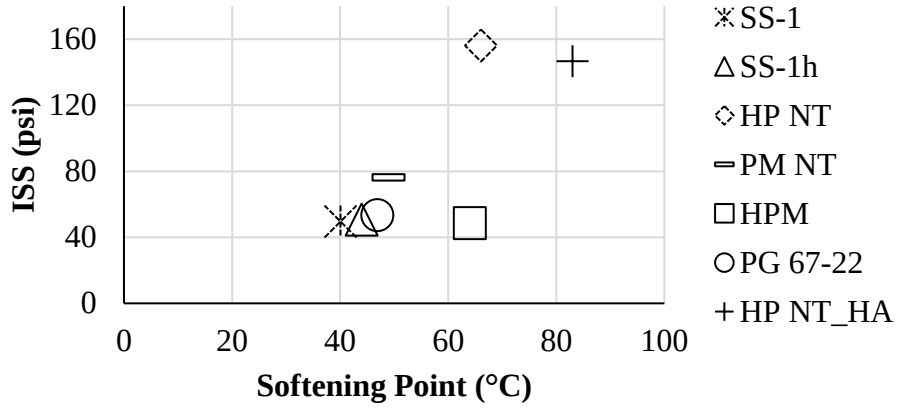

Figure 53. Predicted ISS vs. Softening Point for New AC (½ inch NMAS)/Aged PCC.

4.3.3 Viscosity

Figure 54 to Figure 56 present the relationships between ISS and viscosity for various tack coat materials. These figures suggest a direct correlation between the viscosity of the emulsion and the ISS values. The higher the viscosity of the emulsion, the higher the ISS value. However, there is one particular sample that deviates from this trend. The high polymer-modified emulsion has the highest viscosity among all samples but exhibits lower ISS values than expected. The data demonstrates that a higher percentage of polymer in the emulsion leads to forming a softer material. Consequently, this results in a weaker bond being created. Viscosity alone may not be enough to assess tack coat bonding performance, as demonstrated by the failure to detect the HPM behavior. So, other parameters, such as PGH, should also be considered.

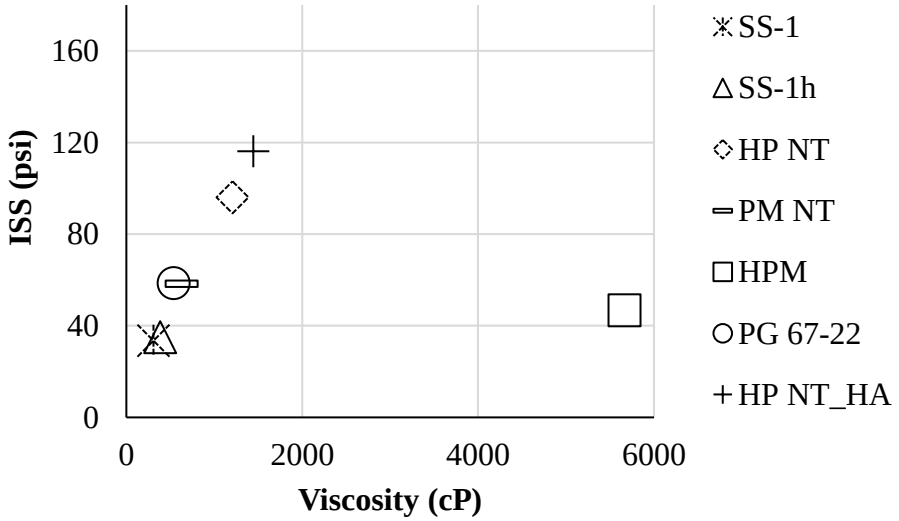

Figure 54. Predicted ISS vs. Viscosity for New AC (½ inch NMAS)/New PCC.

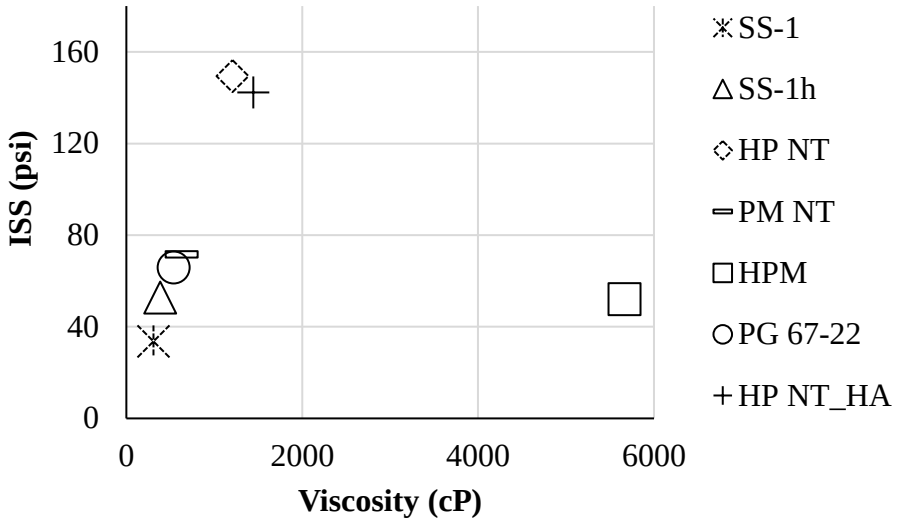

Figure 55. Predicted ISS vs. Viscosity for New AC (¾ inch NMAS)/Aged PCC.

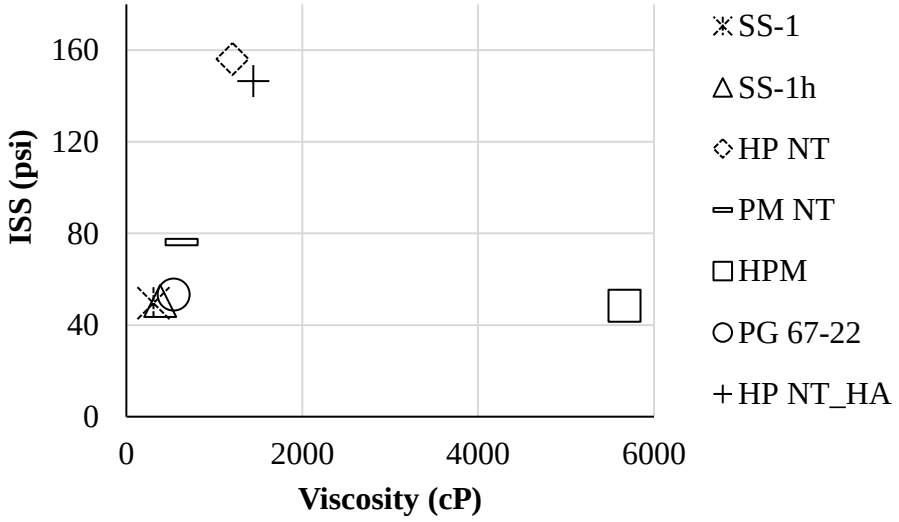

Figure 56. Predicted ISS vs. Viscosity for New AC (½ inch NMAS)/Aged PCC.

Additionally, since the penetration and interlayer shear strength tests were performed at 25°C, a stronger correlation between them seems to exist. In contrast, viscosity and softening point testing were carried out at greater temperatures, which could have caused the data from these tests to have slightly higher variability when correlated to ISS values.

4.3.4 High-Temperature Performance Grade (PGH)

The tack coat material must withstand the same environmental conditions as the binder in the asphalt concrete mixture since the binder's grading is selected based on the project's location environment. Figure 57 to Figure 59 provide evidence of a strong relationship between the tack coat PGH and the ISS results. Specifically, a higher tack coat PGH lead to a higher ISS. Figure 57 demonstrates that materials with a lower PGH than the PGH of the binder in the AC mixture ($\Delta PGH < 0$) perform poorly, with ISS values below 40 psi. The remaining materials exhibit ISS values greater than 40 psi, indicating acceptable performance. This finding aligns with the NCHRP Project 09-40, which reveals that the minimum acceptable laboratory-measured ISS is 40 psi when tested at 25°C using the Louisiana Interlayer Shear Strength Tester (LISST) device.

The same behavior is observed in the aged PCC configurations, considering the 95% CI. The CI represents the range in which the estimated parameter (ISS) value is expected to lie, with a high degree of probability. The data shows that the lower end of the interval is also below 40 psi for both the SS-1 and SS-1h materials. It supports the idea that a satisfactory tack coat performance relies on the PGH being equal to or higher than the PGH of the binder used in the asphalt concrete mixture used as an overlay. Thus, a higher PGH indicates superior adhesive properties of the material, which leads to a stronger bond between the pavement layers.

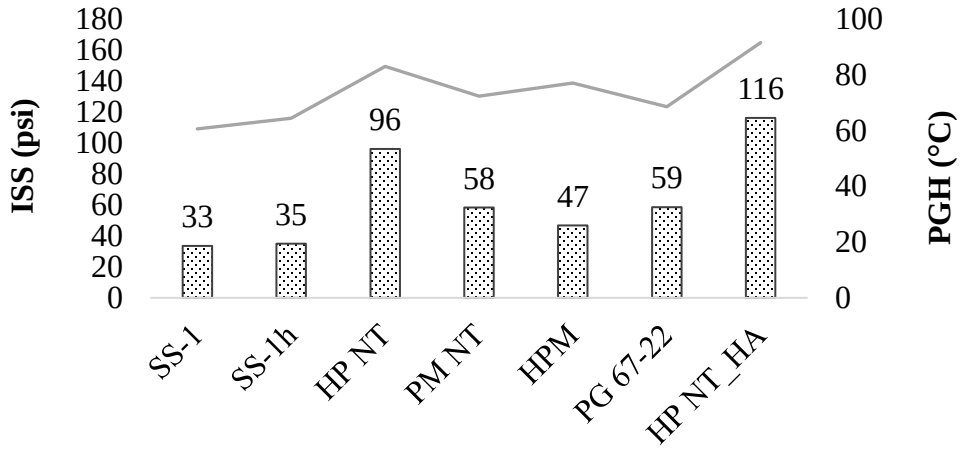

Figure 57. ISS vs. Tack Coat PGH for New AC (½ inch NMAS)/New PCC.

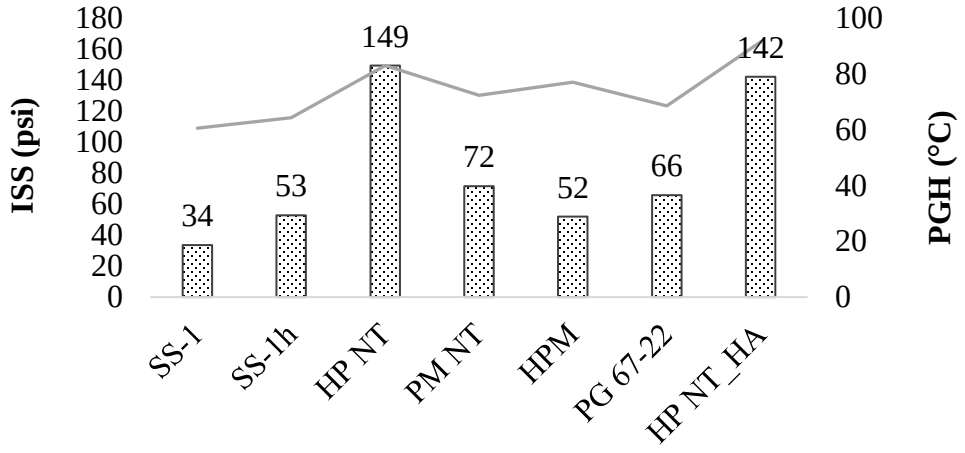

Figure 58. ISS vs. Tack Coat PGH for New AC (¾ inch NMAS)/Aged PCC.

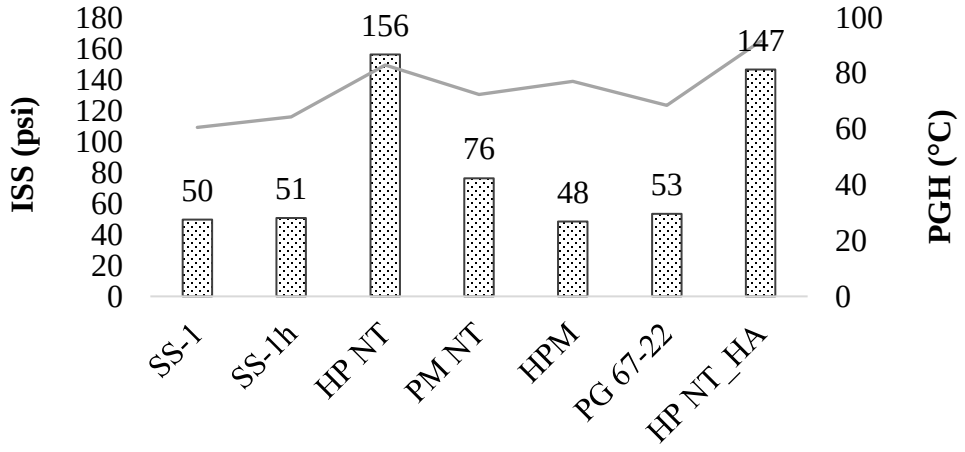

Figure 59. ISS vs. Tack Coat PGH for New AC (½ inch NMAS)/Aged PCC.

In order to evaluate the bonding effectiveness of tack coat materials, a normalization technique was employed using Equation 8. This technique helps eliminate any biases that may arise due to discrepancies in the original data, potentially affecting the overall assessment of the bonding effectiveness.

$$\frac{\text{ISS - Min. ISS}}{\text{ISS (No Tack) - Min. ISS}} \tag{8}$$

Where:

ISS = predicted ISS value at 7% air voids for each tack coat material.

Min. ISS = minimum ISS that provides acceptable performance, 40 psi [14].

ISS (No Tack) = laboratory-measured ISS value for new AC/new AC obtained from NCHP Project 09-64.

The normalization process results can be observed in Figure 60 to Figure 62. It is worth noting that regardless of surface type, all pavement configurations tested exhibited similar data trends. This suggests that the tack coat properties significantly impact the ISS outcomes. During the NCHRP Project 09-64, the ISS measurements were obtained for the new AC samples compacted on top of the new AC. The ISS values were 110.9 psi and 76.7 psi for the ½-inch NMAS mix and ¾-inch NMAS mix, respectively. These values were plugged in on the ratio with their corresponding NMAS used in this study. The lower ISS values observed for the ¾-inch mix might be due to the lower amount of optimum asphalt binder.

If the ratio calculated from Equation 8 is negative it suggests that the anticipated ISS value will fall below the suggested 40 psi, which has been set by NCHRP Project 09-40. This further indicates that the chosen tack coat material did not perform satisfactorily.

The ISS exceeds the recommended minimum value if the ratio falls between 0 and 1. However, the bonding strength contribution of the sample prepared with a particular tack coat is lower than that of the New AC/New AC samples without any tack coat. Conversely, if the ratio exceeds one, it suggests that the tack coat material improves the bonding strength and surpasses the ISS of the New AC/New AC samples prepared without a tack coat.

Softer materials, specifically SS-1 and SS-1h, can be observed to be located either in the negative quadrant or close to the origin. On the other hand, stiffer materials like HP NT and HP NT_HA demonstrate a ratio of 1.5, depending on the surface type. This proves that the PGH parameter is a reliable and straightforward means of evaluating bonding properties.

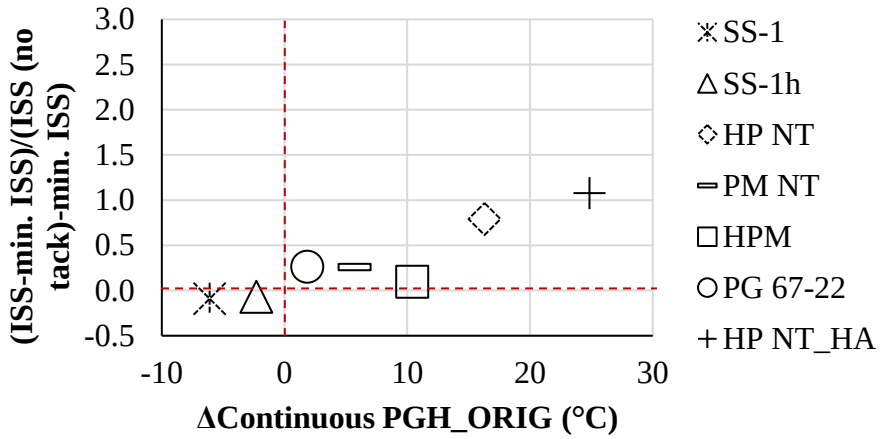

Figure 60. ISS Normalization for New AC (½ inch NMAS)/New PCC.

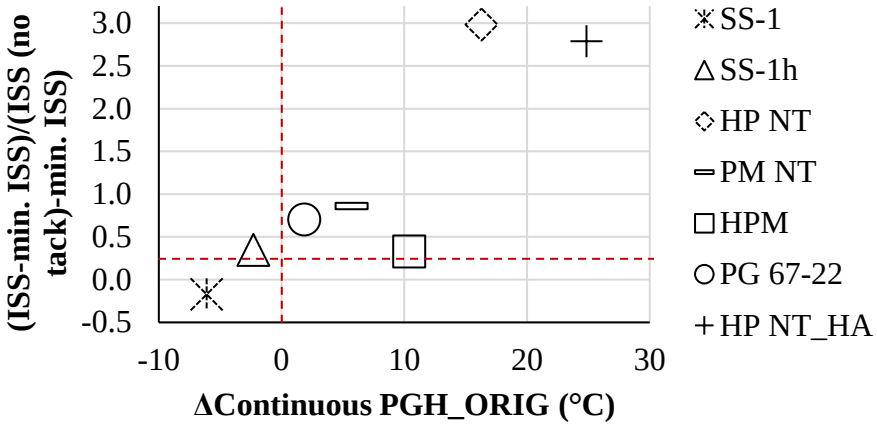

Figure 61. ISS Normalization for New AC (¾ inch NMAS)/Aged PCC.

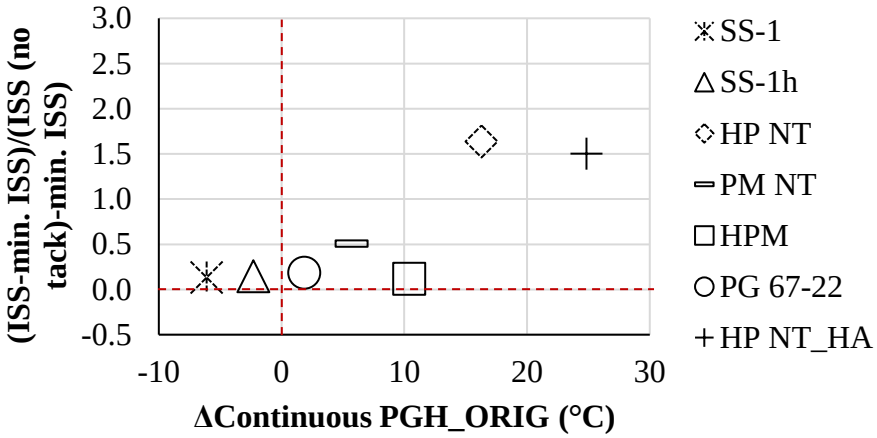

Figure 62. ISS Normalization for New AC (½ inch NMAS)/Aged PCC.

4.4 Interface Surface Textures

Ames Engineering developed the Laser Texture Scanner (LTS), a compact and portable device that can assess the texture of pavement surfaces by scanning their coordinates. The LTS utilizes a laser sensor that scans parallel straight lines with a sampling rate of approximately 0.015 mm per point. Its maximum scan length and width are 104.14 (4.1 in) mm and 76.20 mm (3.0 in), respectively, which allows for a maximum of 1200 line scans with a spacing of 0.064 mm between lines. The device (Figure 63) is positioned on the

surface using three-point contact legs, and it has a feature that enables control of the laser spot intensity [68].

Figure 63. Laser Texture Scanner.

Figure 65 displays a representation of the scanned 3D coordinates of both new and aged PCC surfaces. It should be emphasized that the tests were conducted in the direction of traffic, meaning that the captured data reflects the conditions that a vehicle-mounted laser device would experience on-site. Figure 65 displays an intensity image that captures the texture details of both surfaces. This image is designed to showcase the surface texture with high accuracy and detail.

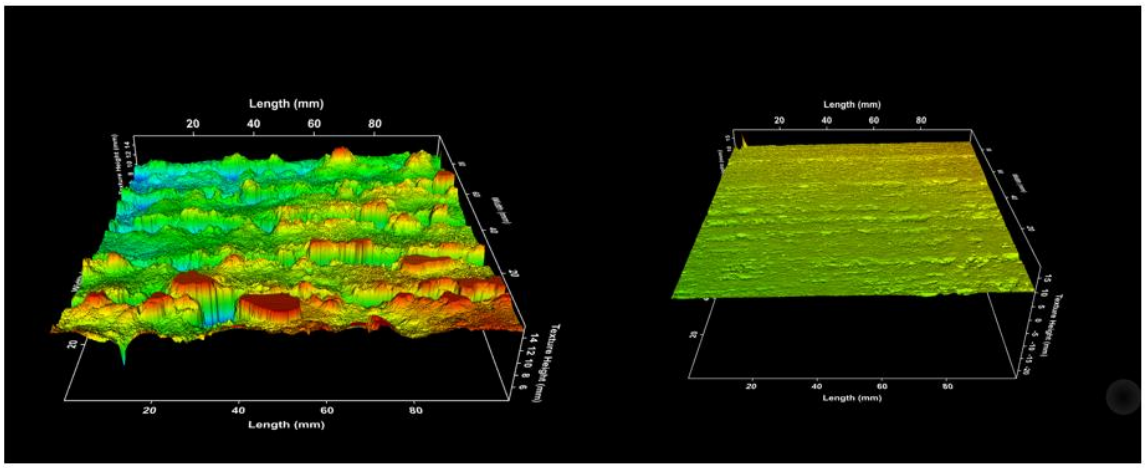

(a) (b)

Figure 64. (a) 3D Coordinates of Scanned New PCC Surface ;(b) 3D Coordinates of Scanned Aged PCC Surface.

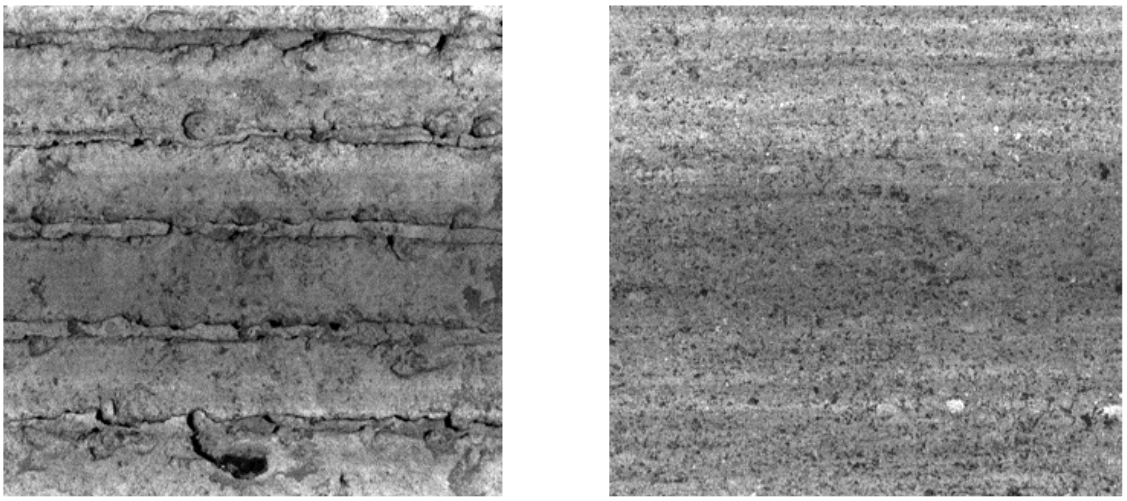

(a) (b)

Figure 65. Intensity Image of (a) New PCC Surface; and (b) Aged PCC Surface.

Since a rougher surface provides greater resistance to sliding by improving interlocking between pavement layers, greater mean profile depth (MPD) and estimated profile depth (EPD) values typically result in higher ISS. However, excessive pavement roughness can cause localized stress concentrations that may reduce ISS and cause premature pavement failure. Tables 6 and 7 present the values of MPD and ETD for both new and aged PCC

surfaces. The coefficient of variation indicates a greater degree of divergence between the data sets for the aged surface. This is likely because the surface's aging process was carried out manually, and it was observed that the surface had a slope that may have influenced the test results.

Previous studies have proposed a positive correlation between high surface texture and ISS values. However, it seems that this relationship may be more complex and influenced by multiple factors. To better understand how surface texture affects bond strength, the roughness parameters for the top layers of asphalt concrete were measured and recorded in Tables 8 and 9.

The data collected showed that the ISS results were affected by the construction technique used for compacting the AC layers. The increased compaction effort on the ½-inch NMAS AC layer on top of the aged PCC slab has improved bonding between the two layers. This is the reason for the higher ISS values observed with lower MPD values for the aged PCC slab configuration when employing ½-inch NMAS AC mixtures, which can be seen in Figure 66.

Table 6. Mean Profile Depth (MPD) Results for New and Aged PCC Surfaces.

Surface Condition	Section ID	MPD (mm)			Avg. MPD	Standard Deviation	Coefficient of Variation (CV), %
		Read 1	Read 2	Read 3			
New PCC	1	1.936	1.937	1.935	1.877	0.058	3.2%
	2	1.818	1.818	1.817			
Aged PCC	1	0.550	0.551	0.551	0.590	0.073	12.0%
	2	0.692	0.692	0.693			
	3	0.529	0.528	0.528			

Table 7. Estimated Texture Depth (ETD) Results for New and Aged PCC Surfaces.

Surface Condition	Section ID	ETD (mm)			Avg. ETD	Standard Deviation	Coefficient of Variation (CV), %
		Read 1	Read 2	Read 3			
New PCC	1	1.749	1.750	1.748	1.702	0.047	2.8%
	2	1.655	1.655	1.654			
Aged PCC	1	0.640	0.641	0.641	0.672	0.058	9.0%
	2	0.754	0.754	0.755			
	3	0.623	0.622	0.622			

Table 8. Mean Profile Depth (MPD) Results for ½-inch and ¾-inch NMAS AC Surfaces.

Surface Condition	Section ID	MPD (mm)			Avg. MPD	Standard Deviation	Coefficient of Variation (CV), %
		Read 1	Read 2	Read 3			
½-inch NMAS	1	0.492	0.491	0.492	0.481	0.040	8.3%
	2	0.427	0.427	0.427			
	3	0.524	0.524	0.522			
¾-inch NMAS	1	1.005	1.005	1.005	0.950	0.049	5.2%
	2	0.958	0.958	0.959			
	3	0.886	0.886	0.886			

Table 9. Estimated Texture Depth (ETD) Results for ½-inch and ¾-inch NMAS AC Surfaces.

Surface Condition	Section ID	ETD (mm)			Average MPD	Standard Deviation	Coefficient of Variation (CV), %
		Read 1	Read 2	Read 3			
½-inch NMAS	1	0.593	0.592	0.593	0.584	0.033	5.6%
	2	0.541	0.541	0.541			
	3	0.620	0.620	0.618			
¾-inch NMAS	1	1.004	1.004	1.004	0.960	0.039	4.1%
	2	0.966	0.966	0.967			
	3	0.909	0.909	0.909			

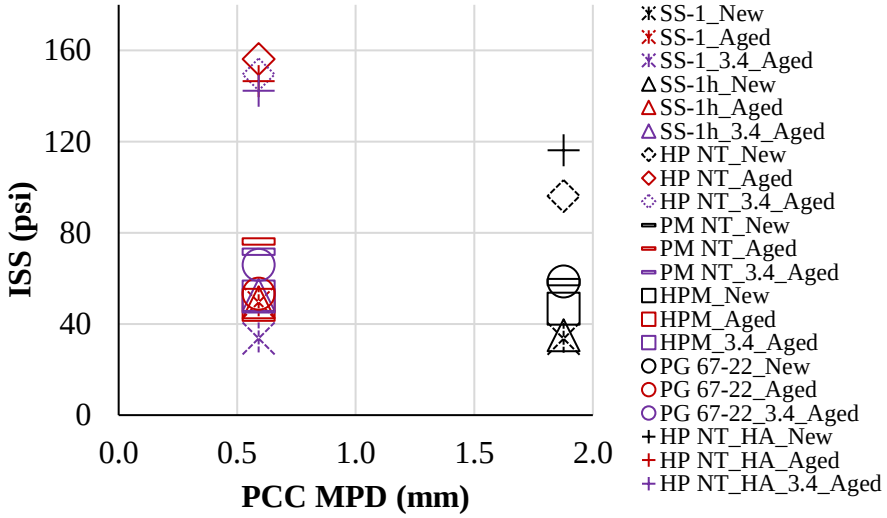

Figure 66. ISS vs. MPD (PCC) Results.

Figure 67 compares the results from the ISS test with the MPD values obtained for the asphalt concrete mixtures. When comparing a ¾-inch AC mix placed on top of an aged PCC with a ½-inch AC mix placed on top of a new PCC, both compacted with the same effort, the ¾-inch configuration still has higher ISS. This is because the ¾-inch mix has a higher MPD than the ½-inch mix, which may have caused the tack coat to penetrate the AC layer, resulting in a stronger bond

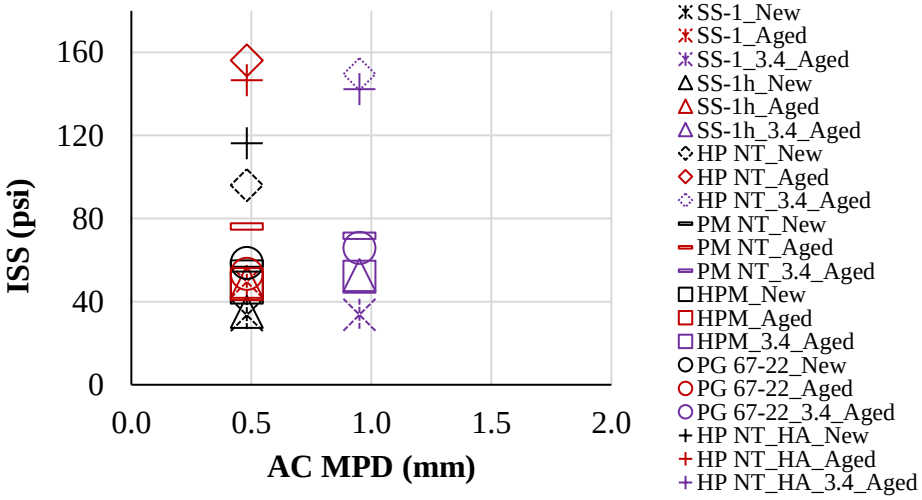

Figure 67. ISS vs. MPD (AC) Results.

Chapter 5: Findings and Recommendations

5.1 Findings

In order to ensure the optimal transfer of traffic and environmental stresses throughout the pavement, it is essential to fully bond the pavement layers to create a single, integrated structure. Good adhesion between the layers reduces shear and permanent deformation, leading to better elastic recovery and longer-lasting pavements. If the interface bond strength is insufficient, it can lead to premature distress and additional costs for the project. Hence, selecting the appropriate tack coat material during pavement construction is crucial to achieving satisfactory performance.

Several factors, including the rheological properties of the tack coat material, construction techniques, and pavement surface area, texture, and type, can affect the bond strength between pavement layers. To assess the performance of different tack coat materials under various loading and environmental conditions, standard specification test methods such as penetration and softening point were used to evaluate all materials studied. The bonding strength was correlated with rheological properties obtained through DSR testing, while the durability performance was correlated with an aging index using 4-mm DSR data.

The tack coat materials chosen for this study cover a wide range of residue stiffness values and polymer modification effects. This selection aimed to encompass a broad range of residual binder properties that could be used in cold and hot climates, regardless of the specific construction techniques utilized. The tests presented in Section 4.1 can capture each material's behavior, indicating that trackless materials are stiffer than slow-setting

emulsions. This difference in behavior is directly related to the formulation of these materials, which includes hard-base asphalt cement.

The absence of a tack coat between pavement layers resulted in debonding during coring for all specimens, regardless of pavement configuration. This indicates that using tack coat materials significantly positively impacts pavement interlayer shear strength, which can be attributed to the adhesive force between the tack coat and surface type.

After extraction, the remaining specimens underwent shear testing at 77 °F (25 °C), according to AASHTO TP 114. All pavement configurations displayed a similar pattern, with samples treated with HP NT and HP NT_HA emulsions demonstrating higher ISS values. Conversely, emulsions containing a softer base binder, such as SS-1 and SS-1h, were expected to have lower ISS values.

Unexpectedly, the aged PCC surface exhibited higher ISS values when compared to the new PCC surface configuration. This difference could be due to the varying percentage of air voids in the asphalt concrete layer obtained during construction, highlighting the impact of the construction techniques on the ISS results. Moreover, it is possible that the outcomes were affected by the tack coat material being absorbed by the PCC surface. In contrast to asphalt concrete, the concrete surface is naturally drier, which could lead to a lower amount of residual binder. This is especially true since the freshly ground PCC surface is more uneven, with the material between the grinding potentially having less impact on the bond strength.

The rheological properties of tack coat materials have been found to have a strong correlation with ISS of composite pavements. Although penetration and softening point

parameters are commonly used to evaluate the quality of tack coat, they may not be sensitive enough to reflect the effects of polymer modification. In contrast, PGH provided a more comprehensive evaluation and was used to predict the performance-related characteristics of tack coats for composite pavements.

Using a tack coat material with one PGH grade higher than the PGH of the binder used in the asphalt concrete results in performance comparable to, or slightly better than, the minimum laboratory-measured ISS of 40 psi, which is necessary to achieve satisfactory field-level tack coat efficiency based on past research. However, when tack coat materials have a PGH two grades higher than the PGH grade of the binder used in the AC layer, a stronger bond is formed, and the failure occurs within the mixture rather than at the tack coat interface.

An aging index was estimated to evaluate the impact of aging on the rheological properties of tack coat materials. A limit was set considering a broader range of tack coat materials, including those contaminated with substances such as diesel. Results indicated that PG 67-22 was the most susceptible to aging, displaying a higher aging index. Nevertheless, all materials studied demonstrated good resistance to aging, as their aging indexes remained below 4.0.

5.2 Recommendations

Based on the research study, the following recommendations can be made:

- Tack coat material selection should consider the PGH of the binder used in the overlay AC mixture for better bonding performance under all loading and environmental conditions for composite pavements.
- Tack coat material should present at least one PGH higher than the binder in the AC layer placed on the tack coat to perform similarly to minimum laboratory measured ISS.
- Unmodified materials with a two or higher performance-grade bump result in a stronger bond, causing failure within the mixture instead of at the tack coat interface. Therefore, recommended high-traffic roads.
- The distillation method is recommended to collect residue from emulsions and test the corresponding required properties for composite pavements.
- An aging index was identified to evaluate the durability of asphalt emulsion/binder materials, with a maximum allowable aging index of 4.0 recommended.
- More fundamental test methods were recommended for the proposed tack coat specification, as they correlated better with ISS, eliminating the need for expensive equipment.
- Consistently achieving the required density of HMA placed on PCC is as critical as selecting the appropriate tack coat material. It should meet the target level to ensure satisfactory results in ISS.

References

[1] A. Rahman, C. Ai, C. Xin, X. Gao, and Y. Lu, "State-of-the-art Review of Interface Bond Testing Devices for Pavement Layers: Toward the Standardization Procedure," *Journal of Adhesion Science and Technology*, vol. 31, no. 2. Taylor and Francis Ltd., pp. 109–126, Jan. 17, 2017. doi: 10.1080/01694243.2016.1205240.

[2] Federal Highway Administration (FHWA) TechBrief, "Tack Coat Best Practices," FHWA-HIF-16-017, Office of Asset Management, Pavements, and Construction, 2016.

[3] Z. Leng, H. Ozer, I. L. Al-Qadi, and S. H. Carpenter, "Interface Bonding Between Hot-Mix Asphalt and Various Portland Cement Concrete Surfaces: Laboratory Assessment," *Transportation Research Record: Journal of the Transportation Research Board*, vol. 2057, no. 1, pp. 46–53, 2008.

[4] I. L. Al-Qadi, S. H. Carpenter, Z. Leng, H. Ozer, and J. S. Trepanier, "Tack Coat Optimization for HMA Overlays: Laboratory Testing," FHWA-ICT-08-023, Office of Asset Management, Pavements, and Construction, 2008.

[5] G. King and R. May, "New Approaches to Tack Application," Presented at the 83rd Annual Meeting of the Transportation Research Board, Washington D.C., 2003.

[6] J. Roffe and F. Chaignon, "Characterization Tests on Bond Coats: Worldwide Study, Impact, Tests, Recommendations," Presented at the 3rd International Conference on Asphalt Mixtures and Pavements, Thessaloniki, Greece, 2002.

[7] Y. Hachiya and K. Sato, “Effect of Tack Coat on Bonding Characteristics at Interface between Asphalt Concrete Layers,” *Proceedings of the 8th International Conference on Asphalt Pavements*, pp. 349–362, 1997.

[8] G. W. Flintsch, B. K. Diefenderfer, and O. Nunez, “Composite Pavement Systems: Synthesis of Design and Construction Practices,” Virginia Department of Transportation (VDOT), Virginia, Technical Report FHWA/VTRC 09-CR2, 2008.

[9] R. Mathews, “Development of a Structural Design Program for HMA Overlaid Fractured PCC Pavements with Emphasis on HMA Tensile Strain Criteria,” M.Sc. Thesis, Department of Civil Engineering, Iowa State University, Ames, IA, 2004.

[10] K. Sobhan and V. Tandon, “Mitigating Reflection Cracking in Asphalt Overlays using Geosynthetic Reinforcements,” *Road Materials and Pavement Design*, vol. 9, pp. 367–387, 2008, doi: 10.3166/RMPD.9.

[11] M. Trevino, T. Dossey, B. F. McCullough, and Y. Yildirim, “Applicability of Asphalt Concrete Overlays on Continuously Reinforced Concrete Pavements,” Center for Transportation Research, The University of Texas at Austin, Austin, 2003.

[12] US Army Corps of Engineers, *Hot-Mix Asphalt Paving Handbook 2000 AC 150/5370-14A*. Washington, DC, 2000.

[13] A. A. Tayebali, M. S. Rahman, M. B. Kulkarni, and X. Qingxia, “A Mechanistic Approach to Evaluate Contribution of Prime and Tack Coat in Composite Asphalt

Pavements," North Carolina State University, Raleigh, Technical Report FHWA/NC/2004-05, 2004.

[14] L. N. Mohammad, M. A. Elseifi, A. Bae, N. Patel, J. Button, and J. A. Scherocman, "Optimization of Tack Coat for HMA Placement," Report 712, National Cooperative Highway Research Program (NCHRP), Washington, DC, 2012.

[15] J. Wang, F. Xiao, Z. Chen, X. Li, and S. Amirkhanian, "Application of Tack Coat in Pavement Engineering," *Construction and Building Materials*, vol. 152. Elsevier Ltd, pp. 856–871, Oct. 15, 2017. doi: 10.1016/j.conbuildmat.2017.07.056.

[16] X. Jia, B. Huang, B. F. Bowers, and T. E. Rutherford, "Investigation of Tack Coat Failure in Orthotropic Steel Bridge Deck Overlay: Survey, Analysis, and Evaluation," *Journal of the Transportation Research Board*, vol. 2444, pp. 28–37, 2014, doi: 10.3141/2444-04.

[17] N. F. Ghaly, I. M. Ibrahim, and E. M. Noamy, "Tack Coats for Asphalt Paving," *Egyptian Journal of Petroleum*, vol. 23, no. 1, pp. 61–65, Mar. 2014, doi: 10.1016/j.ejpe.2014.02.009.

[18] I. L. Al-Qadi, K. I. Hasiba, A. S. Cortina, H. Ozer, and Z. Leng, "Best Practices for Implementation of Tack Coat: Part 1, Laboratory Study," Illinois Center for Transportation, Urbana-Champaign, Technical Report FHWA-ICT-12-004, 2012.

[19] "A Basic Asphalt Emulsion Manual," Asphalt Institute, Manual Series No. 19, Second Edition, Lexington, Kentucky, 2008.

[20] J. S. Chen and C. C. Huang, “Effect of Surface Characteristics on Bonding Properties of Bituminous Tack Coat,” *Journal of Transportation Research Board*, no. 2180, pp. 142–149, Dec. 2010, doi: 10.3141/2180-16.

[21] J. Musselman, R. Moraes, T. Walbeck, and R. C. West, “Methods for Addressing Tack Tracking,” National Center for Asphalt Technology, Auburn, NCAT Report 20-06, 2020.

[22] X. Hu, Y. Lei, H. Wang, P. Jiang, X. Yang, and Z. You, “Effect of Tack Coat Dosage and Temperature on the Interface Shear Properties of Asphalt Layers Bonded with Emulsified Asphalt Binders,” *Constr Build Mater*, vol. 141, pp. 86–93, Jun. 2017, doi: 10.1016/j.conbuildmat.2017.02.157.

[23] L. N. Mohammad, A. Bae, M. A. Elseifi, J. Button, and J. A. Scherocman, “Evaluation of Bond Strength of Tack Coat Materials in Field: Development of Pull-Off Test Device and Methodology,” *Transp Res Rec*, vol. 2126, pp. 1–11, 2009, doi: 10.3141/2126-01.

[24] S. A. Romanoschi and J. B. Metcalf, “Characterization of Asphalt Concrete Layer Interfaces,” *Transp Res Rec*, vol. 1778, pp. 132–139, 2001.

[25] I. Deysarkar, “Test Set-Up to Determine Quality of Tack Coat,” Master of Science, University of Texas, El Paso, El Paso, 2004.

[26] J. Wang, F. Xiao, Z. Chen, X. Li, and S. Amirkhanian, “Application of Tack Coat in Pavement Engineering,” *Construction and Building Materials*, vol. 152. Elsevier Ltd, pp. 856–871, Oct. 15, 2017. doi: 10.1016/j.conbuildmat.2017.07.056.

[27] C. Castorena, M. Rawls, and J. Hyuk-Im, “In-situ Determination of Emulsion Application Rates for Tack Coats and Surface Treatments,” Research and Development, NCDOT Project 2014-03, 2016.

[28] D. Gransberg and D. M. B. James, “Chip Seal Best Practices,” Synthesis 342, National Cooperative Highway Research Program (NCHRP), Washington, DC, 2005.

[29] J. Uzan, M. Livneh, and Y. Eshed, “Investigation of Adhesion Properties Between Asphaltic-Concrete Layers.,” *Asphalt Paving Technology*, vol. 47, pp. 495–521, 1978.

[30] F. Canestrari, F. Cardone, E. Gaudenzi, D. Chiola, N. Gasbarro, and G. Ferrotti, “Interlayer Bonding Characterization of Interfaces Reinforced with Geocomposites in Field Applications,” *Geotextiles and Geomembranes*, vol. 50, pp. 154–162, 2021.

[31] F. Canestrari *et al.*, “Mechanical Testing of Interlayer Bonding in Asphalt Pavements,” in *RILEM State-of-the-Art Reports*, Springer Netherlands, 2013, pp. 303–360. doi: 10.1007/978-94-007-5104-0_6.

[32] N. Sudarsanan, R. Karpurapu, and V. Amrithalingam, “An Investigation on the Interface Bond Strength of Geosynthetic-Reinforced Asphalt Concrete Using Leutner Shear Test,” *Constr Build Mater*, vol. 186, pp. 423–437, Oct. 2018, doi: 10.1016/j.conbuildmat.2018.07.010.

[33] AASHTO TP 114, “Determining the Interlayer Shear Strength (ISS) of Asphalt Pavement Layers,” American Association of State Highway and Transportation Officials (AASHTO), Washington, DC, 2022.

[34] AASHTO TP 115, “Determining the Quality of Tack Coat Adhesion to the Surface of an Asphalt Pavement in the Field or Laboratory,” American Association of State Highway and Transportation Officials (AASHTO), Washington, DC, 2022.

[35] Z. Tang, F. Huang, and H. Peng, “Effect of 3D Roughness Characteristics on Bonding Behaviors Between Concrete Substrate and Asphalt Overlay,” *Constr Build Mater*, vol. 270, Feb. 2021, doi: 10.1016/j.conbuildmat.2020.121386.

[36] R. Das, L. N. Mohammad, M. Elseifi, W. Cao, and S. B. Cooper, “Development and Validation of a Model to Predict Interface Bonding Between Pavement Layers,” *Transp Res Rec*, vol. 2672, no. 28, pp. 22–30, May 2018, doi: 10.1177/0361198118759001.

[37] AASHTO T 361, “Determining Asphalt Binder Bond Strength by Means of the Binder Bond Strength (BBS) Test,” American Association of State Highway and Transportation Officials (AASHTO), Washington, DC, 2022.

[38] Q. Lv and H. U. Bahia, “Factors Affecting the Tracking Performance of Tack Coat Materials,” *Transp Res Rec*, vol. 2673, no. 3, pp. 355–364, Mar. 2019, doi: 10.1177/0361198119834844.

[39] “Evaluation of Pavement Friction,” Synthesis 291, National Cooperative Highway Research Program (NCHRP), Washington, DC, 2000.

[40] G. W. Flintsch, I. L. Al-Qadi, G. W. Flintsch, E. De León, K. K. Mcghee, and I. L. Al-Qadi, "Pavement Surface Macrotexture Measurement and Applications," *Transp Res Rec*, vol. 1860, no. 1, pp. 168–177, 2003.

[41] ASTM E1845, "Standard Practice for Calculating Pavement Macrotexture Mean Profile Depth," Volume 04.03, West Conshohocken, PA, 2016.

[42] AASHTO T 59, "Standard Method of Test for Emulsified Asphalt," American Association of State Highway and Transportation Officials (AASHTO), Washington, DC, 2022.

[43] AASHTO R 78, "Recovering Residue from Emulsified Asphalt Using Low-temperature Evaporative Techniques," American Association of State Highway and Transportation Officials (AASHTO), Washington, DC, 2022.

[44] M. Anderson, "ETF Emulsion Residue Testing Program," AASHTO TSP 2 Emulsion Task Force Meeting, Indianapolis, IN, 2018.

[45] ASTM D7944, "Standard Practice for Recovery of Emulsified Asphalt Residue Using a Vacuum Oven," Volume 04.03, West Conshohocken, PA, 2016. doi: 10.1520/D7944-15.

[46] H. Bahia, A. Sufian, D. Swiertz, B. Solutions, L. Mohammad, and M. Akentuna, "Investigation of Tack Coat Materials Tracking Performance," Wisconsin DOT Report No. 0092-17-06, Madison, WI, 2019.

[47] AASHTO T 315, “Determining the Rheological Properties of Asphalt Binder Using a Dynamic Shear Rheometer (DSR),” American Association of State Highway and Transportation Officials (AASHTO), Washington, DC, 2022.

[48] AASHTO T 313, “Determining the Flexural Creep Stiffness of Asphalt Binder Using the Bending Beam Rheometer (BBR),” American Association of State Highway and Transportation Officials (AASHTO), Washington, DC, 2022.

[49] Federal Highway Administration (FHWA) TechBrief, “Delta Tc Binder Specification Parameter,” FHWA-HIF-21-042, Office of Asset Management, Pavements, and Construction, 2021.

[50] AI IS 240, *Use of the Delta Tc Parameter to Characterize Asphalt Binder Behavior*. Asphalt Institute Technical Advisory Committee, 2019.

[51] AASHTO M 320, “Performance-Graded Asphalt Binder,” American Association of State Highway and Transportation Officials (AASHTO), Washington, DC, 2022.

[52] FHWA TechBrief, “The Multiple Stress Creep Recovery (MSCR) Procedure,” FHWA-HIF-11-038, Office of Asset Management, Pavements, and Construction, April 2011.

[53] AASHTO T 350, “Multiple Stress Creep Recovery (MSCR) Test of Asphalt Binder Using a Dynamic Shear Rheometer (DSR),” American Association of State Highway and Transportation Officials (AASHTO), Washington, DC, 2019.

[54] AASHTO T 316, “Viscosity Determination of Asphalt Binder Using Rotational Viscometer,” American Association of State Highway and Transportation Officials (AASHTO), Washington, DC, 2022.

[55] AASHTO T 49, “Penetration of Bituminous Materials,” American Association of State Highway and Transportation Officials (AASHTO), Washington, DC, 2022.

[56] ASHTO T 53, “Softening Point of Bitumen (Ring-and-Ball Apparatus),” American Association of State Highway and Transportation Officials (AASHTO), Washington, DC, 2022.

[57] G. M. Rowe and S. F. Raposo, “RHEA Rheology Analysis,” User Manual Version 2.1, 2021.

[58] A. M. M. Vega, “Exploring the Black Space of Compressive and Shear Modulus,” Master of Science, University of Arkansas, Fayetteville, 2016.

[59] M. Zeng, H. U. Bahia, H. Zhai, M. R. Anderson, and P. Turner, “Rheological Modeling of Modified Asphalt Binders and Mixtures,” *Association of Asphalt Paving Technologists*, vol. 70, 2001.

[60] A. H. A. Al-Haddad, “Construction of a Complex Shear Modulus Master Curve for Iraqi Asphalt Binder using a Modified Sigmoidal Fitting,” *International Journal of Scientific Engineering and Technology Research*, vol. 04, no. 04, pp. 0682–0690, 2015.

[61] A. Booshehrian, W. S. Mogawer, and R. Bonaquist, “How to Construct an Asphalt Binder Master Curve and Assess the Degree of Blending between RAP and Virgin

Binders," *Journal of Materials in Civil Engineering*, vol. 25, no. 12, pp. 1813–1821, Dec. 2013, doi: 10.1061/(asce)mt.1943-5533.0000726.

[62] ACI 301, "Specifications for Structural Concrete," American Concrete Institute, 2010.

[63] M. Nimeri, H. Nabizadeh, E. Y. Hajj, R. v Siddharthan, S. Elfass, and M. Piratheepan, "Design, Fabrication, and Instrumentation of a Full-Scale Pavement Testing Box," *Airfield and Highway Pavements*, 2019.

[64] Regional Transportation Commission of Washoe County, *Standard Specifications for Public Works Construction*. 2012.

[65] *Mix Design Methods for Asphalt Concrete and Other Hot-Mix Types*, 7th ed. Manual Series No. 02 (MS-2). Asphalt Institute. Lexington, KY, 2014.

[66] AASHTO R 97, "Sampling Asphalt Mixtures," American Association of State Highway and Transportation Officials (AASHTO), Washington, DC, 2019.

[67] A. J. Hand *et al.*, "Developing Laboratory Methods and Specification Language to Test Tack Coat Materials," National Cooperative Highway Research Program (NCHRP), Washington, DC, 2023.

[68] P. A. Serigos, P. Buddhavarapu, G. M. Gorman, F. Hong, and J. A. Prozzi, "The Contribution of Micro- and Macro-Texture to the Skid Resistance of Flexible Pavement," 2016.

Appendix A

Table A.1. PCC Mix Design.

Parameter \ Results	Trial Batch Test Results	Design Target
Water/Cement Material Ratio	0.4	0.4
Sacks Cement	7.5	7.5
3 Day Compressive Strength (psi)	3490	-
7 Day Compressive Strength (psi)	4410	-
14 Day Compressive Strength (psi)	4850	-
28 Day Compressive Strength (psi)	5480	4000
56 Day Compressive Strength (psi)	6010	-
Slump Initial (in)	3.00	3.0
Slump Final (in)	6.0	6.0
Air Content (%)	6.0	6.0
Aggregate Correction Factor	0.3	-
Unit Weight (pcf)	138.9	138.6

Table A.2. PCC Mix Proportions.

Material	Description/Source	Weight (lbs)	Volume (ft^3)
Cement	Nevada Type II	564	2.869
Supplementary Cementitious Materials	Nevada Class N	141	0.978
Coarse Aggregate	#67 Stone	1620	9.985
Fine Aggregate	Concrete Sand	1135	7.020
Water	33.4 gallons	278	4.455
Air Content	6.0%	-	1.620
Admixture	Eucon Air Mac12	7.1 (fl oz)	0.007
Admixture Admixture	Eucon X15	63.5 (fl oz)	0.066
Admixture	Eucon 37	-	-
	Total	3742	27.000

Table A.3. Aggregate Gradation for ¾ inch NMAS PCC Mixture.

Sieve Size	#67 Stone	Concrete Sand	Combined	Specification
2"	100.0	100.0	100.0	–
1 1/2"	100.0	100.0	100.0	100
1"	100.0	100.0	100.0	100
3/4"	94.0	100.0	96.0	80 – 100
1/2"	58.0	100.0	75.0	–
3/8"	30.0	100.0	59.0	46 – 70
No.4	3.0	100.0	43.0	34 – 50
No.8	1.0	88.0	37.0	24 – 42
No.16	1.0	65.0	27.0	17 – 34
No.30	1.0	42.0	18.0	10 – 25
No.50	1.0	20.0	9.0	5 – 15
No.100	1.0	7.0	3.0	2 – 7
No.200	1.0	2.5	1.6	0 – 3
Bin Percentage, %	58.7	41.3	100	–

Table A.4. Aggregate Gradation for ½ inch NMAS HMA Mixture.

Sieve Size	Sieve Size (mm)	1/2"	3/8”	Crusher Fines	Washed Sand	Lime	RAP	Blending % Passing
3/4"	19.0	100.0	100.0	100.0	100.0	100.0	100.0	100.0
1/2"	12.5	99.8	100.0	100.0	100.0	100.0	100.0	100.0
3/8"	9.5	58.8	100.0	100.0	100.0	100.0	95.0	89.9
No.4	4.75	0.8	26.4	100.0	100.0	100.0	71.2	56.2
No.8	2.36	0.6	2.3	75.0	89.8	100.0	52.4	41.2
No.10	2.00	0.5	1.9	68.4	81.0	100.0	48.8	37.6
No.16	1.18	0.5	1.3	52.1	55.3	100.0	40.0	28.1
No.30	0.60	0.4	1.0	38.2	31.1	99.0	30.4	19.2
No.40	0.42	0.4	0.9	33.8	22.2	99.0	25.8	15.9
No.50	0.30	0.4	0.9	30.2	14.5	99.0	21.3	13.1
No.100	0.15	0.3	0.8	24.9	5.1	99.0	15.3	9.3
No.200	0.075	0.3	0.7	20.3	2.5	70.6	11.6	7.0
Pan	-	0.0	0.0	0.0	0.0	0.0	0.0	0.0
Bin Percentage, %		**22.74**	**23.0**	**18.0**	**20.0**	**1.26**	**15.0**	**100.0**

Table A.5. ½ inch NMAS HMA Mixture Properties.

Property	Unit	Design	Specification
Anti-Strip	-	Dry Lime	-
AC Content (Pb)	%	5.9	5.4 – 6.4
Air Voids (Va)	%	4	2.5 – 5.5
VMA	%	14.4	≥ 14
VFA	%	72.2	65 – 78
LA Abrasion	%	19	≤ 37
Soundness Coarse	%	10	≤ 12
Soundness (Na2SO4) Fine	%	11	≤ 15
Fractured Faces (>1)	%	100	≥ 80
Fractured Faces (>2)	%	100	≥ 50
Plastic Flow	0.01 in	15	8 – 20
Stability	lbf	3220	≥ 1800
Absorption (Coarse)	%	3.3	≤ 4
Absorption (Fine)	%	3.7	-
Liquid Limit	%	0	≤ 35
Plasticity Index	%	NP	≤ 6
SPGR (Compacted, Gmb)	-	2.344	-
SPGR (Effective, Gse)	-	2.675	-
SPGR (Max, Gmm)	-	2.442	-
SPGR (Dry, Gsb)	-	2.557	-
SPGR Coarse (Dry, Gsb)	-	2.576	-
SPGR Fine (Dry, Gsb)	-	2.549	-
Unit Weight (Compacted)	lb/ft^3	145.9	-
Unit Weight (Max)	lb/ft^3	152	-

Table A.6. Aggregate Gradation for ¾ inch NMAS HMA Mixture.

Sieve Size	Sieve Size (mm)	3/4"	1/2"	3/8”	Crusher Fines	Washed Sand	Lime	RAP	Blending %Passing
3/4"	19.0	100.0	100.0	100.0	100.0	100.0	100.0	100.0	100.0
1/2"	12.5	37.9	99.8	100.0	100.0	100.0	100.0	100.0	89.4
3/8"	9.5	5.2	58.8	100.0	100.0	100.0	100.0	95.0	76.1
No.4	4.75	1.6	0.8	26.4	100.0	100.0	100.0	71.2	50.3
No.8	2.36	1.5	0.6	2.3	75.0	89.8	100.0	52.4	38.1
No.10	2.00	1.4	0.5	1.9	68.4	81.0	100.0	48.8	34.8
No.16	1.18	1.4	0.5	1.3	52.1	55.3	100.0	40.0	26.0
No.30	0.60	1.3	0.4	1.0	38.2	31.1	99.0	30.4	17.7
No.40	0.42	1.3	0.4	0.9	33.8	22.2	99.0	25.8	14.6
No.50	0.30	1.3	0.4	0.9	30.2	14.5	99.0	21.3	11.9
No.100	0.15	1.2	0.3	0.8	24.9	5.1	99.0	15.3	8.4
No.200	0.075	1.1	0.3	0.7	20.3	2.5	70.6	11.6	6.3
Pan	-	0.0	0.0	0.0	0.0	0.0	0.0	0.0	0.0
Bin Percentage, %		**17.0**	**17.0**	**16.0**	**13.74**	**20.0**	**1.26**	**15.0**	**100**

Table A.7. ¾ inch NMAS HMA Mixture Properties.

Property	Unit	Design	Specification
Anti-Strip	-	Dry Lime	-
AC Content (Pb)	%	5.5	5.0 – 6.0
Air Voids (Va)	%	4	2.5 – 5.5
VMA	%	14.1	≥ 13
VFA	%	72.1	65 – 78
LA Abrasion	%	16	≤ 37
Soundness Coarse	%	7	≤ 12
Soundness (Na2SO4) Fine	%	13	≤ 15
Fractured Faces (>1)	%	100	≥ 80
Fractured Faces (>2)	%	100	≥ 50
Plastic Flow	0.01 in	14	8 – 20
Stability	lbf	3308	≥ 1800
Absorption (Coarse)	%	2.8	≤ 4
Absorption (Fine)	%	3.6	-
Liquid Limit	%	0	≤ 35
Plasticity Index	%	NP	≤ 6
SPGR (Compacted, Gmb)	-	2.355	-
SPGR (Effective, Gse)	-	2.675	-
SPGR (Max, Gmm)	-	2.453	-
SPGR (Dry, Gsb)	-	2.594	-
SPGR Coarse (Dry, Gsb)	-	2.602	-
SPGR Fine (Dry, Gsb)	-	2.558	-
Unit Weight (Compacted)	lb/ft^3	146.5	-
Unit Weight (Max)	lb/ft^3	152.6	-

Table A.8. Summary of Average Test Results for SS-1 Emulsion Residue [67].

Test Method	Property		Test Temp. (°C)	Residue Recovery Method		
				Distillation (AASHTO T 59)	LTE (AASHTO PP 72)	Vacuum Oven (ASTM D 7944)
PG (AASHTO M 320)	Original DSR	G*/sin δ (kPa)	58	1.39	1.73	1.35
		phase angle δ (°)		86.8	86.3	86.9
		G*/sin δ (kPa)	64	0.65	0.80	0.63
		phase angle δ (°)		88.1	87.7	88.2
		G*/sin δ (kPa)	70			
		phase angle δ (°)				
		Continuous PGH_ORIG (°C)		60.6	62.3	60.3
	Continuous PGH (°C)			**60.6**	**62.3**	**60.3**
MSCR (AASHTO T 350)	Jnr @ 3.2 kPa		52	3.13	2.45	3.23
	Jnr @ 0.1 kPa			2.92	2.27	3.00
	%Recovery @ 3.2 kPa			-0.17	0.39	-0.24
	%Recovery @ 0.1 kPa			1.54	3.07	1.81
	Jnr @ 3.2 kPa		58	7.47	5.95	7.69
	Jnr @ 0.1 kPa			6.94	5.50	7.19
	%Recovery @ 3.2 kPa			-2.00	-1.43	-2.05
	%Recovery @ 0.1 kPa			-0.82	0.01	-1.24
	Jnr @ 3.2 kPa		64			
	Jnr @ 0.1 kPa					
	%Recovery @ 3.2 kPa					
	%Recovery @ 0.1 kPa					
Crossover Temperature (°C)				1.0	2.4	1.6
RV (AASHTO T 316)	Rotational Viscosity (cP)		135	308		
Original DSR Absolute Viscosity (Surrogate)	G* (kPa)		60	1.08	1.33	1.03
Penetration (AASHTO T 49)	Penetration		25	125		
DSR Penetration Correlation	G* (kPa)		25	85.0	109.0	82.2
	Calculated Pen Value			138	121	141
Softening Point (AASHTO T 53)	Softening Point R&B			40.1		
DSR Softening Point (Surrogate) (°C)				52.2	48.5	50.5
Tack Coat Formulation Specification Verification Test Results						
Viscosity, Saybolt-Furol, 25°C (77°F), seconds (AASHTO T 59)				25 (20-100)		
Storage Stability Test, 24 hours, % (AASHTO T 59)				0.1 (1.0		
Sieve Test, % (AASHTO T 59)				0.01 (0.1		
Density, lb/gal (AASHTO T 59)				8.51		
Residue by Distillation, %, weight (AASHTO T 59)				61.1 (57		
Penetration, 25°C (77°F), 100 g, 5 seconds, 0.1 mm (AASHTO T 49)				122 (120-		
Ductility, 25°C (77°F), 5 cm/min, cm (AASHTO T 51)				150+ (40		
Ash Content, % (AASHTO T 111)				0.2 (1.0		

Table A.9. Summary of Average Test Results for SS-1h Emulsion Residue [67].

Test Method	Property		Test Temp. (°C)	Residue Recovery Method		
				Distillation (AASHTO T 59)	LTE (AASHTO PP 72)	Vacuum Oven (ASTM D 7944)
PG (AASHTO M 320)	Original DSR	G*/sin δ (kPa)	58		2.07	2.23
		phase angle δ (°)			86.5	86.7
		G*/sin δ (kPa)	64	1.05	0.94	0.99
		phase angle δ (°)		88.0	87.9	88.0
		G*/sin δ (kPa)	70	0.50		
		phase angle δ (°)		88.9		
		Continuous PGH_ORIG (°C)		64.4	63.5	64.0
	Continuous PGH (°C)			**64.4**	**63.5**	**64.0**
MSCR (AASHTO T 350)	Jnr @ 3.2 kPa		52		2.00	1.82
	Jnr @ 0.1 kPa				1.87	1.74
	%Recovery @ 3.2 kPa				0.62	0.64
	%Recovery @ 0.1 kPa				3.13	1.97
	Jnr @ 3.2 kPa		58	4.26	4.91	4.56
	Jnr @ 0.1 kPa			4.07	4.62	4.30
	%Recovery @ 3.2 kPa			-0.93	-1.14	-1.03
	%Recovery @ 0.1 kPa			-0.30	0.07	0.18
	Jnr @ 3.2 kPa		64	9.74		
	Jnr @ 0.1 kPa			9.29		
	%Recovery @ 3.2 kPa			-2.79		
	%Recovery @ 0.1 kPa			-2.33		
Crossover Temperature (°C)				5.9	6.5	6.2
RV (AASHTO T 316)	Rotational Viscosity (cP)		135	385		
Original DSR Absolute Viscosity (Surrogate)	G* (kPa)		60	1.79	1.58	1.65
Penetration (AASHTO T 49)	Penetration		25	80.0		
DSR Pen Correlation	G* (kPa)		25	191.5	144.0	183.0
	Calculated Pen Value			89	104	91
Softening Point (AASHTO T 53)	Softening Point R&B			44.0		
DSR Softening Point (Surrogate) (°C)				52.8	51.9	52.4
Tack Coat Formulation Specification Verification Test Results						
Viscosity, Saybolt-Furol, 25°C (77°F), seconds (AASHTO T 59)				36 (20-100)		
Storage Stability Test, 24 hour, % (AASHTO T 59)				0.18 (1.0 max)		
Sieve Test, % (AASHTO T 59)				0.01 (0.1 max)		
Density, lb/gal (AASHTO T 59)				8.53		
Residue by Distillation, %, weight (AASHTO T 59)				61 (57 min)		
Penetration, 25°C (77°F), 100 g, 5 seconds, 0.1 mm (AASHTO T 49)				78 (60-100)		
Ductility, 25°C (77°F), 5 cm/min, cm (AASHTO T 51)				150+ (40 min)		
Ash Content, % (AASHTO T 111)				0.2 (1.0 max)		

Table A.10. Summary of Average Test Results for HP NT Emulsion Residue [67].

Test Method	Property		Test Temp. (°C)	Residue Recovery Method		
				Distillation (AASHTO T 59)	LTE (AASHTO PP 72)	Vacuum Oven (ASTM
PG (AASHTO M 320)	Original DSR	G*/sin δ (kPa)	76	2.45	3.13	2.90
		phase angle δ (°)		88.9	88.1	88.0
		G*/sin δ (kPa)	82	1.12	1.41	1.31
		phase angle δ (°)		89.1	88.6	88.5
		G*/sin δ (kPa)	88	0.55	0.67	0.63
		phase angle δ (°)		89.1	88.9	88.9
		Continuous PGH_ORIG (°C)		83.0	84.8	84.3
	Continuous PGH (°C)			**83.0**	**84.8**	**84.3**
MSCR (AASHTO T 350)	Jnr @ 3.2 kPa		76	4.06	3.23	3.44
	Jnr @ 0.1 kPa			3.81	2.98	3.24
	%Recovery @ 3.2 kPa			-1.24	-0.59	-0.77
	%Recovery @ 0.1 kPa			1.23	3.21	1.90
	Jnr @ 3.2 kPa		82	9.10	7.31	7.97
	Jnr @ 0.1 kPa			8.67	6.88	7.50
	%Recovery @ 3.2 kPa			-2.75	-2.08	-2.31
	%Recovery @ 0.1 kPa			-1.10	0.22	-0.33
	Jnr @ 3.2 kPa		88			
	Jnr @ 0.1 kPa					
	%Recovery @ 3.2 kPa					
	%Recovery @ 0.1 kPa					
Crossover Temperature (°C)				28.9	29.8	29.4
RV (AASHTO T 316)	Rotational Viscosity (cP)		135	1,209		
Original DSR Absolute Viscosity (Surrogate)	G* (kPa)		60	35.50	44.10	41.30
Penetration (AASHTO T 49)	Penetration		25	5.0		
DSR Pen Correlation	G* (kPa)		25	33,000.0	35,200.0	33,400.0
	Calculated Pen Value			6.0	5.0	6.0
Softening Point (AASHTO T 53)	Softening Point R&B			66.1		
DSR Softening Point (Surrogate) (°C)				71.5	72.9	72.4
Tack Coat Formulation Specification Verification Test Results						
Viscosity, Saybolt-Furol, 25°C (77°F), seconds (AASHTO T				15 (10-150)		
Storage Stability Test, 24 hour, % (AASHTO T 59)				0.29 (1.0 max)		
Sieve Test, % (AASHTO T 59)				0.00 (0.3 max)		
Density, lb/gal (AASHTO T 59)				8.53		
Residue by Distillation, %, weight (AASHTO T 59)				53.0 (50 min)		
Penetration, 25°C (77°F), 100 g, 5 seconds, 0.1 mm (AASHTO				6.0 (30 max)		
ODSR, G*/Sin delta, kPa, 76 °C (AASHTO T 315)				2.429 (1.0		
MSCR, Jnr @ 3.2, kPa, 64 °C (AASHTO T 350)				0.6 (1.5 max)		

Table A.11. Summary of Average Test Results for PM NT Emulsion Residue [67].

Test Method	Property		Test Temp. (°C)	Residue Recovery Method		
				Distillation (AASHTO T 59)	LTE (AASHTO PP 72)	Vacuum Oven (ASTM
PG (AASHTO M 320)	Original DSR	G*/sin δ (kPa)	70	1.30	1.47	1.49
		phase angle δ (°)		83.6	82.70	83.4
		G*/sin δ (kPa)	76	0.67	0.76	0.77
		phase angle δ (°)		83.8	83.5	84.20
		G*/sin δ (kPa)	82			
		phase angle δ (°)				
		Continuous PGH_ORIG		72.4	73.5	73.6
	Continuous PGH (°C)			**72.4**	**73.5**	**73.6**
MSCR (AASHTO T 350)	Jnr @ 3.2 kPa		64	3.68	3.45	3.19
	Jnr @ 0.1 kPa			2.34	2.50	2.04
	%Recovery @ 3.2 kPa			1.71	1.38	2.69
	%Recovery @ 0.1 kPa			23.69	17.0	24.98
	Jnr @ 3.2 kPa		70	9.05	7.65	7.06
	Jnr @ 0.1 kPa			4.92	5.49	4.00
	%Recovery @ 3.2 kPa			-1.39	-1.12	0.52
	%Recovery @ 0.1 kPa			16.72	12.05	24.97
	Jnr @ 3.2 kPa		76			
	Jnr @ 0.1 kPa					
	%Recovery @ 3.2 kPa					
	%Recovery @ 0.1 kPa					
Crossover Temperature (°C)				6.85	7.65	7.7
RV (AASHTO T 316)	Rotational Viscosity (cP)		135	630		
Original DSR Absolute Viscosity (Surrogate)	G* (kPa)		60	4.365	4.87	5.25
Penetration (AASHTO T 49)	Penetration		25	59		
DSR Pen Correlation	G* (kPa)		25	395	314	542.5
	Calculated Pen Value			55.4	69	51
Softening Point (AASHTO T 53)	Softening Point R&B			49		
DSR Softening Point (Surrogate) (°C)				55.4	59.1	55.85
Tack Coat Formulation Specification Verification Test Results						
Viscosity, Saybolt-Furol, 25°C (77°F), seconds (AASHTO T				25 (15-100)		
Storage Stability Test, 24 hour, % (AASHTO T 59)				0.33 (1.0		
Sieve Test, % (AASHTO T 59)				0.00 (0.1		
Particle Charge (AASHTO T 59)				Positive		
Density, lb/gal (AASHTO T 59)				8.55		
Residue by Distillation, %, weight (AASHTO T 59)				56.4 (55 min)		
Oil distillate, % volume (AASHTO T 59)				0.00 (3.0		
Penetration, 25°C (77°F), 100 g, 5 seconds, 0.1 mm (AASHTO				60.0 (40-90)		
Softening Point, °C (AASHTO T 53)				49.8 (49 min)		

Table A.12. Summary of Average Test Results for HPM Emulsion Residue [67].

Test Method	Property		Test Temp. (°C)	Residue Recovery Method		
				Distillation (AASHTO T 59)	LTE (AASHTO PP 72)	Vacuum Oven (ASTM D7944)
PG (AASHTO M 320)	Original DSR	G*/sin δ (kPa)	70	1.69	1.99	1.66
		phase angle δ (°)		65.3	73.5	76.2
		G*/sin δ (kPa)	76	1.07	1.16	0.97
		phase angle δ (°)		62.9	73.6	76.35
		G*/sin δ (kPa)	82	0.73	0.72	
		phase angle δ (°)		59.8	73.0	
		Continuous PGH_ORIG		77.1	77.9	75.6
	Continuous PGH (°C)			**77.1**	**77.9**	**75.6**
MSCR (AASHTO T 350)	Jnr @ 3.2 kPa		64			2.53
	Jnr @ 0.1 kPa					1.10
	%Recovery @ 3.2 kPa					21.40
	%Recovery @ 0.1 kPa					59.05
	Jnr @ 3.2 kPa		70	1.11	3.87	5.60
	Jnr @ 0.1 kPa			0.14	1.36	1.63
	%Recovery @ 3.2 kPa			67.59	21.94	15.59
	%Recovery @ 0.1 kPa			94.42	65.79	67.89
	Jnr @ 3.2 kPa		76	2.78	7.20	
	Jnr @ 0.1 kPa			0.10	1.80	
	%Recovery @ 3.2 kPa			55.57	16.71	
	%Recovery @ 0.1 kPa			96.81	71.03	
Crossover Temperature (°C)				2.6	0.80	6
RV (AASHTO T 316)	Rotational Viscosity (cP)		135	5663.5		
Original DSR Absolute Viscosity (Surrogate)	G* (kPa)		60	4.075	5.675	4.355
Penetration (AASHTO T 49)	Penetration		25	77		
DSR Pen Correlation	G* (kPa)		25	100.55	154	126
	Calculated Pen Value			126	100	111.5
Softening Point (AASHTO T 53)	Softening Point R&B			64		
DSR Softening Point (Surrogate) (°C)				62	60.2	57.15
Tack Coat Formulation Specification Verification Test Results						
Viscosity, Saybolt-Furol, 25°C (77°F), seconds (AASHTO T				23 (20-100)		
Storage Stability Test, 24 hour, % (AASHTO T 59)				0.29 (1.0		
Sieve Test, % (AASHTO T 59)				0.00 (0.1		
Particle Charge (AASHTO T 59)				Positive		
Demulsibility, 35 mL, 0.8% DSS (AASHTO T 59)				65.6 (40		
Density, lb/gal (AASHTO T 59)				8.47		
Residue by Distillation, %, weight (AASHTO T 59)				63.8 (63		
Penetration, 25°C (77°F), 100 g, 5 seconds, 0.1 mm				97.0 (90-		
Elastic Recovery, 10° C (50° F) (AASHTO T 301)				64.0 (60		
Ash Content, % (AASHTO T 111)				0.2 (1.0 max)		

Table A.13. Summary of Average Test Results for PG 67-22 Binder [67].

Test Method	Property		Test Temp. (°C)	Hot Applied PG 67-22
PG (AASHTO M 320)	Original DSR	G*/sin δ (kPa)	64	1.77
		phase angle δ (°)		86.8
		G*/sin δ (kPa)	70	0.83
		phase angle δ (°)		88.0
		G*/sin δ (kPa)	76	
		phase angle δ (°)		
		G*/sin δ (kPa)		
		phase angle δ (°)		
		Continuous PGH_ORIG (°C)		68.6
	Continuous PGH (°C)			**68.6**
MSCR (AASHTO T 350)	Jnr @3.2 kPa		58	2.45
	Jnr @0.1 kPa			2.33
	% Recovery @3.2 kPa			0.11
	% Recovery @0.1 kPa			1.65
	Jnr @3.2 kPa		64	5.72
	Jnr @0.1 kPa			5.40
	% Recovery @3.2 kPa			-1.45
	% Recovery @0.1 kPa			-0.28
	Jnr @3.2 kPa		70	
	Jnr @0.1 kPa			
	% Recovery @3.2 kPa			
	% Recovery @0.1 kPa			
Crossover Temperature (°C)				4.8
RV (AASHTO T 316)	Rotational Viscosity (cP)		135	538
Original DSR Absolute Viscosity (Surrogate)	G* (kPa)		60	3.02
Penetration (AASHTO T 49)	Penetration		25	64
DSR Pen Correlation	G* (kPa)		25	315.5
	Calculated Pen Value			68
Softening Point (AASHTO T 53)	Softening Point R&B			46.9
DSR Softening Point (Surrogate) (°C)				54.6

Table A.14. Summary of Average Test Results for HP NT Hot-Applied Binder [67].

Test Method	Property		Test Temp. (°C)	Hot Applied HP NT
PG (AASHTO M 320)	Original DSR	G*/sin δ (kPa)	88	1.62
		phase angle δ (°)		88.0
		G*/sin δ (kPa)	94	0.71
		phase angle δ (°)		88.2
		G*/sin δ (kPa)		
		phase angle δ (°)		
		G*/sin δ (kPa)		
		phase angle δ (°)		
		Continuous PGH_ORIG (°C)		91.6
	Continuous PGH (°C)			**91.6**
MSCR (AASHTO T 350)	Jnr @3.2 kPa		82	2.52
	Jnr @0.1 kPa			1.50
	% Recovery @3.2 kPa			0.07
	% Recovery @0.1 kPa			20.50
	Jnr @3.2 kPa		88	7.32
	Jnr @0.1 kPa			4.14
	% Recovery @3.2 kPa			-2.16
	% Recovery @0.1 kPa			11.52
	Jnr @3.2 kPa		94	
	Jnr @0.1 kPa			
	% Recovery @3.2 kPa			
	% Recovery @0.1 kPa			
Crossover Temperature (°C)				34.3
RV (AASHTO T 316)	Rotational Viscosity (cP)		135	1,445
Original DSR Absolute Viscosity (Surrogate)	G* (kPa)		60	171.00
Penetration (AASHTO T 49)	Penetration		25	2
DSR Pen Correlation	G* (kPa)		25	75,200.0
	Calculated Pen Value			4
Softening Point (AASHTO T 53)	Softening Point R&B			83.0
DSR Softening Point (Surrogate) (°C)				81.6

Table A.15. Summary of Average Test Results for PG 64-22 Binder [67].

Test Method	Property		Test Temp. (°C)	Hot Applied PG 64-22
PG (AASHTO M 320)	Original DSR	G*/sin δ (kPa)	64	1.41
		Phase Angle δ (°)		86.7
		G*/sin δ (kPa)	70	0.66
		Phase Angle δ (°)		88
		G*/sin δ (kPa)	76	
		Phase Angle δ (°)		
		G*/sin δ (kPa)		
		Phase Angle δ (°)		
		Continuous PGH_ORIG (°C)		66.7
	Continuous PGH (°C)			**66.7**
MSCR (AASHTO T 350)	Jnr @3.2 kPa		58	3.03
	Jnr @0.1 kPa			2.84
	% Recovery @3.2 kPa			-0.11
	% Recovery @0.1 kPa			1.55
	Jnr @3.2 kPa		64	7.23
	Jnr @0.1 kPa			6.72
	% Recovery @3.2 kPa			-1.89
	% Recovery @0.1 kPa			-0.6
	Jnr @3.2 kPa		70	
	Jnr @0.1 kPa			
	% Recovery @3.2 kPa			
	% Recovery @0.1 kPa			
Crossover Temperature (°C)				2.8
RV (AASHTO T 316)	Rotational Viscosity (cP)		135	422
Original DSR Absolute Viscosity (Surrogate)	G* (kPa)		60	2.43
Penetration (AASHTO T 49)	Penetration		25	67
DSR Pen Correlation	G* (kPa)		25	269
	Calculated Pen Value			75
Softening Point (AASHTO T 53)	Softening Point R&B			48.5
DSR Softening Point (Surrogate) (°C)				54.1

Table A.16. ISS Test Results of New AC (½ inch NMAS)/New PCC.

Tack Coat	Application Rate	%AV	ISS, psi	Average ISS, psi	STD, psi	CV, %	95% CI
SS-1	M	4.8	43.7	35.9	6.3	18%	15.8
SS-1	M	10.8	28.1				
SS-1	M	7.8	35.9				
SS-1	H+	10.0	6.6	11.8	4.0	34%	9.9
SS-1	H+	10.0	12.5				
SS-1	H+	15.3	16.4				
SS-1h	M	12.1	25.2	24.1	0.9	4%	2.3
SS-1h	M	10.7	24.0				
SS-1h	M	10.8	23.0				
SS-1h	H+	8.9	30.1	25.4	6.9	27%	17.1
SS-1h	H+	8.1	30.5				
SS-1h	H+	9.3	15.7				
HP NT	M	8.7	72.8	98.7	20.9	21%	52.0
HP NT	M	3.0	99.1				
HP NT	M	8.3	124.1				
HP NT	H+	4.6	123.8	93.6	22.2	24%	55.1
HP NT	H+	8.8	85.5				
HP NT	H+	8.5	71.4				
PM NT	M	7.5	41.7	54.7	10.0	18%	24.7
PM NT	M	6.8	56.7				
PM NT	M	5.5	65.8				
PM NT	H+	5.0	74.5	65.2	6.6	10%	16.5
PM NT	H+	7.7	61.6				
PM NT	H+	6.6	59.5				
HPM	M	7.9	46.2	55.5	14.6	26%	36.2
HPM	M	5.7	44.2				
HPM	M	5.3	76.1				
HPM	H+	5.0	66.9	45.2	15.3	34%	38.1
HPM	H+	6.2	33.4				
HPM	H+	5.6	35.4				
PG 67-22	M	7.9	72.1	68.8	2.4	4%	6.1
PG 67-22	M	7.5	67.9				
PG 67-22	M	8.3	66.4				
PG 67-22	H+	7.7	50.6	45.6	12.9	28%	32.0
PG 67-22	H+	5.9	58.2				
PG 67-22	H+	7.1	28.0				
HP NT_HA	M	7.0	112.9	113.0	2.5	2%	6.2
HP NT_HA	M	8.4	116.1				
HP NT_HA	M	5.7	110.0				
HP NT_HA	H+	5.1	137.1	122.6	15.2	12%	37.7
HP NT_HA	H+	5.2	129.1				
HP NT_HA	H+	7.9	101.6				

Table A.17. ISS Test Results of New AC (¾ inch NMAS)/Aged PCC.

Tack Coat	Application Rate	%AV	ISS, psi	Average ISS, psi	STD, psi	CV, %	95% CI
SS-1	M	12.1	23.81	14.0	7.0	50%	17.3
SS-1	M	13.5	8.82				
SS-1	M	11.0	9.23				
SS-1	H+	12.2	11.48	14.7	4.5	30%	11.1
SS-1	H+	11.6	11.67				
SS-1	H+	10.0	21.04				
SS-1h	M	6.8	46.3	55.4	20.6	37%	51.1
SS-1h	M	6.7	83.9				
SS-1h	M	7.4	36.1				
SS-1h	H+	12.5	23.6	37.5	11.4	31%	28.4
SS-1h	H+	10.3	37.1				
SS-1h	H+	7.6	51.7				
HP NT	M	5.7	168.2	151.5	18.5	12%	46.0
HP NT	M	6.0	160.6				
HP NT	M	7.4	125.6				
HP NT	H+	11.7	107.2	140.8	26.9	19%	66.9
HP NT	H+	9.1	142.2				
HP NT	H+	7.0	173.1				
PM NT	M	6.4	19.8	38.3	14.5	38%	36.1
PM NT	M	7.1	39.9				
PM NT	M	9.2	55.3				
PM NT	H+	12.8	98.4	84.6	30.4	36%	75.6
PM NT	H+	12.3	113.0				
PM NT	H+	9.2	42.4				
HPM	M	5.9	78.7	51.9	22.7	44%	56.5
HPM	M	6.2	23.1				
HPM	M	7.3	53.8				
HPM	H+	11.2	33.5	48.5	14.7	30%	36.5
HPM	H+	7.6	43.6				
HPM	H+	6.5	68.5				
PG 67-22	M	7.5	87.3	72.6	12.0	17%	29.9
PG 67-22	M	9.0	57.8				
PG 67-22	M	8.3	72.6				
PG 67-22	H+	11.1	23.8	35.2	12.5	35%	31.0
PG 67-22	H+	8.3	52.6				
PG 67-22	H+	15.5	29.2				
HP NT_HA	M	6.6	179.4	160.8	24.0	15%	59.6
HP NT_HA	M	6.0	176.1				
HP NT_HA	M	8.2	126.9				
HP NT_HA	H+	11.6	91.3	108.8	15.1	14%	37.6
HP NT_HA	H+	11.4	107.0				
HP NT_HA	H+	9.2	128.2				

Table A.18. ISS Test Results of New AC (½ inch NMAS)/Aged PCC.

Tack Coat	Application Rate	%AV	ISS, psi	Average ISS, psi	STD, psi	CV, %	95% CI
SS-1	M	5.2	49.3	59.0	7.7	13%	19.2
SS-1	M	4.4	59.5				
SS-1	M	5.2	68.2				
SS-1	H+	5.3	50.1	53.9	5.2	10%	13.0
SS-1	H+	4.7	61.3				
SS-1	H+	7.0	50.3				
SS-1h	M	7.1	44.8	62.2	12.4	20%	30.9
SS-1h	M	5.4	68.7				
SS-1h	M	5.2	73.0				
SS-1h	H+	3.8	58.2	52.7	6.9	13%	17.0
SS-1h	H+	4.3	56.9				
SS-1h	H+	6.1	43.1				
HP NT	M	4.1	152.4	174.3	16.4	9%	40.6
HP NT	M	3.0	191.7				
HP NT	M	3.0	178.8				
HP NT	H+	5.7	158.9	160.9	5.4	3%	13.4
HP NT	H+	2.3	168.3				
HP NT	H+	6.8	155.5				
PM NT	M	4.6	86.7	93.0	9.9	11%	24.7
PM NT	M	2.9	107.0				
PM NT	M	2.7	85.3				
PM NT	H+	2.7	86.0	89.0	9.2	10%	22.7
PM NT	H+	2.7	101.5				
PM NT	H+	4.5	79.7				
HPM	M	4.4	42.5	50.3	8.2	16%	20.4
HPM	M	3.3	61.7				
HPM	M	4.0	46.9				
HPM	H+	4.6	63.9	66.6	9.6	14%	23.8
HPM	H+	4.6	79.5				
HPM	H+	6.1	56.5				
PG 67-22	M	4.6	52.0	67.5	11.4	17%	28.4
PG 67-22	M	3.6	71.5				
PG 67-22	M	3.4	79.1				
PG 67-22	H+	3.1	64.8	65.1	0.4	1%	1.0
PG 67-22	H+	3.7	65.6				
PG 67-22	H+	4.4	64.8				
HP NT_HA	M	4.8	164.5	172.3	6.2	4%	15.5
HP NT_HA	M	3.2	179.8				
HP NT_HA	M	2.9	172.5				
HP NT_HA	H+	3.0	140.3	148.2	10.2	7%	25.3
HP NT_HA	H+	3.2	141.7				
HP NT_HA	H+	4.6	162.5				

Table A.19. Analysis of Variance for New AC (½ inch NMAS)/New PCC.

Source	DF	Adj SS	Adj MS	F-Value	P-Value
Air Voids Level (AV), %	1	1555.3	1555.34	8.07	0.008
Tack Coat Types	6	30349.2	5058.20	26.23	0.000
Application Rate Level	1	405.9	405.93	2.10	0.156
Error	33	6364.0	192.85		
Lack-of-Fit	32	6347.0	198.34	11.67	0.228
Pure Error	1	17.0	16.99		
Total	41	51964.3			

Table A.20. Analysis of Variance for New AC (¾ inch NMAS)/Aged PCC.

Source	DF	Adj SS	Adj MS	F-Value	P-Value
Air Voids Level (AV), %	1	1903	1902.9	3.00	0.032
Tack Coat Types	6	69563	11593.8	18.26	0.000
Application Rate Level	1	0	0.0	0.00	0.996
Error	33	20947	634.8		
Total	41	110024			

Table A.21. Analysis of Variance for New AC (½ inch NMAS)/Aged PCC.

Source	DF	Adj SS	Adj MS	F-Value	P-Value
Air Voids Level (AV), %	1	534.3	534.3	3.98	0.035
Tack Coat Types	6	76117.5	12686.3	94.51	0.000
Application Rate Level	1	253.6	253.6	1.89	0.179
Error	33	4429.8	134.2		
Total	41	92862.2			

Table A.22. Turkey and Bonferroni Pairwise Tack Coat Comparison for New AC (½ inch NMAS)/New PCC.

Tack Coat Types	N	Mean	Grouping		
HP NT_HA	6	114.199	A		
HP NT	6	94.014	A		
PG 67-22	6	56.528		B	
PM NT	6	56.245		B	
HPM	6	44.694		B	
SS-1h	6	32.964		B	
SS-1	6	31.396		B	
No Tack	3	0.000			C

Means that do not share a letter are significantly different.

Table A.23. Turkey and Bonferroni Pairwise Tack Coat Comparison for New AC (¾ inch NMAS)/Aged PCC.

Tack Coat Types	N	Mean	Grouping		
HP NT	6	140.840	A		
HP NT_HA	6	133.635	A		
PM NT	6	63.024		B	
PG 67-22	6	57.232		B	
SS-1h	6	44.131		B	
HPM	6	43.391		B	
SS-1	6	25.009		B	
No Tack	3	0.000			C

Means that do not share a letter are significantly different.

Table A.24. Turkey and Bonferroni Pairwise Tack Coat Comparison for New AC (½ inch NMAS)/Aged PCC.

Tack Coat Types	N	Mean	Grouping			
HP NT	6	167.124	A			
HP NT_HA	6	157.503	A			
PM NT	6	87.171		B		
PG 67-22	6	64.283			C	
SS-1h	6	61.518			C	
SS-1	6	60.488			C	
HPM	6	59.386			C	
No Tack	3	0.000				D

Means that do not share a letter are significantly different.